Volume 44 | Number 11 | 7 June 2015 | Pages 3349–3862

Chem Soc Rev

Chemical Society Reviews
www.rsc.org/chemsocrev

ISSN 0306-0012

ROYAL SOCIETY OF CHEMISTRY

REVIEW ARTICLE
Federico Bella, Michael Grätzel *et al.*
Aqueous dye-sensitized solar cells

Chem Soc Rev

REVIEW ARTICLE

View Article Online
View Journal | View Issue

Cite this: *Chem. Soc. Rev.*, 2015, **44**, 3431

Aqueous dye-sensitized solar cells

Federico Bella,*[a] Claudio Gerbaldi,[a] Claudia Barolo[b] and Michael Grätzel*[c]

Received 3rd December 2014

DOI: 10.1039/c4cs00456f

www.rsc.org/csr

Nowadays, dye-sensitized solar cells (DSSCs) are the most extensively investigated systems for the conversion of solar energy into electricity, particularly for implementation in devices where low cost and good performance are required. Nevertheless, a key aspect is still to be addressed, being considered strongly harmful for a long time, which is the presence of water in the cell, either in the electrolyte or at the electrode/electrolyte interface. Here comes the present review, in the course of which we try our best to address the highly topical role of water in DSSCs, trying to figure out if it is a poisoner or the keyword to success, by means of a thoroughly detailed analysis of all the established phenomena in an aqueous environment. Actually, in the last few years the scientific community has suddenly turned its efforts in the direction of using water as a solvent, as demonstrated by the amount of research articles being published in the literature. Indeed, by means of DSSCs fabricated with water-based electrolytes, reduced costs, non-flammability, reduced volatility and improved environmental compatibility could be easily achieved. As a result, an increasing number of novel electrodes, dyes and electrolyte components are continuously proposed, being highly challenging from the materials science viewpoint and with the golden thread of producing truly water-based DSSCs. If the initial purpose of DSSCs was the construction of an artificial photosynthetic system able to convert solar light into electricity, the use of water as the key component may represent a great step forward towards their widespread diffusion in the market.

1. Introduction

Due to the gradual, but constant and inescapable depletion of fossil fuels and the increasing energy demand to support the current model of economic growth, mankind is facing a global energy problem.[1,2] Amongst the number of alternative resources, renewable energies are rapidly becoming the leading solution to fulfil the growing needs of power sources.[3,4] In this respect, wind power, solar energy, hydropower, geothermal energy, biomass and biofuel are extensively investigated for a few decades both from the scientific/academic and industrial viewpoints.[5]

At present, solar energy is considered the most promising renewable resource: every day, the Sun shines on the Earth, thus providing around 3×10^{24} J of green energy per year, which exceeds by a factor of 10^4 the present global population consumption.[6–8] A simple calculation leads self-evidently to the conclusion that covering only around 0.1% of the Earth's surface by means of energy conversion devices having an efficiency of about 10% would satisfy the present global energy needs. These encouraging numbers are inducing the scientific community to make even greater efforts towards the direction of improving solar energy conversion technologies as well as proposing new intriguing solutions.[9,10] To have an idea of the magnitude of this effort, a rapid search on a scientific database (*e.g.*, Scopus), using the simple keyword "solar energy", provides more than 10 000 publications for each of the recent years.

The creation of a potential difference, or electric current, in a material upon exposure to light is possible because of the photovoltaic (PV) effect, and – depending on the materials used – three generations of solar energy devices have been developed to date.[11–13] Among all, the mostly studied device of the last generation is the dye-sensitized solar cell (DSSC), being a low-cost and high efficiency solar energy-to-electricity converter. Firstly assembled and demonstrated by O'Regan and Grätzel in 1991,[14] they are composed of only five components (Fig. 1): a transparent conductive oxide (TCO) substrate,[15] a nanostructured n-type semiconductor,[16] a visible-light absorber dye,[17] an electrolyte[18] and a counter electrode.[19] With the key idea of mimicking the natural photosynthesis, DSSCs are being pursued as eco-friendly devices, which could be easily fabricated.[20,21] In a dye-sensitized solar cell, upon absorption of light, dye molecules reach an excited state and, with an appropriate energy level alignment of all the

[a] *GAME Lab, CHENERGY Group, Department of Applied Science and Technology – DISAT, Politecnico di Torino, Corso Duca degli Abruzzi 24, 10129 Torino, Italy. E-mail: federico.bella@polito.it; Tel: +39 0110904638*
[b] *Department of Chemistry and NIS Interdepartmental Centre, Università degli Studi di Torino, Via Giuria 7, 10125 Torino, Italy*
[c] *Laboratory of Photonics and Interfaces, Swiss Federal Institute of Technology (EPFL), Station 6, 1015 Lausanne, Switzerland. E-mail: michael.graetzel@epfl.ch; Tel: +41 216933112*

components, charge separation occurs at the interface between the dye-sensitized semiconductor and the electrolyte. While electrons are injected into the conduction band (CB) of the semiconductor (usually titanium dioxide, TiO_2) and transported to the conductive electrode, the regeneration of the oxidized dye takes place at the counter electrode by means of an electron-donor species (typically a liquid electrolyte based on the redox couple iodide/triiodide, I^-/I_3^-).[22] Multidisciplinarity, academic and industrial interests have boosted the number of publications per year (Fig. 2), resulting in about 4000 international peer-reviewed0papers in the 2013–2014 period of time. Some of these articles, which led to the identification of new materials with concrete applications also in other research fields,[23,24] are highly cited: each of them counts even more than 1000 citations.[25–28]

The most performing DSSCs (efficiencies up to 13% have been recently demonstrated[29]) use organic solvent-based liquid electrolytes. These have the relevant drawback of high vapour pressure and a severe environmental impact. Moreover, several organic solvents are toxic and/or explosive, thus seriously limiting their practical applications in DSSCs because of safety issues. Although several alternatives to organic solvents have been proposed (*i.e.*, plastic crystals and solid-state conductors[30,31]), the biggest – sometimes ignored – issue still remaining unsolved

Federico Bella

Federico Bella received MSc in Industrial Chemistry at the Università di Torino and the PhD in Electronic Devices at the Italian Institute of Technology. He is a post-doc researcher at the Department of Applied Science and Technology of the Politecnico di Torino, managing the research activity in the field of third generation solar cells in the Group for Applied Materials and Electrochemistry (GAME-Lab). His interests include dye-sensitized solar cells, sodium-ion batteries, polymer electrolytes for energy application and multivariate chemometric techniques. He is a young member of the Board of the Italian Chemical Society. He has published more than 25 articles in the last two years in the fields of energy, electrochemistry and materials science.

Claudio Gerbaldi

Claudio Gerbaldi received his PhD in Materials Science and Technology from Politecnico di Torino in 2006. In 2011, he became an assistant professor and, in 2014, an associate professor at the same Department of Applied Science and Technology of the Politecnico di Torino. In the Group for Applied Materials and Electrochemistry (GAME-Lab), he currently coordinates the research activity on nanostructured electrodes, as well as bio-inspired materials and innovative polymer electrolytes for the development of eco-friendly energy storage and conversion devices. Among others, he has received the ''UniCredit Award'' for the Young Innovation in Research (2007) and has published ~75 ISI articles with ~250 annual citation counts in recent years.

Claudia Barolo

Claudia Barolo received her PhD in Chemistry from Università di Torino in 2001. In 2006, she became an assistant professor and, in 2014, an associate professor in Industrial Chemistry at the Department of Chemistry of the same university. Her research activity is mainly focused on the synthesis and characterization of functional molecules and hybrid materials for technological applications (photonics, nanotechnology, biotechnology). As an expert in the field of sensitizers for solar cells, she is the recipient of several national and international research grants, industrial collaborations, and, since 2011 she has been a member of the Technical and Scientific Committee of Dyepower consortium. She has published more than 55 ISI articles with ~200 annual citation counts in recent years.

Michael Grätzel

Michael Grätzel directs the Laboratory of Photonics and Interfaces at the École Polytechnique Fédérale de Lausanne. He pioneered the use of mesoscopic materials in energy conversion and storage systems, in particular photovoltaic cells, lithium ion batteries and photoelectrochemical devices for water splitting by sunlight. He has received the Albert Einstein World Award of Science, the Gutenberg Research Award, the Galvani Medal, the Faraday Medal and the Millenium Technology Grand Prize. He has published ~1100 papers, 50 reviews/book chapters and is the inventor/co-inventor of >50 patents. His studies have been cited over 140 000 times (h-index 170), making him one of the 10 most highly cited chemists in the world.

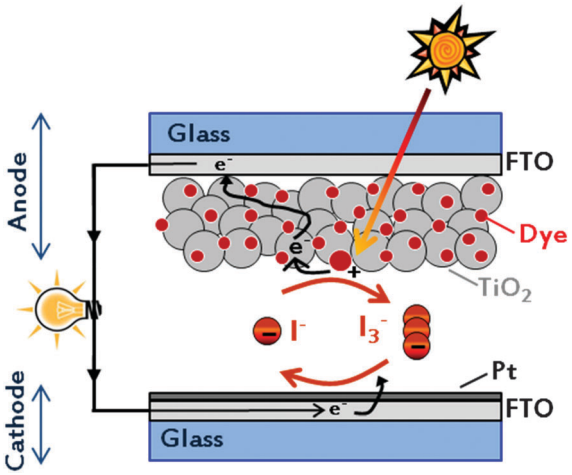

Fig. 1 Schematic representation of the components and of the basic operating principle of a DSSC.

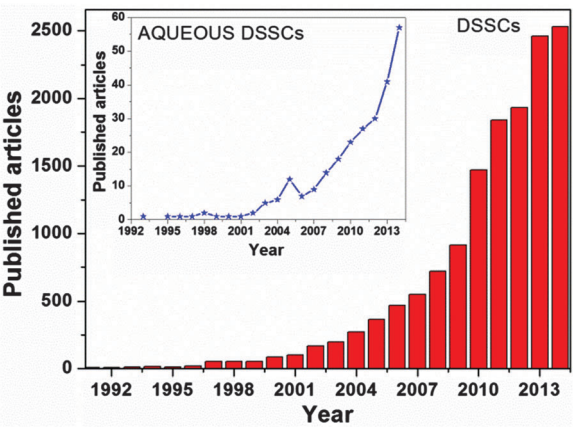

Fig. 2 Number of research articles published per year in the field of DSSCs. Inset: data for aqueous DSSCs. Source: SCOPUS Database.

in standard aprotic DSSC systems is the contamination of the cell by means of moisture/water. This often affects both the cell performance and the long-term stability, even if robust encapsulation systems and specifically conceived barrier materials are utilised. In fact, traces of water are always present in the electrolytic solution and in the pores/voids of the semiconductor electrode film, being eventually introduced during cell assembly or upon operation under ambient conditions (tiny defects in the encapsulation are often present). This phenomenon is even more accentuated when the production of flexible DSSCs is envisaged,[32,33] quite rapidly permeated by water molecules (*i.e.*, 0.01 g m^{-2} day^{-1}) even in the presence of rather expensive barrier layers; in fact, it has been calculated that the water content in the electrolyte may be >10% after one year of real outdoor use.[34] These results have led to the general opinion that water is detrimental, in fact a poisoner, for DSSCs.

The aim of this review article is to thoroughly unravel the specific role of water as an electrolyte component in DSSCs. First of all, it is fundamental to understand how the presence of water can influence the device performance; many studies have been proposed over the years in this respect. Crossing experimental data obtained by using very different techniques as well as theoretical simulations would help in identifying the interactions between water molecules and DSSC components. Then, we consider very much interesting and surprising to show how, in the last few years, the scientific community has turned its efforts in the direction of DSSCs fabricated with water-based electrolytes. Indeed, being less expensive, non-flammable and more environmentally friendly, these novel devices would also not suffer from water contamination issues, with the added value of easily solvating many potential redox mediators. Photoanode modifications, introduction of novel additives and surfactants, selection of specifically conceived redox couples, preparation of suitable cathodes and stabilization of electrolytes have progressively led to the fabrication of 100% aqueous DSSCs. Achieving high performance in a fully aqueous cell represents the *Holy Grail* for DSSCs, and brings back the attention to their initial purpose: the realisation of an artificial photosynthetic system able to convert solar visible light energy into electricity, by using a unique solvent, water, the solvent of life.

2. Electrolytes for DSSCs: state of the art

The electrolyte has been identified as one of the component which most significantly influences DSSC efficiency and stability, since it has a key role in the regulation of the electron transfer kinetics. According to their physical consistency, electrolytes may be classified into three main classes: liquid, quasi-solid and solid.

Traditional liquid electrolytes consist of a redox couple and a few additives dissolved into an organic solvent. As previously stated, the standard redox mediator is the I^-/I_3^- couple, but several valid alternatives have been proposed. In particular, cobalt complexes[35] have exceeded the performance of the standard redox pair, achieving efficiencies up to 13%.[29] Other redox mediators, such as $SCN^-/(SCN)_3^-$,[36] $SeCN^-/(SeCN)_3^-$,[37] Br^-/Br_3^-,[38] sulphur-based systems,[39] copper complexes,[40] ferrocene derivatives[41] and stable nitroxide radicals,[42] have also been proposed. Each of these systems is characterized by peculiar thermodynamic and kinetic properties, which must be well matched with the other cell components. Moreover, also counterions of redox mediators must be properly selected, since it has been reported that the photocurrent decreases and the photovoltage increases while increasing the cation radius, due to the variation of the TiO_2 CB energy (E_c) and the associated influence on the electron injection efficiency.[43]

Additives are often introduced in appropriate amounts to increase the PV parameters; among them, nitrogen-containing heterocyclic compounds and guanidinium thiocyanate (GuSCN) are the most frequently used. While the former improve cell photovoltage by shifting the band edge of TiO_2 and increasing the electron lifetime,[44] the latter enhances the photocurrent by positively moving the flatband potential of the photoelectrode, thus increasing the electron injection yield.[45]

As regards organic solvents, acetonitrile (ACN), valeronitrile (VAN), 3-methoxypropionitrile (MPN), methoxyacetonitrile (MAN), ethylene carbonate (EC), propylene carbonate (PC), γ-butyrolactone (GBL) and *N*-methylpyrrolidone (NMP) are the most commonly used, due to their high dielectric constant and low viscosity. Since all these solvents can be considered as electron acceptors, a classification of their donor number (*i.e.*, the enthalpy of reaction of the solvent with a strong electron acceptor) was proposed,[46] and it was proved that an increase in the electron-donor (or basic) character led to higher cell potentials and lower photocurrents.[47] The worst drawback of organic solvents is their high volatility, thus room temperature ionic liquids (RTILs), being non-flammable and non-volatile organic compounds, are widely used as additives or solvents in order to guarantee good chemical and thermal stabilities.[48] However, RTILs often show high viscosity values, and specific improvements of their rheological characteristics are necessary to ensure an efficient ion transport. The enormous research efforts carried out in the field of liquid electrolytes have been already thoroughly discussed in several review articles.[49–53]

Limited long-term stability, difficulty in hermetic sealing and leakage of the liquid electrolyte have been identified as relevant drawbacks in view of real indoor and outdoor applications of DSSCs.[54–56] A possible solution is represented by the entrapment of the liquid electrolyte by means of a polymeric or inorganic network. Polymeric quasi-solid electrolytes can be prepared in the form of gels[57] or membranes,[58,59] where a huge amount of crosslinked matrices has been investigated.[60–62] As an alternative, inorganic nanoparticles (NPs) have been adopted to jell liquid electrolytes, creating a quasi-solid (paste-like) network containing self-assembled channels able to ensure sufficient ionic transport.[63–65] To date, quasi-solid electrolytes are considered the optimum compromise between efficiency and durability,[66] and the recent advances in this subject have been collected in some review articles.[67–69]

Solid electrolytes are based on a completely different working principle: holes transferred from the dye are transported *via* hopping between the electronic states of the solid electrolyte to the metallic or polymeric counter electrode. Crystalline p-type semiconductors,[70] organic hole-conducting molecules,[71] as well as conductive polymers[72] have been widely studied.[73–75] However, the poor intrinsic conductivity, the low electron transfer from the dye molecules, the poor penetration into the mesoporous TiO_2 and the faster recombination phenomena do not allow solid cells to be more efficient than their liquid and quasi-solid counterparts. Studies on solid DSSCs have recently led to the development of perovskite solar cells (PSCs), in which compounds like $CH_3NH_3PbI_xCl_{3-x}$ act as the light harvester as well as the conductor of both electrons and holes.[76–78] PSCs have achieved efficiencies above 19%[79] (certified value: 17.9%,[80]) and, although very young, will surely be able to establish themselves as a leading device for solar energy conversion.

The introduction of water in liquid, quasi-solid and solid electrolytes causes a very complex set of effects on the PV performance of the resulting DSSCs. The initial section of this review will focus on their detailed investigation, while the rest of the manuscript will deal with cells in which water is purposely added to the electrolyte with gradually increasing percentages, giving rise to so-called ''aqueous DSSCs''.

3. Harmful effects due to water contamination

As anticipated in the Introduction, the presence of water was initially viewed as a strongly negative aspect for DSSCs. Where does water in cells come from? Unless DSSCs are assembled in a N_2- or Ar-filled glove-box (procedure almost never encountered in the literature), water is present during all the manufacturing steps. Indeed, it can be adsorbed on the anodic semiconductor, be present in the solvents and in the solutions used to make the dye-uptake or the liquid electrolyte filling, permeate the polymer films used for device sealing. The effects of water on the PV performance, and the stability and the visual aspects of DSSCs have been extensively studied by adopting several experimental techniques and/or through computational studies, which are reported in the following Sections (3.1–3.5). For ease of understanding, we will report the water content as percentage by weight (wt%) or volume (vol%); however, in the case of very low quantities we will adopt the molar concentration (for H_2O, 1.0 M corresponds to 1.8 wt%).

3.1 Effects on photovoltaic parameters

A couple of years after inventing the DSSCs, Grätzel and coworkers proposed the first study on the stability of *cis*-X_2bis(2,2′-bipyridyl-4,4′-dicarboxylate)-ruthenium(II) ($X = Cl^-$, Br^-, I^-, CN^- and SCN^-) sensitizers.[81] All of the cells showed an initial 20–30% decay in short-circuit current density (J_{sc}), which was attributed to the absorption of residual UV light as well as to the contamination by water molecules. Such detrimental effects were attributed to the electronic and chemical equilibration of the dye-loaded TiO_2 with the liquid electrolyte, the water uptake from ambient air being envisaged as their main cause. Indeed, when a water-tight cell sealant was used, the initial decay in the performance of the cell was suppressed.

The first analytical investigation of water contamination dates back to 1998, when Lindquist and coworkers showed that J_{sc} decreased (Fig. 3A) and open-circuit voltage (V_{oc}) increased (Fig. 3B) when the water content in the electrolytic solution (LiI 0.10 M and I_2 10 mM in MAN) increased from 0 to 2.2 M.[43] It was proposed that water molecules, being strongly adsorbed onto the TiO_2 surface, coordinated with the surface Ti atoms[82] and blocked the reaction of I_3^- with the electrons in the TiO_2 CB. As a result, V_{oc} increased proportionally to the amount of water introduced in the cell. Such a phenomenon was so strong as to balance and quantitatively overcome the negative shift of the CB which was caused by the addition of water to the aprotic electrolytic solution.[83] Anyway, despite the improvement in V_{oc}, cell performance decreased due to the neat reduction of J_{sc} values. In their preliminary studies, Lindquist and coworkers motivated this effect by arguing the following hypotheses: desorption of the N3 dye from the TiO_2 surface, weakening of

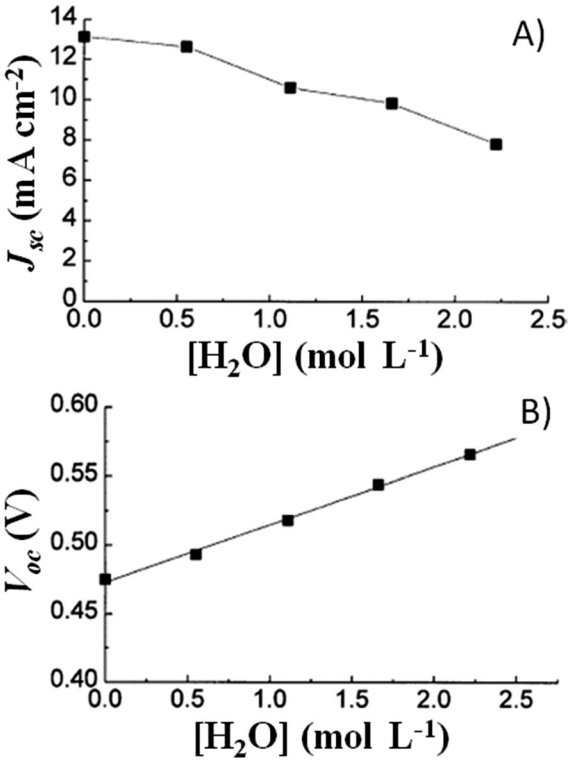

Fig. 3 Variation of J_{sc} (A) and V_{oc} (B) values, measured a 0.82 sun, due to water addition in the liquid electrolyte. Electrolytes: LiI 0.10 M and I_2 10 mM in MAN/H_2O. Dye: N3. Adapted and reprinted from ref. 43.

the TiO_2–dye interaction, photoinduced substitution of the –NCS ligand of the dye and change in the absorption properties of the sensitizer molecules due to the variation in the solvent polarity. For sure, the most intriguing phenomenon was observed when the contaminated electrolyte was replaced by a freshly prepared water-free one: J_{sc} was fully restored (from 1.93 to 2.62 mA cm^{-2}), while V_{oc} retained a higher value (0.535 V *vs.* the initial 0.453 V). As a result, the overall cell efficiency (η) increased (from 5.2% to 6.4% at an irradiation intensity P_{in} of 0.15 sun), and Lindquist's group compared the effect observed in the water-contaminated systems to that provided by the traditionally used pyridine derivative additives.[84]

3.2 Spectroscopic investigation of water-promoted effects

Fourier transform infrared (FTIR) studies reported in Fig. 4A–C showed that when the working electrodes were immersed in an electrolyte (LiI 0.50 M and I_2 50 mM in MPN) containing 5 vol% H_2O, the broadening as well as decreased intensity of the –NCS ligand absorption band (2100 cm^{-1}) was observed. In the same study, Hagfeldt and coworkers found a small absorption peak at 1575 cm^{-1}, which was assigned to the symmetric bending of the water molecules, either bonded to the N719 dye or adsorbed onto the nanostructured TiO_2 film.[85] UV-Vis spectra (Fig. 4D–F) showed blue-shifted absorption maxima with respect to the reference (λ_{max} = 551 nm), both under dark (λ_{max} = 529 nm) and under normal illumination conditions (λ_{max} = 500 nm); these shifts were probably caused by the exchange of the –NCS ligands of the dye with water molecules and/or OH^- anions in the contaminated electrolyte.

To ascertain the eventual influence of hydrogen bonds and hydrophobic interactions on the water-contaminated cell components, the use of water isotopes (*i.e.*, H_2O, D_2O and $H_2{}^{18}O$) has been proposed by Yang and coworkers,[86] who exploited the potential prospects of this procedure usually applied in geology, biology and medicine.[87,88] By monitoring the time-dependent surface reaction occurring on the photoelectrodes in the presence of water isotopes, the diffuse-reflectance infrared Fourier transform (DRIFT, Fig. 5) technique showed that the intensity of the SCN^- ligand remarkably decreased when the water content in the electrolyte (LiI 0.50 M, I_2 50 mM and TBP 0.50 M in ACN; TBP = 4-*tert*-butylpyridine) increased (from 0 to 5 wt%). Additionally, the peak intensity of SCN^- decreased with prolonged soaking time, due to the progressive replacement of the –SCN ligand with water molecules or OH^- ions.[89] This was confirmed by the appearance of a strong band at 3000–3600 cm^{-1}, due to water adsorption on the nanostructured TiO_2 lattice.[90] Moreover, the interaction of Li^+ cations (from LiI) with the free SCN^- anions led to the formation of LiNCS, as indicated by the peak at 2079 cm^{-1}.[91] Considering the sensitizer structure as a whole, it resulted that only the bipyridine ligands of the sensitizer did not take part in the degradation process. When water isotopes were used, Yang and coworkers measured that the degradation rate increased in the order of $H_2O > D_2O > H_2{}^{18}O$, fully consistent with the diffusion rate of these isotopes in the electrolyte, which is inversely proportional to the square root of their molecular masses.[92] As regards the PV performance, the bonding between Li^+ and SCN^- ions gave rise to negative shifts in the TiO_2 Fermi level, which resulted in lower V_{oc} values for aqueous DSSCs, in contrast to the previously discussed results by Lindquist and coworkers.[43]

3.3 Imaging techniques and visual aspects: how cells change over time

Photocurrent imaging techniques represent a valuable investigation method to provide information on problems related to DSSC efficiency as well as long-term stability.[93,94] Cell mapping is usually carried out by means of a He–Ne laser (632 nm), inducing a photocurrent point by point, which is registered through a lock-in amplifier. Using such a technique, Tributsch and coworkers observed the bleaching of the electrolyte, as a result of the disappearance of I_3^- ions.[95] This resulted in the increase of the internal resistance, because the I_3^- reduction reaction at the counter electrode stopped. Interestingly, this was the first work to go in contrast to the others: the effect of water was not geared solely to the dye stability, but also the electrolyte underwent major changes. Even if the formation of iodate (IO_3^-) from I_3^- was expected by Tributsch and coworkers, FTIR analysis revealed the absence of iodate in the electrolyte. Nevertheless, the FTIR spectrum of the electrolyte in the region of the OH-stretching mode showed increased water concentration values in the solvent (ACN). Moreover, the water content increased with time, and aging studies showed that the corresponding OH-stretching mode became the main signal in the spectrum after 84 days. Thus, it was proposed that water could

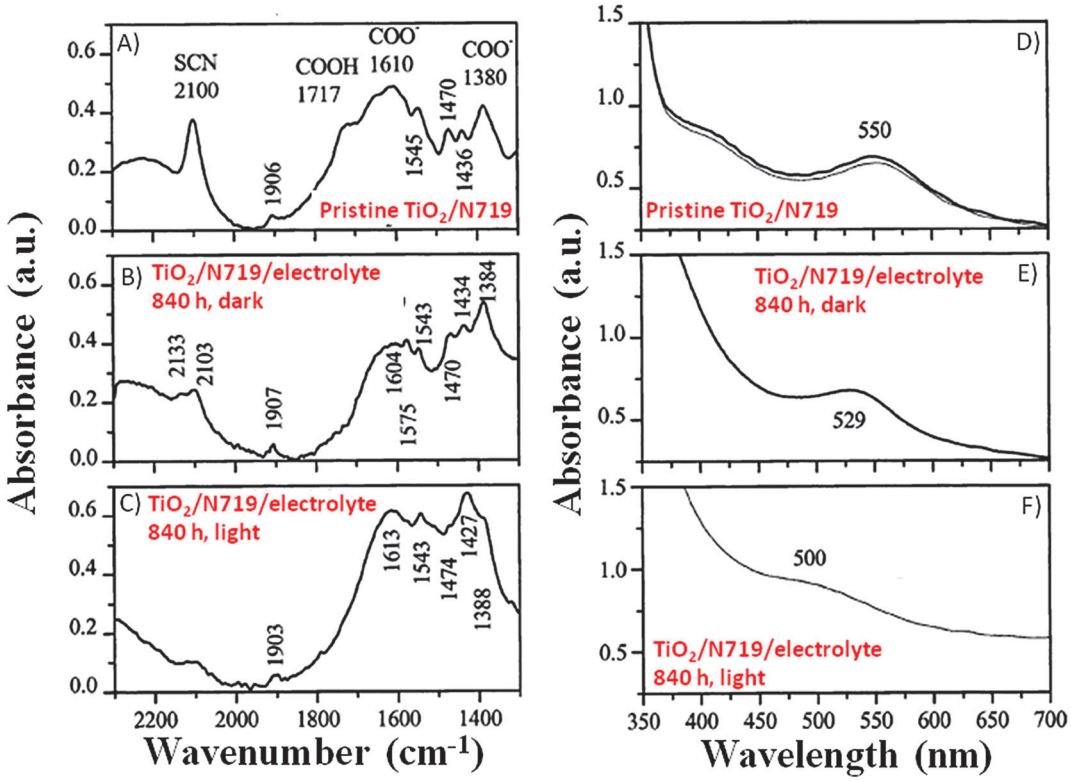

Fig. 4 FTIR (left side) and UV-Vis (right side) spectra of: (A, D) non-treated working electrodes in an Ar atmosphere; (B, E) working electrodes being soaked in a liquid electrolyte (LiI 0.50 M and I_2 50 mM in MPN) with 5 vol% H_2O under dark for 840 h; (C, F) working electrodes being soaked in the same liquid electrolyte under visible light illumination for 840 h. FTIR spectra of the treated samples were normalized based on the TiO_2 absorption maximum of the reference sample at 832 cm^{-1}. Adapted and reprinted from ref. 85.

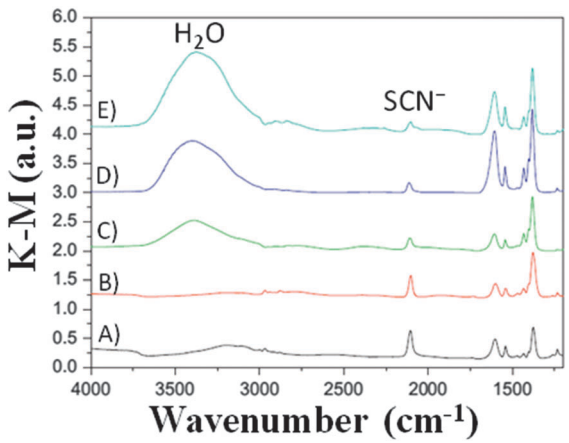

Fig. 5 DRIFT spectra of N719/TiO_2 films immersed in liquid electrolytes (LiI 0.50 M, I_2 50 mM and TBP 0.50 M in ACN) having different water contents for 192 h: (B) 0 vol% H_2O; (C) 1 vol% H_2O; (D) 2 vol% H_2O; (E) 5 vol% H_2O. The response of the photoelectrode before immersion is also shown (A) for comparison purposes. Adapted and reprinted from ref. 86.

activate as a weak base TBP, commonly used as a V_{oc} improver.[44] This would have caused the instability of the I_3^- anions: as well-known from basic ion chemistry, I_3^- ions become unstable and IO_3^- is formed when the pH increases up to 8–10.[96] However, the expected absorption of IO_3^- at 800 cm^{-1} was not detected,[97] thus its adsorption on the TiO_2 electrode was proposed.

Spatially resolved photocurrent mapping[98] has also been proposed by Cameron and coworkers, who coupled Z907 dye-sensitized photoelectrodes with ACN- as well as water-based electrolytes.[99] When vacuum-filled, the ACN-containing cells showed a homogeneous performance all over their volume (Fig. 6A), with the exception of an area of high photocurrent at the top of the device, where dye coverage was higher. As regards aqueous cells, the map showed an area with high photocurrent spreading out from the filling hole (Fig. 6B), where maybe electrolyte filling was relatively poor. To overcome such a defect, aqueous cells were vacuum treated at 80 °C: homogeneous current densities were obtained across the whole area of the cell (Fig. 6C), due to an improved electrolyte penetration. Anyway, all of the aqueous cells underwent a loss of photocurrent (and dye as well) nearby the filling holes; Cameron and coworkers hypothesized that TBP-based alkali solutions could desorb dye from TiO_2, especially around the filling holes. After the previous study by Tributsch and coworkers,[95] this was the second research article where a synergistic effect between water and TBP was observed to have detrimental effects on the device stability.

3.4 Modelling interactions between water and cell components

After being experimentally consolidated that water interacts with the molecules of dye adsorbed onto the semiconductor

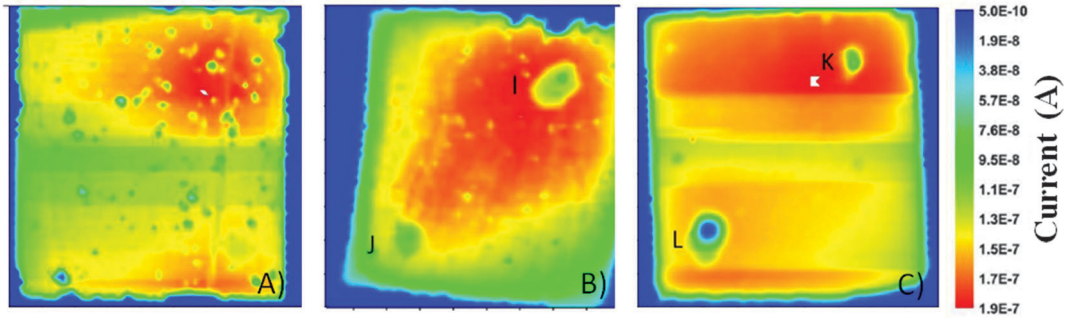

Fig. 6 Photocurrent maps for: (A) vacuum-filled ACN-based cell; (B) vacuum-filled aqueous cell; (C) high temperature vacuum-filled aqueous cell. The positions of the filling holes and the corresponding cold spots are indicated by the letters I–L. The side of each image is 1 cm. Adapted and reprinted from ref. 99.

active material particles, several mechanistic studies have been proposed to investigate this phenomenon. De Angelis and coworkers performed an *ab initio* molecular dynamics simulation and an extensive time-dependent density functional theory (TDDFT) excited state calculation of a squaraine dye[100,101] anchored to an anatase slab exposing the (101) surface,[102] surrounded by 90 water molecules.[103] Water was observed to adsorb, also in overlayer configuration,[104] at the TiO_2 surface. As a result, the blocking function toward recombination of injected electrons with oxidized species in the electrolyte proposed by Lindquist and coworkers[43] was confirmed. As regards the squaraine dye, the TDDFT study demonstrated that an intensive solvent reorganization around the TiO_2-bonded carboxylic group led to a transition from the starting bridged-bidentate to the monodentate adsorption configuration. The latter was stable for ~6 ps; then, the proton anchored at the surface was transferred to the anionic carboxylic group, resulting in the desorption of the dye, which is illustrated in Fig. 7.

Apart from the dye to water interaction, the concurrent presence of TiO_2 to water as well as organic solvent to water interactions should also be considered in DSSC modelling. It is important to recall that aprotic solvents (*e.g.*, ACN and MPN) are responsible for the high DSSC efficiency,[105] due to their high dielectric constant and solubilisation ability *versus* many inorganic and organic salts and additives.[106,107] Furthermore, transient adsorption spectroscopy (TAS) demonstrated that, when photoanodes were immersed in ACN, a 50% increase in the signal intensity occurred, indicating that aprotic solvents increased the electron injection efficiency. In this respect, Tateyama and coworkers modelled the effect of ubiquitous water contamination in an ACN-based electrolyte solution[108] by means of DFT methods implemented in Car–Parrinello molecular dynamics (CPMD).[109,110] Surprisingly, considering the solvation shell $(ACN)_{46}(H_2O)_1$ ($[H_2O]$ = ~0.50 M), it was illustrated that ACN molecules prevented water from coming in contact with the (101) TiO_2 surface by means of a network of hydrogen bonds. However, CPMD also indicated that water molecules that were already adsorbed onto the photoanode before cell assembly were hardly removed because of their strong interaction with the anatase (101) surface. This strong water to TiO_2 interaction (Fig. 8) was observed to be stable up to

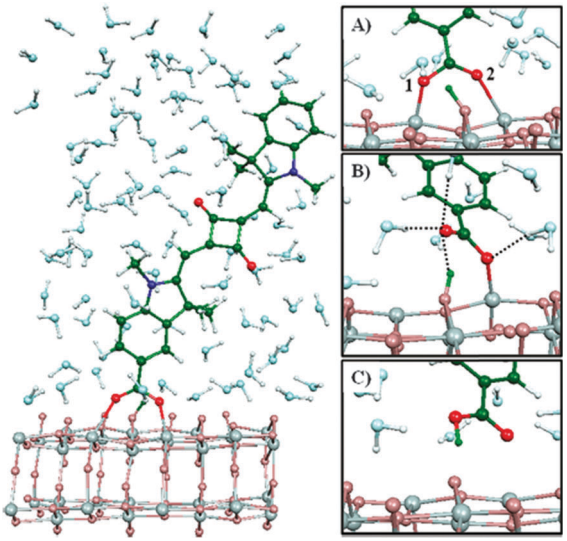

Fig. 7 Squaraine dye adsorbed onto an anatase slab, surrounded by 90 water molecules. In the right hand-sided images, relevant configurations sampled during the TDDFT study are shown: (A) initial bridged-bidentate configuration with labeled oxygen atoms; (B) monodentate configuration; (C) dissociated dye. Note the different proton positions (green). Dashed lines in (B) represent hydrogen bonds to the carboxylic group. Reprinted from ref. 103.

400 K, and could be detrimental for DSSC performance. In fact, photogenerated holes could migrate to water molecules (due to the oxygen atoms charges), thus producing water cation radicals able to interact with the dye molecules onto the TiO_2 surface. Therefore, the common procedure to operate in an anhydrous environment during DSSC fabrication was strongly recommended by the authors.

3.5 Effects of sealing conditions and device area

The experimental conditions of DSSC manufacture have been studied by Dittrich and coworkers,[111] who focused their attention on oxygen- and water-related surface defects on the photoanode, such as oxygen vacancies (or Ti^{3+} donor states) and hydroxy surface complexes. Cells were assembled either with or without pre-treatment under vacuum. It was observed that J_{sc} values decreased when the TiO_2 surface was pre-treated under vacuum, due to the

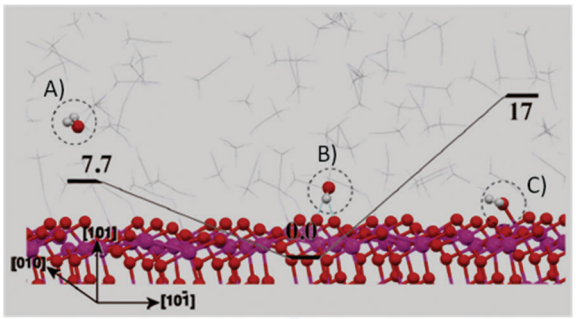

Fig. 8 Structures (with energy values in kcal mol^{-1}) of the TiO_2/bulk-ACN interfaces contaminated with water. (A) Water molecules exist in bulk ACN; (B) the most stable structure of water molecule in bulk ACN and water adsorbed on the TiO_2 surface *via* a hydrogen bond through the H atom in water; (C) water adsorbed onto the TiO_2 surface *via* a hydrogen bond through the O atom in water. Adapted and reprinted from ref. 108.

formation of recombination paths for injected electrons.[112,113] The decrease of J_{sc} was observed to be more pronounced when the cells were pre-treated under a mixed vacuum/water environment, the interaction of –OH groups with TiO_2 being very intense on defective sites.[114] In contrast, chemisorption of water improved V_{oc} values in both vacuum and oxygen pre-treated cells, as a result of the increase of the barrier height between the TiO_2 CB and the redox mediator potential (E).

All of the studies so far reported focusing on water contamination highlighted several detrimental phenomena occurring in different DSSC components: negative shift of the TiO_2 CB, weakening of the TiO_2–dye interaction up to dye desorption, photoinduced substitution of the –NCS ligand and the related change in the absorption properties of the sensitizer, disappearance of I_3^- ions, unwelcome interaction of water with both additives (TBP) and salts (LiI). Moreover, thinking about DSSCs large-scale applications it is important to consider that all of these drawbacks are exponentially emphasized with the increase in the overall volumetric dimension of the device. Considering 5 cm × 5 cm cells assembled under an ambient atmosphere (50–60% RH), Kitamura and coworkers observed the progressive decolouration of the photoelectrodes, accompanied by a 40% decrease in J_{sc} after 800 h at ambient temperature and under dark conditions.[115] This effect was prevented by assembling the cells in the inert atmosphere of an Ar-filled dry glove box (0.1% RH).

At present, two options are available. Specific technologies that may 100% avoid water contamination during the whole manufacturing process of DSSCs as well as during their entire operational life have to be adopted. Alternatively, scientists have to propose dyes, electrodes and electrolytes which can properly operate under a partial or fully aqueous environment, taking advantage of the amount of positive aspects that water would guarantee to third generation PV devices, as stated in the introductory section of this review. We believe that the first option is hardly feasible in terms of cost as well as manufacturing issues (especially because DSSCs are considered promising also for their ease of manufacture), while the development of water-based or fully aqueous DSSCs is certainly the most exciting and promising prospect as will be detailed and analysed in the following sections.

4. Back to 1988: aqueous photoelectrochemical cells

Before discussing the recent findings concerning aqueous DSSCs, it is important to move a step back to a few years before their invention (1991). Indeed, it must be enlightened that the photoelectrochemical cells developed in the 1980–1990 decade were intended to operate with fully aqueous electrolytes.[116,117]

In 1988, Grätzel and coworkers reported on the surprisingly broad band sensitization of TiO_2 to visible light by means of *cis*-Ru(II)$L_2(H_2O)_2^{2-}$ (L = 2,2′-bipyridyl-4,4′-dicarboxylate).[118] A high surface area fractal anatase film deposited onto a Ti sheet acquired an intense violet coloration due to adsorption of the dye from an acidic aqueous solution. The regenerative photoelectrochemical cell containing a KI 0.10 M and I_3^- 1.0 mM aqueous electrolyte provided an efficiency of 2% (J_{sc} = 0.38 mA cm^{-2}, V_{oc} = 0.520 V, fill factor FF = 0.70; P_{in} = 0.7 sun). Interestingly, the photocurrent remained stable after 4 days of illumination, thus confirming the remarkable stability of the sensitizer; moreover, a maximum incident photon to current efficiency (IPCE) value of 62% was observed. In this study, water was present in the sensitizer molecule, in the dye-uptake solution and in the electrolyte as well.

In 1988, RuL_3^{4-} (L = 2,2′-bipyridyl-4,4′-dicarboxylate) was proposed by Grätzel and coworkers as another promising sensitizer for aqueous photoelectrochemical cells;[119] it was also coupled with a new Br-based redox couple (LiBr 1.0 M, Br_2 1.0 mM and $HClO_4$ 1.0 mM). Upon irradiation with a 1.58 W m^{-2} monochromatic light (470 nm), the cell demonstrated a remarkable efficiency of 12% (short-circuit current I_{sc} = 135 μA, V_{oc} = 0.720 V, FF = 0.74; IPCE = 56%); at that time, this was the highest monochromatic conversion yield achieved using a dye-sensitized regenerative photoelectrochemical cell.

With the advent of DSSCs in 1991,[14] aprotic organic solvents replaced water, and cells operating in an aqueous environment were no longer investigated for the following 10–15 years.

5. The trend is being reversed: aqueous electrolytes

In the twenty-first century, scientists started again to focus their research efforts on more deeply investigating the effects of water in DSSCs, the final challenging goal being the full replacement of the traditionally used organic solvents. The seminal paper published in 2010 by O'Regan and coworkers may be undoubtedly considered the fundamental contribution for the scientific community in this context.[120] The authors varied the relative fractions of MPN and water to prepare electrolytes (PMII 2.0 M, I_2 50 mM, GuSCN 0.10 M and TBP 0.5 M; PMII = 1-propyl-3-methylimidazolium iodide) having 0, 20, 40, 60, 80 and 100 vol% H_2O with respect to MPN. Three noticeable insights were proposed in this work: the use of a

hydrophobic dye (TG6), the introduction of 1% Triton X-100 (see Section 7) to avoid phase separation in the aqueous electrolyte and the selection of a high PMII concentration, which concurrently acted as an iodide source and a surfactant. As shown in Table 1, being iodide more soluble in water than tri-iodide, the addition of water shifted E towards positive values. Moreover, no detrimental effect on cell performance was observed up to 40 vol% H_2O. The basic functions of DSSCs (injection, regeneration and transport) worked properly even when using electrolytes having high water contents. Furthermore, the 80 vol%-based cell showed only 7% and 8% losses in J_{sc} and V_{oc}, respectively, after 1000 h under 1 sun (35 °C with UV-filter). The desorption of the hydrophobic dye TG6[121,122] was not detected.

Interestingly, it was observed that, by reducing the irradiation intensity, the performance mismatch between aqueous and non-aqueous electrolytes decreased. As shown in Fig. 9, O'Regan and coworkers observed that the fraction of photocurrent lost at low P_{in} and the saturation photocurrent at higher P_{in} values were correlated, and an increase in performance variation between identical cells at high water content was present. This represented a key issue: if in Section 3 we reported that the presence of water affected the PV parameters, the stability over time and the visual appearance of DSSCs, now also the worsened reproducibility emerges. Such a scenario opened the debate in the scientific community, and the following arguments were proposed:

– A reduction in the dye excited-state lifetime occurred due to the increase in the dielectric constant when moving from organic solvents towards water.[123] However, even if losses at the injection step could be independent of P_{in}, they were not expected to strongly vary when identical cells were considered.

– Electrons could be lost by increased recombination with the oxidized dye molecules, due to the increase of E (see Table 1), which reduced both the driving force and the rate constant for dye regeneration. However, even if losses from this route are usually strongly dependent upon P_{in}, O'Regan and coworkers performed photovoltage transient experiments which demonstrated that the variation in the electron recombination lifetime was reduced by a factor of two over all the different water contents.

– The real explanation of the behaviour showed in Fig. 9 involved phase segregation inside the pores of TiO_2, due to non-homogeneity in the pore sizes as well as in the dye coverage. In fact, the concurrent presence of (i) pores having high I_2/TBP phases, (ii) high H_2O/I^- phases and (iii) empty pores resulted in a reduced redox couple diffusion throughout the photoanode. Since phase segregation was sensitive to the exact pore structure, the variation in performance within identical cells at high water content was explained.

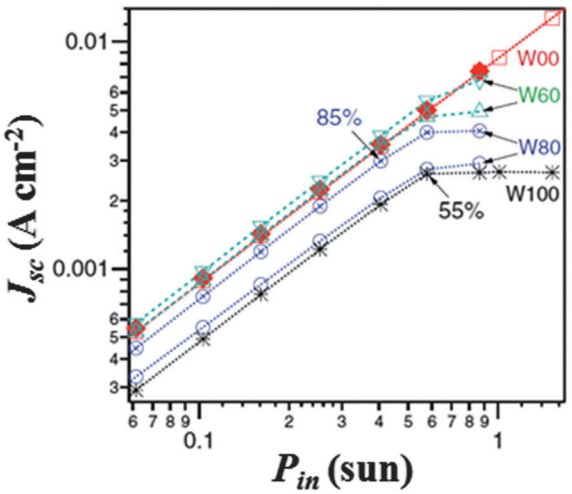

Fig. 9 J_{sc} *vs.* P_{in} for selected water-free and water-based DSSCs (see Table 1). Percentages are J_{sc} relative to the water-free cell at the same P_{in} value. Adapted and reprinted from ref. 120.

Following the insights proposed in the work by O'Regan's group, it is reasonable to assume that the above reported segregation phenomena occurring in water electrolytes should not occur when non-mesoporous films are considered. Nevertheless, to the best of our knowledge and the present literature reports, no scientific group has undertaken this research path so far.

Other literature reports showed as well that the presence of a specifically selected amount of water in the electrolyte can increase the PV conversion efficiency. Weng and coworkers observed that, by increasing the water concentration up to 2.2 M, V_{oc} and FF values increased monotonically, while J_{sc} showed a continuous decrease, as reported in Table 2.[124] Efficiency increased from 3.8% to 4.5% in the presence of a 1.7 M H_2O solution in a standard liquid electrolyte (LiI 0.50 M and I_2 50 mM in MPN/H_2O). The authors made the following hypotheses regarding the reasons for the V_{oc} improvement: an increased electron injection efficiency, a decreased electron density and a retardation of decay rate. Time-resolved infrared absorption spectroscopy, a useful technique to directly detect the CB as well as the trapped electrons,[125–127] showed that – in the presence of water – the optical phonon scattering, which indicates surface trapped states, was observed. It revealed that hydroxide group interaction with TiO_2 gave rise to an increase in the surface-trap states.[114] The interfacial back electron transfer process was retarded in an aqueous environment, and the electron injection efficiency increased up to 1.7 M of water.

Mixtures of water and organic solvents have been recently investigated by Frank and coworkers.[128] Regardless the water content, Table 3 shows that V_{oc}, FF and η values were higher for the ACN:VAN-based DSSCs than for the MPN-based counterparts,

Table 1 E values for aqueous electrolytes and PV parameters (P_{in} = 1 sun) of the corresponding DSSCs. Electrolytes: PMII 2.0 M, I_2 50 mM, GuSCN 0.1 M and TBP 0.5 M in H_2O/MPN. Dye: TG6. Adapted and reprinted from ref. 120

H_2O (vol%)	E (V)	J_{sc} (mA cm^{-2})	V_{oc} (V)	FF	η (%)
0	0.058	11.3	0.73	0.67	5.5
20	0.077	11.8	0.73	0.67	5.7
40	0.103	11.1	0.73	0.68	5.5
60	0.117	8.9	0.75	0.67	4.5
80	0.129	6.5	0.75	0.68	3.3
100	0.136	4.7	0.74	0.69	2.4

Table 2 PV parameters (P_{in} = 1 sun) of DSSCs assembled with electrolytes prepared at various concentrations of water. Electrolytes: LiI 0.50 M and I_2 50 mM in MPN/H_2O. Dye: N3. Adapted and reprinted from ref. 124

H_2O (M)	J_{sc} (mA cm^{-2})	V_{oc} (V)	FF	η (%)
0	16.5	0.47	0.49	3.8
0.6	15.8	0.49	0.53	4.1
1.2	15.1	0.52	0.55	4.3
1.7	14.1	0.54	0.59	4.5
2.2	12.1	0.55	0.62	4.1

Table 3 PV parameters (P_{in} = 1 sun) of DSSCs assembled with electrolytes containing different amounts of water and organic solvents. Electrolyte: PMII 1.0 M, I_2 0.15 M, GuSCN 0.10 M and NBBI 0.50 M. Dye: Z907. Adapted and reprinted from ref. 128

Organic solvent	H_2O (vol%)	J_{sc} (mA cm^{-2})	V_{oc} (V)	FF	η (%)
MPN	0	15.77	0.647	0.658	6.72
MPN	10	16.15	0.662	0.643	6.87
ACN:VAN	0	14.63	0.661	0.725	7.01
ACN:VAN	10	15.67	0.680	0.706	7.52

while J_{sc} followed the opposite trend. As regards water addition in the liquid electrolyte (PMII 1.0 M, I_2 0.15 M, GuSCN 0.10 M and NBBI 0.50 M; NBBI = *N*-butylbenzimidazole), it enhanced both J_{sc} and V_{oc} for any of the organic solvents used, but lowered FF values. Such a behaviour was quite different with respect to what reported by Weng and coworkers,[124] who used N3 dye instead of Z907. Further investigation was carried out by means of electrochemical impedance spectroscopy (EIS) under bias light at 680 nm. It showed that the addition of water decreased the difference in the potential values between E_c and E of about 28 mV: this resulted from a downward shift of 10 mV for E toward positive electrode potentials, along with a 38 mV downward shift of the TiO_2 CB. All of these changes in the potential values of the different energy levels were attributed to an increased proton concentration at the photoanode surface.[129,130] By combining transport and recombination measurements, it was evidenced that the addition of water increased the charge-collection efficiency.[131,132] This effect, together with the higher charge-injection efficiency derived from the downshift of the TiO_2 CB upon water addition,[133] led to improved J_{sc} values. Frank and coworkers also expected a reduced V_{oc} due to the lower gap in the potential between E_c and E; however, the addition of water increased the photovoltage of about 15–19 mV (Table 3). Such a behaviour was justified by considering the decreased recombination in aqueous cells by a factor of 4–5.[86,134] As regards the decreased FF values, an increase in the dark exchange current was detected, which was attributed to a larger dark electron concentration in the presence of water.[84] Outstandingly, the *J*–*V* characteristics of the DSSCs assembled using electrolytes prepared both with and without the addition of water showed essentially the same aging behaviours upon 1000 h of continuous light soaking. This represents a key issue, quite in contrast with what reported in Section 3: does the presence of water have an influence on the cell stability or not? Dye nature, electrolyte composition or dye-electrolyte combination: what the preponderant factor is? From Frank and coworkers study, it seems that the adoption of a thermally stable electrolyte solvent (MPN/H_2O) and a hydrophobic dye (Z907) can lead to equally stable water-free and water-based DSSCs.

Table 4 PV parameters (P_{in} = 1 sun) of DSSCs assembled with electrolytes based on water and/or ethanol–water mixtures recovered from industrial effluents. Electrolyte: KI 0.50 M and I_2 25 mM. Adapted and reprinted from ref. 138

Solvent	Dye	J_{sc} (mA cm^{-2})	V_{oc} (V)	FF	η (%)
H_2O	N3	2.70	0.37	0.60	0.6
H_2O	N719	2.00	0.40	0.63	0.5
H_2O : EtOH 65 : 35	N3	4.68	0.47	0.59	1.3
H_2O : EtOH 65 : 35	N719	4.04	0.48	0.57	1.1

The remarkable advantage in terms of safety as well as eco-compatibility of replacing organic solvents by water has been already detailed in the introductory section. However, it should be also considered that some industrial processes (*i.e.*, biotechnology and food industry) produce water–ethanol mixtures as effluents, the separation of which is not economically advantageous. The recovery of these wastewaters surged as a hot research topic only recently,[135–137] after the pioneering work of Miyasaka and coworkers, who proposed their reuse in aqueous DSSCs.[138] Table 4 shows the enhancement of J_{sc} values when using EtOH–H_2O solutions, which was attributed to the activation of the mesoporous TiO_2/electrolyte (KI 0.50 M and I_2 25 mM) interface. Pristine photoanodes were found not to be hydrophilic enough to absorb water into their interior pores, thus the addition of alcohols improved their wettability because of the higher affinity with the surface functionalities present at the inner surface of the mesopores. Moreover, the addition of ethanol reduced both the surface tension and the viscosity of the aqueous electrolyte, thus increasing the effective area of the electrochemically active TiO_2–electrolyte interface with respect to the pure aqueous system, in which a hydrogen-bonded large cluster of water molecules could not effectively penetrate the whole mesoporous structure. As a result, efficiency values were doubled.

The brief analysis of the recent scientific reports has evidenced a real turnaround in the DSSC research community: water is no longer intended to be a poisoner to be utterly avoided, in fact it started to be gradually introduced in progressively larger amounts. This novel trend is accompanied by electrochemical and spectroscopic investigation of the new phenomena and new interfaces, to guarantee the useful insights towards the improvement of the device characteristics. As will be explained in the following sections, each cell component is currently the subject of thorough investigation from the physical as well as engineering viewpoint in order to ensure its highest possible efficiency in an aqueous environment.

6. Additives for aqueous electrolytes

Nowadays, it is widely known that the introduction of specifically selected additives in the electrolyte may guarantee remarkable improvements in the PV performance of a DSSC.[139–141] Indeed, for the same dye, while J_{sc} is closely related to the type

and concentration of the redox mediator under use, V_{oc} can be ameliorated by introducing nitrogen-containing heterocyclic compounds, such as pyridines, aminotriazole, pyrimidine, aminothiazole, pyrazole and quinoline. Above all, in 1993 Grätzel and coworkers introduced TBP.[81] Being adsorbed onto the surface of the TiO_2 photoelectrode, it prevented the leakage of the injected electrons in the electrolyte and also prevented I_3^- from contacting the surface of the photoanode. As reported in the course of this review, TBP has been already introduced in some aqueous electrolytes; however, it showed rather low solubility in water. Thus, alternative additives have been proposed for aqueous DSSCs (in this section) or their solubilisation has been achieved through the introduction of surfactants (see Section 7).

N-Alkylbenzimidazole derivatives represent another category of organic additives which were found to behave similarly to TBP. Indeed, *N*-methylbenzimidazole (NMBI) is often added in liquid electrolytes both for TiO_2-[142] and ZnO-sensitized DSSCs.[143,144] Yang and coworkers proposed several bis-benzimidazole derivatives containing an ethylene glycol repeating unit (BBEG$_n$, see Fig. 10) for aqueous DSSCs (DMPII 0.50 M, LiI 0.10 M, I_2 50 mM and TBP/BBEG$_n$ 0.50 M in ACN/H_2O; DMPII = 1,2-dimethyl-3-propylimidazolium iodide) and evaluated the cell durability.[145] As listed in Table 5, V_{oc} and FF values were found to be higher in all the water-based cells. This was ascribed to the strong adsorption of water onto the TiO_2 surface, which blocked the reaction between I_3^- ions and injected electrons; moreover, as previously stated by O'Regan's group,[120] the electrochemical potential of the iodine-based redox mediator in water-based cells was positively shifted. As a drawback, the addition of water led to the detachment of the adsorbed N719 dye molecules, thus limiting the flux of the injected electrons from the excited states of the dye which adversely influenced J_{sc} values.

As shown in Table 5, the novel BBEG$_n$ additives proposed by Yang and coworkers did not guarantee improved performances if compared to TBP. Nevertheless, the resulting devices demonstrated enhanced stability upon the aging test, while TBP-based cell efficiency dropped significantly (62% in 135 h). Indeed, the chemical structure of BBEG$_n$ additives incorporated ethylene glycol linkages between two benzimidazoles, which produced H-bond bonding sites for the water molecules. In this way, ethylene glycol linkages sequestered the water molecules, thus preventing their interaction with the TiO_2-dye linkage as well as the dye –SCN functional group. Moreover, the BBEG$_n$/H_2O phase solvated I_3^- ions, thus decreasing their concentration in the dyed TiO_2 surface and avoiding back electron transfer phenomena. Summarising, by the proper use of specifically selected and optimised additives, aqueous DSSCs may become as much stable as (or eventually even more stable than) their standard aprotic counterparts. In this respect, the search for new additives for water-based liquid electrolytes is currently under intensive investigation in many research laboratories.

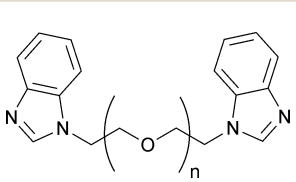

Fig. 10 Chemical structure of benzimidazole-based additives (BBEG$_n$) used in aqueous DSSCs, ref. 145.

Table 5 PV parameters (P_{in} = 1 sun) of DSSCs assembled with electrolytes based on pure ACN or ACN–H_2O mixtures. Electrolytes: DMPII 0.50 M, LiI 0.10 M, I_2 50 mM and TBP/BBEG$_n$ 0.50 M. Dye: N719. Adapted and reprinted from ref. 145

Additive	H_2O (vol%)	J_{sc} (mA cm^{-2})	V_{oc} (V)	FF	η (%)
TBP	0	14.99	0.73	0.65	7.14
TBP	10	5.05	0.80	0.70	2.82
BBEG$_n$, n = 1	0	11.31	0.78	0.60	5.27
BBEG$_n$, n = 1	10	4.19	0.80	0.69	2.31
BBEG$_n$, n = 3	0	13.04	0.78	0.62	6.29
BBEG$_n$, n = 3	10	5.75	0.80	0.64	2.96

7. Surfactants: key ingredients for aqueous DSSCs

An electrolyte of a DSSC is a fairly complex chemical system: the solvent should be able to solubilise both inorganic salts and non-polar species (*i.e.*, iodine and additives such as TBP and NMBI). When the aqueous electrolyte contains a mixture of water and organic solvents, homogeneity and stability of all the components in solution are fairly easy to be obtained (once optimized their concentrations), as described so far. On the other hand, if a fully aqueous DSSC has to be fabricated, a way to solubilise all of the aforementioned electrolyte components has to be found. This is a particularly complex work, which requires the modification or the functionalization of the traditionally used chemical compounds, or the introduction of a new class of additives: surfactants. The ability of surfactants in lowering the surface (or interfacial) tension between two liquids or between a liquid and a solid is well-established;[146] their application as detergents, wetting agents, emulsifiers, foaming agents and dispersants are vitally important in our daily life.[147,148] The scientific community considers surfactants as key ingredients for drug delivery systems[149] as well as environmental decontamination and rehabilitation procedures.[150] Several applications are also envisaged in the field of energy conversion and storage[151] due to the unique properties of surfactants particularly in the synthesis and functionalization of porous anodic[152,153] and cathodic[154,155] nanostructures.

For what concerns aqueous DSSCs, surfactants have initially been used to segregate water molecules within the micellar phase, thus promoting its solubility in the organic liquid electrolyte. The use of Triton X-100, $C_{14}H_{22}O(C_2H_4O)_n$, a non-ionic surfactant having a hydrophilic polyethylene oxide chain and an aromatic hydrocarbon lipophilic or hydrophobic group, was proposed by Kim and coworkers.[156] They introduced Triton X-100 in the 20 mM concentration into an aqueous liquid electrolyte (LiI 0.10 M, HDMII 0.60 M, I_2 50 mM and TBP 0.50 M in MPN/H_2O, HDMII = 1-hexyl-2,3-dimethylimidazolium iodide), and observed increased V_{oc} and FF values while increasing the amount of water (0.0–4.4 M); conversely, J_{sc}

monotonically decreased. A peak efficiency value of 5.9% when $[H_2O]$ = 2.2 M was obtained (Table 6).

Three hypotheses may be elaborated to justify the increased V_{oc} values observed in surfactant-laden liquid electrolytes:

– The reduction in the back electron transfer from the TiO_2 CB to the I_3^- ions in the electrolyte: in fact, I_3^- ions have higher solubility in the hydrophilic Triton X-100/H_2O phase than at the interface with the photoanode.

– The negative shift of the flat band potential of TiO_2: some of the protons transferred by the sensitizer (which contains –COOH groups) to the TiO_2 surface are removed by the hydrophilic Triton X-100/H_2O phase, thus leading to a shift of the flat band potential which becomes less positive than that occurring in the absence of the surfactant-added aqueous phase.[157,158]

– The positive shift of E.

J_{sc} decreased because of the reduced number of injected electrons, due to the improved V_{oc} caused by the increase of the barrier height for their injection.[159] Interestingly, the trend observed for the photocurrent differed from that expected by Kim and coworkers by means of chronoamperometry and EIS measurements. Indeed, an increase of the limiting current for the oxidation of I^- was detected. This accounted for the enhancement in the diffusion of I^- ions in the presence of Triton X-100 and water, as also indicated by the decrease in the series (R_s) as well as charge transfer resistance at the counter electrode (R_{CE}) measured for aqueous DSSCs (Table 6). Along with the observed decrease in viscosity, this should have resulted in improved J_{sc} and FF values.

The long-term stability of Triton X-100-added DSSCs was surprisingly high (−19% after 7 days under dark), even higher than the corresponding aprotic cell (−67%), thanks to the increased stability of J_{sc}. In fact, Triton X-100 was able to strongly retain the molecules of solvent, thus suppressing their evaporation; its aqueous phase could even extract the water traces which were inevitably introduced during cell fabrication.[160] The harmful effects caused by the presence of water during irradiation (*i.e.*, hydrogen evolution and photocatalytic processes) were avoided, thus demonstrating that a surfactant-added aqueous DSSC can perform better than a standard cell. However, for the sake of the reader we must point out that the cells of this article were not sealed with a rigorous procedure; indeed, a 67% efficiency decrease in a week only is not a data comparable with the state of the art of sealed liquid DSSCs.[161,162]

Data reported in Section 5 show that the performance of 100% water-based DSSCs is still low compared with those of traditional DSSCs, and one of the reasons is surely the incomplete wetting of the dye-coated TiO_2 interface by the aqueous electrolyte. In this context, it is well known that the addition of a surfactant increases the wettability and minimizes the separation between materials in two different phases. Yan and coworkers investigated a series of surfactants in organic solvent-free DSSCs (NaI 2.0 M, I_2 0.20 M and GuSCN 0.10 M): hexadecyltrimethylammonium bromide (CTAB), *N*,*N*,*N*-trimethyl-3-(perfluorooctyl sulfonamido)-propan-1-aminium iodide (FC-134), bis(2-ethylhexyl) sulfosuccinate sodium salt (AOT) and triethylammonium perfluorooctane sulphonate (FK-1).[163] As can be seen in Table 7, both anionic (AOT, FK-1) and cationic (CTAB, FC-134) surfactants dramatically improved the PV performances of N719-sensitized DSSCs. At the same time, higher charge-transfer resistance values were measured at the TiO_2/electrolyte interface, and the resulting reduced charge recombination and increased electron lifetime were attributed to the enhanced interfacial compatibility due to the addition of the surfactants.[164,165] On the other hand, Mott–Schottky experiments and capacitance measurements suggested that the surfactant addition did not shift the TiO_2 CB edge, thus contradicting what previously reported by Kim and coworkers.[156] In the presence of surfactant-added aqueous electrolytes, photoanodes showed reduced contact angle (CA) values compared to the corresponding surfactant-free ones (Fig. 11), thus further demonstrating the improved wettability of the photoanode/electrolyte interface.[166,167]

Sunlight-to-electricity conversion of surfactant-added DSSCs was improved under low P_{in}; as an example, the efficiency of the FC-134 (0.2 wt%)-laden cell increased from 3.96 to 4.66% when P_{in} decreased from 1.0 to 0.5 sun. The lower efficiency yielded under full sunlight irradiation intensity, maybe due to the inefficient charge screening of the electron transport in the mesoporous TiO_2,[168,169] paved the way to the use of aqueous cells in a relatively dark environment, where DSSCs are increasingly establishing themselves as the leading device.[170,171] As regards the long-term stability, the surfactant-free cell provided only 17% of the initial efficiency after 50 days under constant 1.0 sun illumination (at room temperature, RT, with UV-filter), where the CTAB-laden one was able to retain the 48%. Such an improvement was assigned to the surfactant molecules adsorbed at the surface of the photoanode. The resulting coating layer prevented I_3^- ions from contacting the dye-coated TiO_2 active material particles, reduced the recombination rate and avoided the sensitizer degradation by enhancing the dye-regeneration rate.

Table 6 PV (P_{in} = 1 sun) and electrochemical parameters of DSSCs assembled with electrolytes containing different amounts of water. Electrolytes: LiI 0.10 M, HDMII 0.60 M, I_2 50 mM, TBP 0.50 M in MPN/H_2O. Dye: N719. Adapted and reprinted from ref. 156

H_2O (M)	J_{sc} (mA cm^{-2})	V_{oc} (V)	FF	η (%)	R_s (Ω)	R_{CE} (Ω cm^{-2})
0.0	13.44	0.74	0.53	5.3	20.97	2.74
1.1	12.10	0.79	0.57	5.4	20.90	2.18
2.2	11.77	0.81	0.62	5.9	20.79	2.12
3.3	11.65	0.82	0.59	5.7	20.83	1.64
4.4	10.38	0.81	0.61	5.1	20.74	1.36

Table 7 PV parameters (P_{in} = 1 sun) of DSSCs assembled with electrolytes encompassing different kinds of surfactants. Electrolyte: NaI 2.0 M, I_2 0.20 M and GuSCN 0.10 M in H_2O. Dye: N719. Adapted and reprinted from ref. 163

Surfactant	J_{sc} (mA cm^{-2})	V_{oc} (V)	FF	η (%)
None	7.50	0.51	0.66	2.51
CTAB (0.1 wt%)	8.94	0.51	0.69	3.14
AOT (0.1 wt%)	8.44	0.50	0.71	2.98
FK-1 (0.1 wt%)	9.99	0.51	0.69	3.55
FC-134 (0.1 wt%)	9.69	0.51	0.70	3.56
FC-134 (0.2 wt%)	10.97	0.53	0.68	3.96

Fig. 11 CA measurements of different aqueous electrolytes at the surface of dye-coated TiO_2 films. Adapted and reprinted from ref. 163.

Due to its positive effect, AOT was recently employed by Jang and coworkers with the aim of controlling both the total and the local concentration of the redox couple (BMII 0.70 M, I_2 30 mM, GuSCN 0.10 M and TBP 0.50 M in ACN/VAN; BMII = 1-butyl-3-methylimidazolium iodide).[172] By means of its $-SO_3^-$ group,[173] AOT can be chemisorbed onto the TiO_2 nanoparticles, thus hindering the access of I_3^- anions and facilitating the access of I^- ones to enhance the dye regeneration rate. Upon concurrent addition of water, the absorbance of I_3^- at 363 nm decreased due to the triiodide hydrolysis reaction: one of the resulting products was I^-, which further assisted the dye regeneration efficiency (from 71% to 78%). Table 8 shows that such a combined effect of water and AOT led to the improvement in both J_{sc} and V_{oc} values; the R_{CE} was improved as well, thus demonstrating that the triiodide reduction reaction at the counter electrode/electrolyte interface occurred much more efficiently in the AOT/water-laden devices. At present, the 10.8% efficiency value obtained by Jang and coworkers (see the insight outlined in Fig. 12) is the highest value ever measured for a DSSC containing water. However, we cannot call it "aqueous DSSC", as the amount of water added to the electrolyte was minimal (10 mM).

Table 8 PV parameters (P_{in} = 1 sun) of DSSCs assembled with electrolytes laden with water and/or AOT. Electrolyte: BMII 0.70 M, I_2 30 mM, GuSCN 0.10 M, TBP 0.50 M in ACN/VAN. Dye: N719. Adapted and reprinted from ref. 172

Additives	J_{sc} (mA cm^{-2})	V_{oc} (V)	FF	η (%)	R_{CE} (Ω)
None	15.3	0.832	0.73	9.3	6.93
AOT (1.0 mM)	16.5	0.829	0.74	10.1	4.93
H_2O (10 mM)	16.9	0.850	0.71	10.2	6.89
AOT + H_2O	17.5	0.850	0.73	10.8	4.83

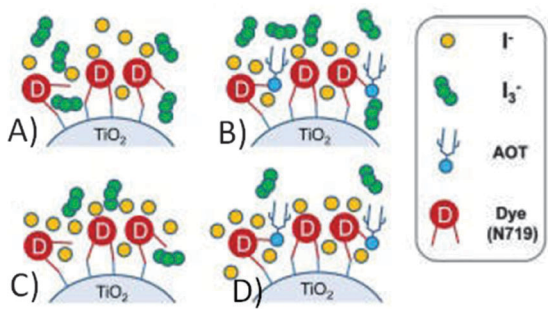

Fig. 12 Local concentration control of the I_3^-/I^- redox couple by the hydrogen bonding interaction between the AOT and the carboxyl group of the N719 dye. (A) AOT- and water-free system; (B) in the presence of AOT, I_3^- is hindered from approaching the TiO_2/dye surface; (C) accelerated hydrolysis of I_3^- by water; (D) AOT and water are simultaneously added to reduce the recombination rate and to enhance the dye regeneration yield. Adapted and reprinted from ref. 172.

8. Exploiting water to introduce new redox couples

As stated in Section 2, several redox mediators have been proposed during the past decades;[50] among others, the iodide/triiodide couple[51] and cobalt complexes[29] have proven to be the most stable and the best performing, respectively. Nevertheless, due to their ability in solubilising compounds which are insoluble in conventional aprotic organic solvents, the use of water as a solvent opened up new possibilities in the preparation and selection of the redox mediator.

The first exotic redox couple for aqueous DSSCs was a cerium-based compound. It was proposed by Teoh and coworkers in 2008.[174] $Ce(NO_3)_3$ 0.10 M and $Ce(NO_3)_4$ 50 mM were dissolved in a 35 : 65 EtOH : H_2O mixture. This electrolyte was coupled with a variety of commercial and natural sensitizers, such as crystal violet, mercurochrome, chlorophyll, extracts of *Bongainvillea brasiliensis*, *Garcinia suubelliptica*, *Ficus Reusa* and *Rhoeo spathacea*. Indeed, due to their simple preparation techniques, wide availability and low cost, natural dyes could be the best option for an aqueous, thus truly eco-friendly solar energy conversion device. As a further insight, Teoh and coworkers used their electrolyte with a 38 nm-thick Schottky barrier[175] composed of Au NPs deposited onto the photoanode, in order to improve the efficiency of the electron injection.[176,177] As a result, electrons in the LUMO of the dye passed through the Au thin layer by tunnelling the TiO_2 CB, thus avoiding the electron recombination reaction. J_{sc} and V_{oc} values measured in the presence of commercial dyes were found to be lower than those of natural dyes; the highest efficiency (η = 1.49%, J_{sc} = 10.9 mA cm^{-2}, V_{oc} = 0.496 V, FF = 0.27) was obtained in the presence of *Rhoeo spathacea* (RhS).

A cerium-based aqueous electrolyte (30 : 70 in EtOH : H_2O) was also coupled with natural pigments, such as the green and the red parts of *Codiaeum varie* and *Aglaonema*. Moreover, with the aim of improving the photovoltage, Su and coworkers[178] coupled this system with a ZrO_2 photoanode characterised by a wide band gap energy (5.8 eV) and a CB higher than that of TiO_2.[179,180] When the green part of *Codiaeum varie* (CV-G) was used, a V_{oc} of 0.624 V was achieved, definitely higher than those usually measured for natural pigment-sensitized TiO_2-based DSSCs.[181] Furthermore, the effective dielectric constant and refractive index of the ZrO_2 layer were experimentally tuned, and the light transmission of the photoanode was improved, resulting in a cell efficiency of 0.69% (J_{sc} = 0.52 mA cm^{-2}, FF = 0.53).

Working in aqueous media allows the application of redox couples such as $Fe(CN)_6^{4-/3-}$, which can overcome iodate formation, light absorption and corrosiveness typical of standard iodine-based mediators. In 2012, Spiccia and coworkers introduced the ferrocyanide/ferricyanide redox couple in a truly water-based electrolyte: 0.40 M $K_4Fe(CN)_6$, 40 mM $K_3Fe(CN)_6$, 0.10 M KCl and 0.1 vol% Tween 20, dissolved in H_2O at pH 8.[182] The redox

Table 9 PV parameters (P_{in} = 1 sun) of DSSCs assembled with $Fe(CN)_6^{4-/3-}$- and I^-/I_3^--based electrolytes, in the presence of different solvents. Dye: MK-2. Adapted and reprinted from ref. 182

Redox couple	Solvent	J_{sc} (mA cm^{-2})	V_{oc} (V)	FF	η (%)
$Fe(CN)_6^{4-/3-}$	H_2O	7.21	0.761	0.75	4.10
I^-/I_3^-	ACN	11.86	0.769	0.66	6.05

potentials of $Fe(CN)_6^{4-/3-}$ and I^-/I_3^- being similar,[183] a typical hydrophobic carbazole dye (MK-2) was used; besides showing an high molar extinction coefficients,[184] it allowed the use of relatively thin TiO_2 films, thus resulting in reduced interfacial area for recombination as well as improved charge extraction. Moreover, it showed only faint signs of desorption when stored under water for 30 days (conversely, the complete desorption of Z907 dye was observed in the same conditions). $Fe(CN)_6^{4-/3-}$-based DSSC showed an efficiency equal to 4.1% (Table 9); J_{sc} was the only value which decreased with respect to the corresponding I^-/I_3^-/ACN-based cell (MPII 0.60 M, LiI 0.10 M, I_2 0.20 M and TBP 0.50 M; MPII = 1-methyl-3-propylimidazolium iodide). It was supposed that ferrocyanide, being able to sensitize TiO_2,[185] contributed as a co-sensitizer, but its performance was obviously lower than that of MK-2. By means of intensity modulated photovoltage and photocurrent spectroscopies, also combined with charge extraction analysis,[186] it was demonstrated that the $Fe(CN)_6^{4-/3-}$-based electrolyte guaranteed a three orders of magnitude faster rate of recombination if compared to the reference couple. Besides, no difference in V_{oc} values was observed, which was related to the negative CB shift of 150 mV induced by $Fe(CN)_6^{4-/3-}$. The only drawback of this new redox couple was the performance decay measured under unfiltered white light illumination, which was caused by the well-known photolysis and photocatalytic decomposition of the ferrocyanide/ferricyanide redox couple.[187,188] By introducing a 480 nm long-pass filter, no performance decay was observed. Anyway, modification of the TiO_2 surface or its replacement with an alternative wide band-gap semiconductor should be considered for the fabrication of cells stable under full solar irradiation; otherwise, also the replacement of the cyanide ligands with stronger binding units may be taken into account.

Experimental investigation showed that the poor solubility of I_2 in water is the major limiting factor affecting aqueous DSSC performance. Even if this drawback can be solved by adopting suitable surfactants (see Section 7), the challenge of finding non-corrosive redox couples, which may also guarantee weak light absorption in the visible light region, has encouraged researchers to test sulphur-based systems, such as thiolate/disulphide.[189–192] Despite most of these species demonstrating rather low water solubility, Sun and coworkers identified a water-soluble thiolate/disulphide redox couple. It consisted of 1-ethyl-3-methylimidazolium 4-methyl-1,2,4-triazole-3-thiolate (TT^-EMI^+) and 3,3′-dithiobis[4-methyl-(1,2,4)-triazole] (DTT) (Fig. 13,[193]). The resulting truly aqueous electrolyte (TT^-EMI^+ 0.20 M, DTT 0.20 M, TBP 0.50 M and Triton X-100 1 vol%) was coupled with a hydrophobic dye having a short methoxyl chain in the donor unit (D45, Table 14), which increased the probability of interaction with

Fig. 13 Structures of the TT^-EMI^+/DTT-based redox couple. Adapted and reprinted from ref. 193.

Table 10 PV parameters (P_{in} = 1 sun) of DSSCs assembled with TT^-EMI^+/DTT- and I^-/I_3^--based electrolytes, in the presence of different dyes and solvents. Adapted and reprinted from ref. 193

Redox couple	Solvent	Dye	J_{sc} (mA cm^{-2})	V_{oc} (V)	FF	η (%)
TT^-EMI^+/DTT	H_2O	D45	7.2	0.650	0.55	2.6
TT^-EMI^+/DTT	H_2O	D51	9.5	0.610	0.59	3.5
TT^-EMI^+/DTT	ACN:VAN	D45	3.5	0.570	0.53	1.1
I^-/I_3^-	ACN:VAN	D45	11.7	0.790	0.61	5.6

the redox system. An efficiency equal to 2.6% was recorded (Table 10). Replacing water with ACN did not modify E, but led to the desorption of the dye from the TiO_2 surface. When compared to a traditional I^-/I_3^--based system (DMHII 0.60 M, LiI 60 mM, I_2 40 mM and TBP 0.40 M in ACN/VAN; DMHII = 3-hexyl-1,2-dimethylimidazolium iodide), the aqueous electrolyte showed remarkably reduced diffusion coefficients, being $D(TT^-)$ and D(DTT) equal to 4.01×10^{-6} and 1.87×10^{-6} cm^2 s^{-1}, respectively, while $D(I^-)$ and $D(I_3^-)$ were equal to 1.70×10^{-5} and 1.10×10^{-5} cm^2 s^{-1}, respectively, thus almost one order of magnitude different. However, since PV measurements under different light intensities did not show any enhancement in the performance under weak light intensity, low electrolyte diffusion coefficients were not likely to be responsible for the low J_{sc} recorded; on the other hand, it was observed that D45 regeneration was slowed down by a factor of four in the presence of TT^-EMI^+/DTT. When D45 dye was replaced by D51 (Table 14), efficiency jumped up to 3.5% (Table 10), which was attributed to the higher extinction coefficient and broader absorption spectrum of the sensitizer. During the stability test, aqueous DSSCs were able to assure only 63% of their initial efficiency after 4 h of light soaking at RT. However, despite FF values decreasing due to the poor stability of DTT in solution, Sun and coworkers highlighted that the optimization of the electrolyte composition could be considered as an effective strategy to overcome stability issues in aqueous DSSCs.

As previously stated, the recent efficiency records of DSSCs have been obtained using cobalt complexes as redox mediators.[29,35] Being transition metal ion complexes, they are highly soluble in water which accounts for their suitable application in aqueous DSSCs. Indeed, Spiccia and coworkers easily dissolved 0.20 M of $[Co(bpy)_3]^{2+}$ and 40 mM of $[Co(bpy)_3]^{3+}$ in water, along with the addition of NMBI (0.70 M) as a V_{oc}-booster and various amounts of poly(ethylene glycol) (PEG 300) to minimize phase separation between the hydrophobic dye (MK-2) and the aqueous electrolyte.[194] A bell-shaped performance trend was observed as a function of the amount of PEG 300 added; the best energy conversion efficiency of 4.2% (J_{sc} = 8.3 mA cm^{-2}, V_{oc} = 0.685 V,

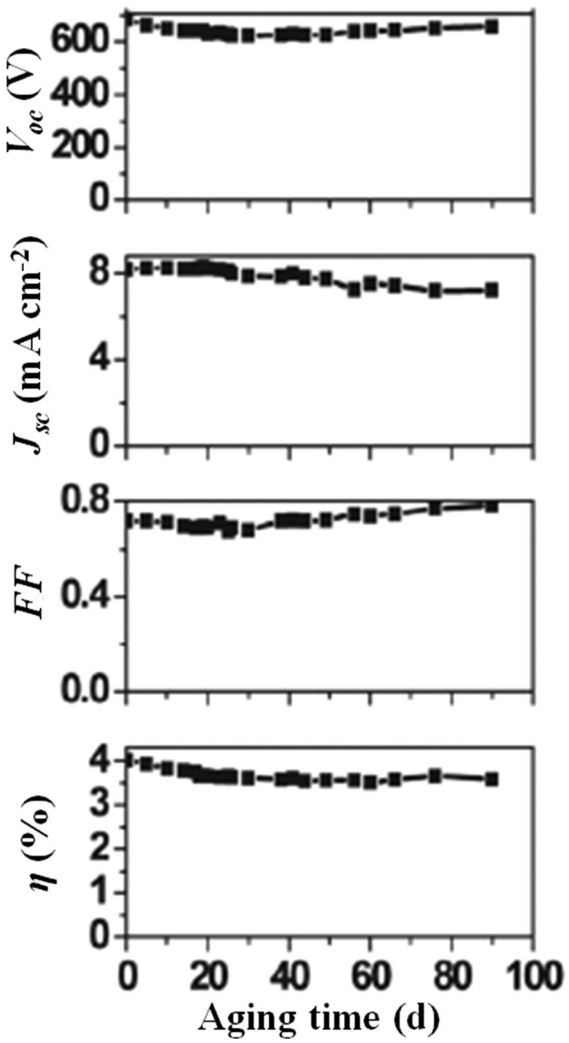

Fig. 14 Long-term stability under dark of a DSSC assembled with an aqueous electrolyte composed of $[Co(bpy)_3]^{2+}$ 0.20 M, $[Co(bpy)_3]^{3+}$ 40 mM, NMBI 0.70 M and PEG 300 1 vol%. Dye: MK-2. Adapted and reprinted from ref. 194.

FF = 0.72) was achieved upon addition of 1 wt% PEG 300. Noteworthy, such an additive was able to concurrently guarantee the highest possible electron recombination resistance and the lowest diffusion resistance of the redox species. The durability of cobalt-based electrolytes being a topic of great interest right now,[195] aqueous DSSCs were investigated for their stability under prolonged aging conditions by Spiccia and coworkers, demonstrating a limited 10% decrease of the initial efficiency after more than three months under dark (Fig. 14).

9. Photoanode activation: a way to improve the interfacial characteristics between electrodes and aqueous electrolytes

Nowadays, it is widely established that the interface between the photoanode and the aqueous electrolyte is a key point remarkably affecting the efficiency of water-based DSSCs. This is in fact an important issue even for standard DSSCs, where the surface modification of the photoanode is usually carried out by means of barrier layers,[196] N-doping,[197] hybrid organic–inorganic linkers,[198] nanodecorations[199] and physical techniques.[200] Furthermore, for the first time, the solid electrolyte interphase formation (SEI layer, well known and investigated in the field of Li-ion batteries,[201]) has been recently evidenced even in DSSCs, which implies a novel series of challenging research goals for the scientific community.[202]

A simple interfacial activation for aqueous DSSCs was proposed by Miyasaka and coworkers, by means of treating the mesoporous layer with gaseous active oxygen prior to dye adsorption.[203] In particular, the TiO_2 layer was concurrently etched by air rich in O_3 (300 ppm) and exposed to UV light for 60 min. Water CA values decreased from 71 to 22°, which highlighted the improved hydrophilicity of the electrode. An efficient permeation of the aqueous redox electrolyte (KI 0.50 M and I_2 25 mM in H_2O : EtOH 65 : 35) through the mesoporous electrode structure was achieved; both J_{sc} and V_{oc} increased, from 4.94 to 5.80 mA cm^{-2} and from 0.55 to 0.60 V, respectively. As a result, efficiency noticeably increased from 1.7% to 2.2%. Noteworthy, TBP (5 vol%), being insoluble in water, was introduced in the dye-uptake solution and not in the electrolyte. Authors hypothesized that TBP could be considered as a base and, when adsorbed onto the TiO_2 surface, could improve the rate of deprotonation of the carboxyl groups of the Ru complex to reinforce the bonding between dye and TiO_2, thus leading to improved electron injection efficiencies. In other words, TBP provided itself as a ligand for the Ru complex, forming a mixed ligand complex with tetrabutylammonium (TBA).

An alternative way to modify the photoanode could be the introduction of a Schottky barrier, which can increase the electron injection efficiency.[175] To this purpose, Lai and coworkers prepared Au NPs modified by tetraoctylammonium bromide, which were then anchored at the TiO_2 surface by means of (3-mercaptopropyl)trimethoxysilane.[204] A self-assembly monolayer process was performed and, by successively repeating the preparation steps, a layer-by-layer Au NPs coating was formed on the conducting substrate (Fig. 15). Being the I^-/I_3^- couple corrosive towards Au, a Fe^{2+}/Fe^{3+} redox mediator was used, despite its high sensitivity to hydrolysis in aqueous solutions due to the formation of iron aquo complexes with water. To possibly avoid such a drawback, mixtures of H_2O/EtOH in the 65 : 35 ratio were selected for the preparation of the electrolyte ($FeCl_2$ 0.10 M, $FeCl_3$ 50 mM and $LiNO_3$ 0.10 M).[205] In the presence of four Au NP layers, J_{sc} more than doubled (*i.e.*, from 2.76 to 5.96 mA cm^{-2}); FF increased as well (*i.e.*, from 0.23 to 0.35). However, the efficiency of the aqueous DSSC remained rather low (*i.e.*, 0.95% against 0.26% for the Au-free cell), maybe because of the redox mediator instability and/or the selection of the dye (merbromin, MB, hardly known for its high efficiency).

In liquid DSSCs, the diffusive nature of the ion flow throughout the electrolyte creates an upper limit to the current (diffusion limited current, J_{dl}) that can pass across the cell. It is controlled by the diffusion coefficient of the limiting species

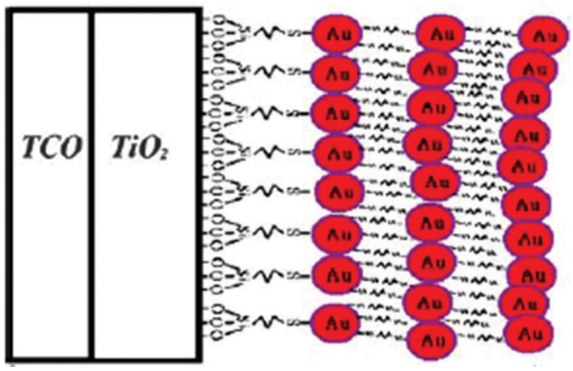

Fig. 15 Layer-by-layer Au NP assembly onto the TiO_2 electrode to act as a Schottky barrier in aqueous DSSCs. Adapted and reprinted from ref. 204.

(I_3^- ions), their concentration, the cell thickness as well as the thickness and morphology of the TiO_2 photoanode. While in organic solvent-based liquid electrolytes the J_{dl} values ($\sim$30 and $\sim$100 mA cm^{-2} in MPN and ACN, respectively) are larger than J_{sc} values, under incomplete wetting conditions the reduced cross sectional area through which ions can diffuse causes lower J_{dl} values. Since the latter situation may occur in aqueous DSSCs, O'Regan and coworkers proposed several strategies to improve the rather critical wettability of Z907-dyed TiO_2.[206,207] Among the different surfactants being investigated, chenodeoxycholic acid (CDCA) demonstrated the highest values of J_{sc} (3 fold increase) and J_{dl} (10 fold increase): this beneficial effect was attributed both to the hydrophobic centre portion of the molecule (compatible with Z907) and the hydrophilic –OH groups. Despite the improved wetting ability, the low J_{sc} value ($\sim$2 mA cm^{-2}) indicated that some limitation could be derived from injection and/or collection processes. Even if the main recombination pathway has recently been proposed to be the reduction of free iodine (rather than the triiodide),[208] it was noted that the binding coefficient (K_M) of I^- and I_2 was much weaker in water ($K_M = 10^3$) compared to what measured in organic solvents ($K_M = 4 \times 10^6$ in ACN).[209] Thus, the recombination in aqueous electrolytes should result much faster than in organic electrolytes, accompanied by a substantial decrease in the collection efficiency. To better unravel this phenomenon, I_2 concentration was reduced, resulting in increased J_{sc} (lower amount of free I_2 led to slower recombination) and decreased J_{dl} (I_3^- is the limiting species for the diffusion current in the electrolyte). Similar experiments were performed using the D149 dye observing an analogous trend. Only higher J_{dl} values were obtained, due to the chemisorption of D149 by means of a single –COOH group, which resulted in a higher CDCA surface concentration. In general, the I_2 concentration was maintained higher than 10 mM, as lower values gave unstable cells. Although the topic of dyes for aqueous cells will be comprehensively detailed in Section 10, it is appropriate to report here that this study was also carried out using an N719 sensitizer, stabilised by adding HNO_3 (pH 3) in water.

Another strategy to optimize the photoanode/electrolyte interfacial characteristics is the introduction of novel additives in the electrolyte. In this respect, O'Regan and coworkers observed a positive effect on both wetting and collection efficiency by means of guanidinium and iodide ions, respectively.[206] In particular, by using a high concentration of guanidinium iodide (GuI 8.0 M), a remarkable increase in the J_{sc} values (from 7.89 to 10.02 mA cm^{-2}) was obtained. On the other hand, V_{oc} remained unchanged, due to the balance of the following two opposite phenomena: the reduction of the recombination rate due to the decrease of free iodine amount and the lowering of the redox potential of the solution due to the increased iodide concentration. Efficiencies up to 4.06% were obtained (GuI 8.0 M and I_2 20 mM in H_2O; dye: D149/CDCA), but the long-term stability of GuI-based cells was lower than that of GuSCN/NaI-based ones, more likely because – as suggested by the authors – GuI could cause the desorption of CDCA from the surface, thus leading to the dewetting of the inner pore structure. Based on these considerations, the reader can certainly appreciate the charming and delicate balance at the base of the fabrication of an efficient DSSC.

A completely different approach for the photoanode activation has been very recently proposed in the article by Spiccia and coworkers,[210] who modified the surface properties of TiO_2 nanoparticles by means of octadecyltrichlorosilane (ODTS) in order to create an insulating layer able to reduce electron recombination by restricting the access of the cobalt redox couple at the titania surface. Condensation reaction occurred directly between Ti–OH groups and ODTS, and also by alkyl group intercalation between MK-2 dye molecules (Fig. 16A). This resulted in a strengthened insulating layer, thanks to the formation of Si–O–Si and Si–O–Ti crosslinkages induced by further condensation processes activated after the introduction of the fully aqueous electrolyte ($[Co(bpy)_3]^{2+}$ 0.20 M, $[Co(bpy)_3]^{3+}$ 40 mM, NMBI 0.70 M and PEG 300 1 wt%). As clearly visible in Table 11, the V_{oc} of ODTS-treated photoanodes increased with soaking time, while FF decreased due to mass transport limitations in the titania mesopores.[211] ODTS-treated cells showed improved J_{sc} values than ODTS-free ones, more likely because of a negative shift in the CB of the photoanode or a suppression of the interfacial electron recombination of the injected electrons with the oxidized cobalt species (Fig. 16B[128]). The first hypothesis was discarded due to the similar capacitance values provided by the different photoanodes. On the other hand, ODTS showed to be useful to improve both the electron recombination resistance and the electron lifetime by increasing soaking time values, due to a higher coverage of the exposed surface sites by the alkyl siloxane (Fig. 16C). Efficiencies up to 5.64% were obtained, which did not decrease even after 500 h of storage under dark. Moreover, molecular dynamics simulations were performed (Fig. 16D): for the untreated system, the distance d(Co-TiO_2) decreased significantly from 25 to 8 Å with the dynamic simulation time, while it remained almost constant for the ODTS-treated system. This confirmed that, for the ODTS-treated cells, the $[Co(bpy)_3]^{3+}$ ions did not come in contact with the titania surface, thus lowering the chance of recombination.

Until now, a semiconductor different from TiO_2 has not been employed in aqueous DSSCs. To this purpose, a good material to be explored could be zinc oxide (ZnO), whose

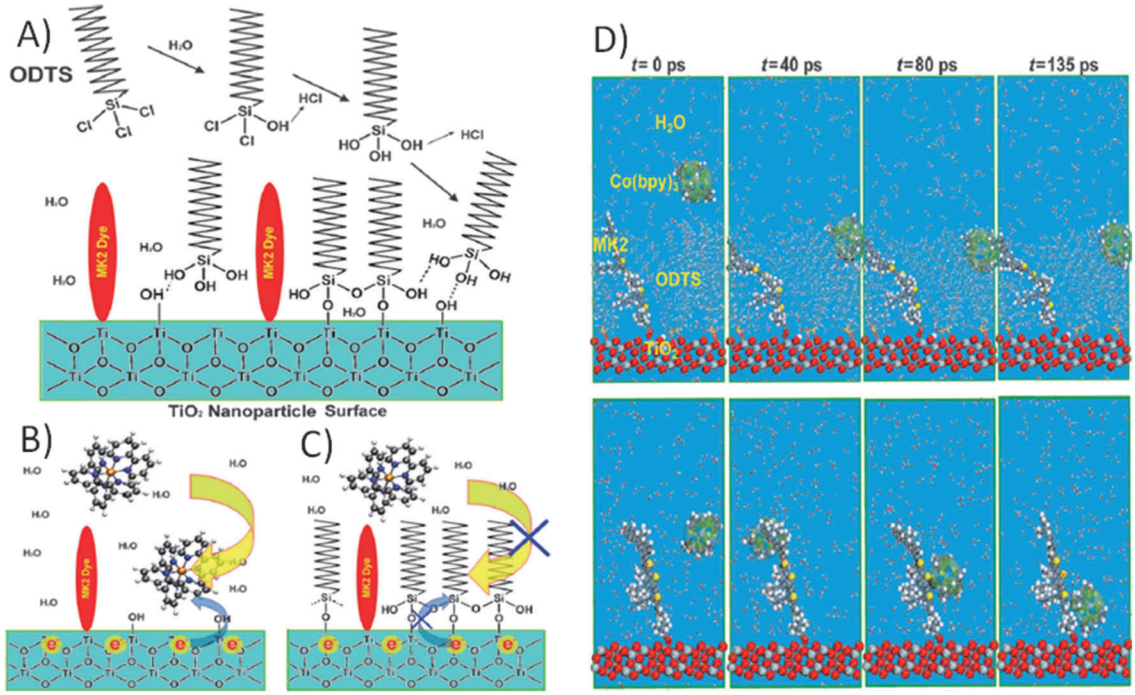

Fig. 16 (A) Proposed reaction process for alkyl siloxane anchoring to the dye-coated TiO_2 NPs treated with an ODTS solution; (B) electron recombination in non-ODTS treated aqueous DSSCs; (C) inhibition of electron recombination by aqueous DSSCs fabricated with ODTS treated photoanodes; (D) snapshot of the simulated systems of the ODTS-untreated and treated TiO_2 cluster as a function of the simulation time. In the ODTS-untreated system (bottom), the MK-2 molecule was attached at the TiO_2 cluster, whereas the ODTS-treated dyed TiO_2 photoanode (top) was obtained by attaching the crosslinked hydrolysed ODTS molecules at the vacant sites. Both systems were immersed in an explicit water environment. Adapted and reprinted from ref. 210.

Table 11 PV parameters (P_{in} = 1 sun) of fully aqueous DSSCs assembled with ODTS-free or ODTS-treated photoanodes. Electrolyte: $[Co(bpy)_3]^{2+}$ 0.20 M, $[Co(bpy)_3]^{3+}$ 40 mM, NMBI 0.70 M and PEG 300 1 wt%. Dye: MK-2. Adapted and reprinted from ref. 210

Treatment time (min)	J_{sc} (mA cm^{-2})	V_{oc} (V)	FF	η (%)
0	8.45	0.687	0.70	4.09
5	10.17	0.821	0.68	5.64
20	9.52	0.861	0.63	5.16

wettability and morphology can be highly tailored, as already demonstrated by research groups that usually employ this material in lithium batteries.[212–215]

10. Dyes and stability in water: still a long road to succeed

Representing the vital component of a DSSC, the sensitizer (or dye) has been extensively investigated in the last decades.[216–218] The main target of the scientific community efforts has been the discovery, elaboration and application of novel organometallic complexes,[219–221] the preparation of metal-free dyes,[222–224] the extension of the spectrum in the near IR regions[225–227] and the invention of new synthetic methodologies being green and readily up-scalable at the industrial level.[228–230] As regards aqueous DSSCs, the number of articles published until now that propose novel dyes *ad hoc* elaborated for the purpose has been very limited. This is rather surprising. As reported in the previous sections of this review, several research groups more likely used common organometallic and organic dyes (maybe focusing rather on hydrophobic ones) for the fabrication of aqueous cells, the main focus being the modification of electrolyte components and the functionalization of the photoanode surface.

Bearing in mind the long-term stability as an utmost important target for a dye in aqueous DSSCs, Grätzel and coworkers initially focused their efforts on the introduction of long apolar chains able to laterally interact with Ru-based complexes; by this way, an aliphatic network was intended to form which might avoid both the TiO_2-dye debonding and the approaching of triiodide to the photoanode surface.[231] A long-term stability test compared the performance of N3 and $[Ru(H_2dcbpy)(mhdbpy)(NCS)_2]$ dyes (where H_2dcbpy = 4,4′-dicarboxy-2,2′-bipyridine and mhdbpy = 4-methyl-4′-hexadecyl-2,2′-bipyridine) in the presence of increasing water contents in the electrolyte (I_2 10 mM in HMII/H_2O; HMII = 1-hexyl-3-methylimidazolium iodide). Data depicted in Fig. 17 show that, in the presence of electrolytes encompassing 5 and 10 vol% H_2O, respectively, the performance of N3-based cells was lower with respect to that of the devices assembled with the hydrophobic dye, these latter being stable, thanks to the presence of the aliphatic chains which assured complete insolubility in water.

Thanks to their broad absorption spectra and excellent light-harvesting ability, Ru complexes would represent the sensitizer of choice for aqueous DSSCs. Nevertheless, in order to obtain cells demonstrating sufficient durability, efforts must be devoted

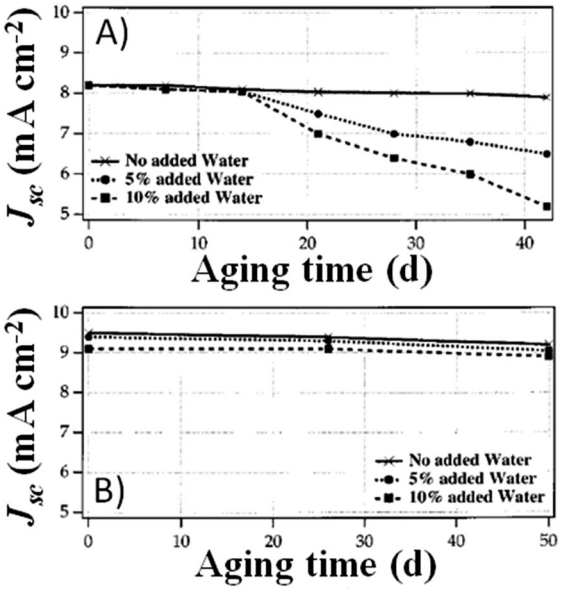

Fig. 17 Long-term stability (P_{in} = 0.015 mW cm^{-2}) of DSSCs assembled with RTIL-based electrolytes (I_2 10 mM in HMII) encompassing different H_2O contents. Dyes: (A) N3; (B) [Ru(H_2dcbpy)(mhdbpy)$(NCS)_2$]. Adapted and reprinted from ref. 231.

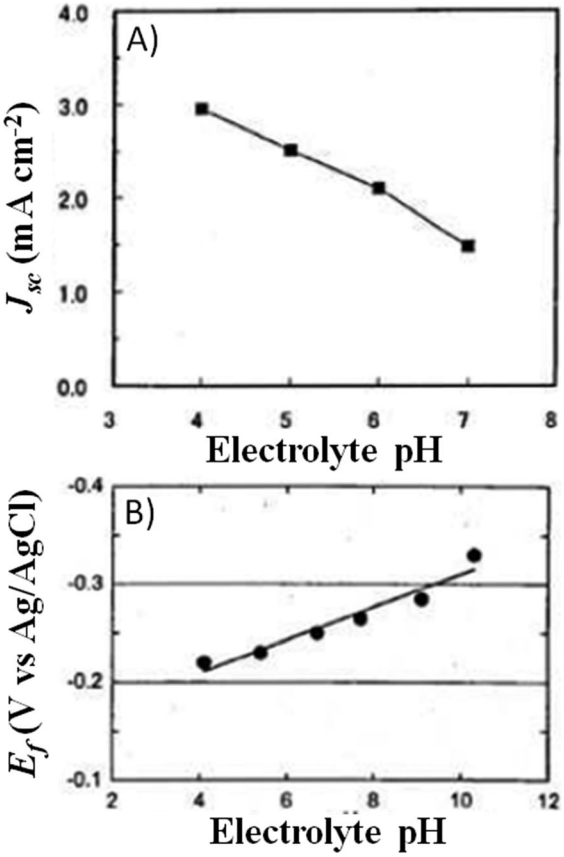

Fig. 18 (A) pH dependence of J_{sc} values (P_{in} = 1 sun) obtained for an aqueous DSSC sensitized with N719. Electrolyte: KI 0.50 M and I_2 25 mM; (B) dependence of the Fermi level electrochemical potential (E_f) of the mesoporous TiO_2 electrode on the pH of the above reported electrolyte. The potential data were based on the measurement of the onset potential of dark cathodic current. Adapted and reprinted from ref. 138.

to ameliorate the bonding between dye molecules and TiO_2 NPs.[232] Miyasaka and coworkers compared two photoanodes having equal amounts of N719 and N3 sensitizer molecules adsorbed onto the surface of the TiO_2 layer.[138] In the presence of a truly aqueous electrolyte (KI 0.50 M and I_2 25 mM), efficiencies of 0.6% and 0.5% were calculated when using N3 and N719 dyes, respectively. The cell assembled using the N719 dye showed lower J_{sc} (upon adsorption, TBA groups caused a negative Fermi level shift of the semiconductor[233]) and higher V_{oc} values (TBA is a base capable of negatively shifting the Fermi level as well as the TiO_2 CB) compared to the one using N3. The differences in J_{sc} were also ascribed to the adsorption strength of the dyes at the TiO_2/aqueous electrolyte interface; in fact, being more hydrophilic than N3, N719 has a higher solubility in water (3.5×10^{-3} *vs.* 1.2×10^{-3} M). The four –COOH groups of the N3 dye molecule ensure a more efficient electronic interaction at the oxide interface which, as a result, guarantees a much more stronger adsorption at the interface with the active material particles, thus improved stability under water. Moreover, the performances of all the aqueous DSSCs were found to be pH-dependent (Fig. 18A), particularly in terms of J_{sc} values which were negatively affected when a high pH (adjusted by addition of phosphate buffer solutions) was adopted; in contrast, V_{oc} was not affected. The J_{sc} decrease reflected a positive shift of the CB potential of TiO_2, as reported in Fig. 18B. However, the detachment of the dye from the electrode could also be promoted by the experimented high pH values as well.

The behaviour upon aging of Ru-based aqueous DSSCs was investigated by Miyasaka and coworkers, who observed a 50% progressive decrease of the photocurrent after 2.5 months (under dark, RT).[138] Reference cells containing organic solvent-based electrolytes showed reduced lifetime, because of solvent evaporation. After several weeks the bleaching of iodine was detected in aqueous DSSCs. Anyway, a significant intrinsic surplus value of DSSCs is that electrolyte can be fully replaced to restore cell performance, as it was confirmed in the article by Miyasaka and coworkers where the cell efficiency was recovered by replacing the degraded aqueous electrolyte with a freshly prepared one. Of course, the procedure of electrolyte replacement is much more easy and safe when an aqueous system is envisaged than an organic volatile one that carries around severe environmental hazards.

Further surface characterization of N3-, N719- and Z907-dyed electrodes was performed by Hahlin and coworkers by means of photoelectron spectroscopy (PES),[234] a useful technique to get specific information on the electronic as well as the molecular surface structures of the photoanode.[235–237] The dye-sensitized samples were exposed to a mixed H_2O/EtOH solution in the 30 : 70 ratio for 20 min, and then assembled in organic solvent-based DSSCs (TBAI 0.60 M, LiI 0.10 M, I_2 50 mM, GuSCN 50 mM and TBP 0.50 M in ACN; TBAI = tetrabutylammonium iodide). Water exposure led to a decrease in J_{sc} exceeding 20% for the N3- and N719-based systems, while V_{oc} decreased only for the N719-based cell; Z907-sensitized electrodes did not show any appreciable variation. Additionally, a

20 nm shift of the IPCE maximum was observed for both cells, thus clearly indicating modification in the electronic structure of the adsorbed molecules. Changes in the amount of surface adsorbed N3, N719, and Z907 dyes were finely detected by measuring the photoemission intensity from the core level Ru-$3d_{5/2}$ relative to the Ti-$2p_{3/2}$: only in the case of N3 and N719 dyes, the Ru/Ti ratio decreased by about 80% and 50%, respectively. As regards the hydrophobic Z907 dye, water-induced dye desorption was not detected, and by studying the S/Ru ratio it was concluded that no substantial permanent chemical modification, such as ligand exchange, occurred to the molecule. In agreement with the experiments of Miyasaka and coworkers,[138] it was observed that the N719 dye layer was more sensitive to water compared to the N3 one, and its S-2p and N-1s signals were mostly affected by the aqueous environment. As a result, clear shifts of the HOMO levels towards higher binding energies occurred for both the dyes (*i.e.*, 0.17 and 0.26 eV for N3 and N719, respectively), thus leading to an increased gap between the energy levels of the HOMO and the LUMO, and subsequently a blue shift in the absorption spectrum.

As previously mentioned, very little studies have been published on the preparation of dyes having specific characteristics to be effectively used in aqueous cells. A seminal work of Ko and coworkers reported about new organic sensitizers (JK-259 and JK-262) containing 4-(2-(2-methoxyethoxy)-ethoxy)phenylamine as the electron donor molecule and cyanoacrylic acid as the electron acceptor molecule bridged by the 9,9-bis(2-(2-methoxy-ethoxy)-ethyl)-9*H*-fluorenyl linker (Table 14).[238] The 2-(2-methoxy-ethoxy)ethyl unit was introduced to ameliorate the water compatibility, and a TBP treatment onto the TiO_2 films ensured the photoanode stability. JK-259 and JK-262 showed efficiency values of 1.16% and 2.10%, respectively, in a fully aqueous electrolyte (PMII 2.0 M, I_2 50 mM, GuSCN 0.10 M, TBP 0.50 M and Triton X-100 1 wt%). However, due to the very low J_{sc} values, these efficiencies were $>50\%$ lower when compared to those measured in the corresponding organic solvent-based DSSCs. The authors justified the decrease in the photocurrent on the basis of detachment of the adsorbed dye through the hydrolysis of the TiO_2–water surface linkage, which is rather contradictory to the aim of their work which was intended for the preparation of a dye stable in water. Apart from this curious aspect, we may argue that research in this field should be much more effective because plenty of possibilities are available for performance and stability improvements.

Ko and coworkers further investigated aqueous DSSCs using three different organic sensitizers, namely D5L6,[239] D21L6[240] and JK-310; in particular, the latter two contained (hexyloxy)-phenylamine and 4-(2-(2-methoxyethoxy)-ethoxy)phenylamine as electron donor units.[241] As clearly visible in Table 14, all of these dyes have a water-soluble substituent and were coupled with an aqueous electrolyte (PMII 2.0 M, I_2 50 mM, GuSCN 0.10 M, TBP 0.50 M and Triton X-100 1 wt% in MPN : H_2O 50 : 50). PV measurements (Table 12) showed that V_{oc} gradually increased with the incremental addition of water (*i.e.*, from 0 to 50%); in contrast, J_{sc} sharply decreased under the same conditions. Again, dyes were found to easily detach due to their partial hydrophilic nature, resulting in the reduction of both photocurrent and efficiency. Such a result further confirmed that the step of tailor-making the dyes in order to get improved photoanode wettability must be carefully counterbalanced by the water solubility value of such organic molecules.

Table 12 PV parameters (P_{in} = 1 sun) of DSSCs assembled with different organic dyes and liquid electrolytes. Electrolytes: PMII 2.0 M, I_2 50 mM, GuSCN 0.10 M, TBP 0.50 M and Triton X-100 1 wt% in MPN or MPN/H_2O. Adapted and reprinted from ref. 241

Dye	H_2O (vol%)	J_{sc} (mA cm^{-2})	V_{oc} (V)	FF	η (%)
D5L6	0	10.50	0.66	0.75	5.20
	50	6.22	0.75	0.73	3.40
D21L6	0	12.57	0.71	0.74	6.56
	50	7.46	0.77	0.77	4.41
JK-310	0	12.28	0.70	0.72	6.18
	50	6.62	0.75	0.76	3.77

As an alternative to the synthesis of new dyes, an impressive work of modification of known sensitizers to make them efficient and stable in an aqueous environment started in 2014. Bisquert and coworkers demonstrated an efficient synthetic protocol to modify the existing cyanoacrylate moiety of organic dyes (whose carboxylate linkage is susceptible to hydrolysis[242]) with a highly water-stable hydroxamate anchoring group *via* a condensation reaction.[243] The well known MK-2 dye[184,244,245] was chosen as a target substrate, and its hydroxamate-derivative (MK-2HA, Table 14) was significantly (30–50%) less susceptible to desorption in water, as a result of the stronger interaction of the novel anchoring group with the surface of TiO_2.[246,247] The enhanced water tolerance was also attributed to the higher pK_a of MK-2HA dye and to the less strained chelate bite angle in hydroxamic acids compared with carboxylic acid analogues. Interestingly, TAS measurements carried out on both dyes revealed that the lifetime of the charge-separated state increased with increasing immersion time in the DMF–H_2O solution used to evaluate the water stability of sensitizers. Thus, such a ''soaking and desorption'' approach, which probably contributed to the removal of dye aggregates from the semiconductor surface,[171] was proposed as a potentially effective treatment to improve the recombination dynamics of DSSC photoanodes. In these experiments, MK-2HA-sensitized photoanodes showed no change in the electron injection efficiency upon exposure to the desorption solution, while MK-2 ones lost nearly 65%, due to the sensitivity of the dye–TiO_2 interface toward water. Cells with MK-2 and MK-2HA dyes were fabricated and water was purposefully added to the electrolyte (MPII 2.0 M, LiI 0.10 M, I_2 0.20 M and TBP 0.50 M in ACN/H_2O). In 200 h aging test under dark, MK-2-based DSSCs with 10 and 20 wt% water had decreased efficiency by 15% and 50% compared to the anhydrous control, mainly due to the 50% reduced J_{sc}. As regards MK-2HA-based cells, there was no significant difference in the efficiencies (slightly lower than 4%) measured with aqueous (10 wt%) and anhydrous electrolytes. Moreover, FF and V_{oc} of water-based DSSCs increased with time: authors hypothesized that the water content in the electrolyte could serve to accelerate the desorption of aggregates, leading to more favourable interfacial electron transfer dynamics.

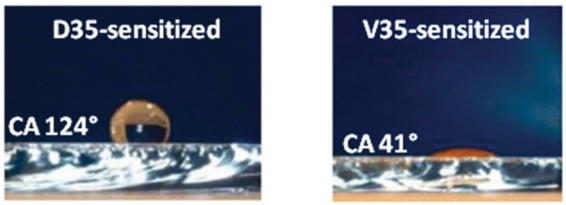

Fig. 19 Crossed sections of working electrodes sensitized with D35 (left) and V35 (right) with a drop of deionized water positioned on the top. CA values are also reported. Adapted and reprinted from ref. 249.

D35 is another well known dye in the DSSC field,[248] and Boschloo and coworkers synthesized its hydrophilic analogous, by substituting the hydrophobic alkyl chains with glycolic ones.[249] The resulting hydrophilic dye (V35, Table 14) showed an extraordinary interaction with water, and the authors claimed that the use of wettability-improver surfactants was not necessary (as can be seen in Fig. 19), thus reducing cell cost and avoiding possible mass transport problems. The new dye was initially coupled with a fully aqueous electrolyte containing only NaI and I_2, and then gradually modified as reported in Table 13. Interestingly, efficiency increased when KI replaced NaI, probably due to the ability of glycolic chains (like crown ethers) to coordinate small cations (such as Na^+).[250,251] Performance was further improved by doubling the concentration of KI, thus lowering the amount of free iodine. The addition of GuSCN had a negative effect, while CDCA improved efficiency up to 2.20%. Moreover, V35 dye was further investigated in aqueous DSSCs employing alternative cathodic materials at different pH values, as will be described in Section 11.

Pigments extracted from natural matrices may result in a valuable alternative to synthetic dyes.[252,253] Despite the efficiencies obtained are still lower compared to the reference Ru-based dyes, thanks to their low cost and ready availability, these pigments are nowadays very much considered by those research groups who are focused on the development of the so-called biophotovoltaic devices.[181,254,255] In Section 8, the very recent work of Su and Lai on natural pigments coupled with alternative redox mediators has been mentioned,[178] but the very first demonstration of the good compatibility between pigments and water was provided by Rabani and coworkers.[256] In 2001, they exploited the promising prospects as a sensitizer of the seed coats of the pomegranate (PG) fruit, which is a rich source of anthocyanins.[257] By operating under strong acidic conditions (pH 1) and after having ascertained that Na^+ was the most effective counter ion in photocurrent generation, the resulting aqueous DSSC (NaI 1.0 M and I_2 0.10 M) demonstrated a J_{sc} value of 2.2 mA cm^{-2} and a V_{oc} of 0.44 V (FF was not reported). Stability tests showed no appreciable decrease of the photocurrent after 24 h illumination. It is important to recall here that the size of the photoanode NPs is a key factor affecting the performances of natural pigment-based cells. In their investigation, Rabani and coworkers used 5 nm diameter NPs which guaranteed small pores, thus preventing or minimizing the adsorption of undesired molecules (*i.e.*, foreign impurity phases deriving from the original matrix) which could result in reduced photocurrent by means of visible light absorption competition.

Table 13 PV parameters (P_{in} = 1 sun) of V35-sensitized DSSCs assembled with different fully aqueous electrolytes. Adapted and reprinted from ref. 249

Electrolyte	J_{sc} (mA cm^{-2})	V_{oc} (V)	FF	η (%)
NaI 2.0 M and I_2 20 mM	2.30	0.500	0.67	0.80
KI 2.0 M and I_2 20 mM	4.07	0.550	0.70	1.55
KI 4.0 M and I_2 20 mM	4.78	0.570	0.65	1.76
KI 4.0 M, I_2 20 mM and GuSCN 0.50 M	3.33	0.555	0.67	1.25
KI 4.0 M, I_2 20 mM and CDCA sat.	4.86	0.600	0.76	2.20

An overview of the dyes used so far for aqueous DSSCs is given in Table 14, together with the redox mediators with which they have been tested. Very recently, novel metal-free dyes containing an anthracene/phenothiazine unit in the spacer have been synthesized and proposed for aqueous DSSCs, and a cell performance equal to 4.96% was achieved.[258]

11. Low-cost and water-compatible cathodes

Being the most popular choice for high-efficiency DSSCs, platinum has been widely recognized as the benchmark material at the cathode side, due to its high catalytic activity and excellent conductivity.[259] As a result, for many years, research on novel cathodic materials has been considered rather a secondary issue by the scientific community, especially if compared to the impressive efforts addressed to the improvement of the other cell components. Nevertheless, Pt presents a series of drawbacks, the most significant being the high cost and the scarce availability, which have restricted so far the mass production of DSSCs,[260] as already occurred to fuel cells and related systems using Pt as a catalyst.[261] Moreover, Pt may readily undergo severe dissolution in electrolytes containing the iodine-based redox couple, resulting in the formation of PtI_4 and reduced cell performances;[262] Pt is not compatible with the recently proposed sulphur-based redox shuttles as well.[189] For all these reasons, we may reasonably argue that the breakthrough in the widespread diffusion of DSSCs may be realised only when counter electrodes at sustainable costs and stable long-term performance are developed.[263] In this respect, transition metal compounds (*i.e.*, carbides, nitrides) have drawn considerable attention as alternatives to Pt cathodes, due to their excellent catalytic activity towards electrolytes based on both sulphur- and cobalt-based redox couples.[264,265] Organic polymers (*i.e.*, PEDOT, PPy, PANI, *etc.*) demonstrated promising prospects as flexible and transparent cathodes.[266,267] In the last two years, low-dimensional carbonaceous materials (*i.e.*, CNTs arrays and graphene films) started to be widely studied and applied, especially in iodine-free DSSCs.[268,269]

As previously reported in the course of this review (Section 8), redox couples to be used in aqueous DSSCs are often different from the standard ones conceived for aprotic media. The use of water as a solvent (sometimes mixed with ACN or MPN) makes the electrolyte/cathode compatibility a new topic to be deeply investigated. Obviously, aqueous electrolytes being a recent

Table 14 Structural formulas of sensitizers usually employed in aqueous DSSCs, together with the redox pairs with which were coupled. Further details about the other cell components and the PV performance are reported in the manuscript and in Table 20

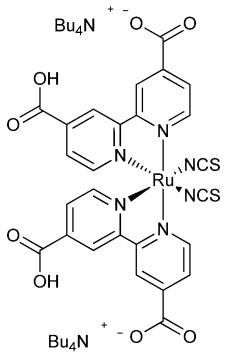

N719

Always with I^-/I_3^- with increasing H_2O content: 0.018 wt%,[172] 4 wt%,[156] 10 wt%,[145] 65 wt%,[138] and in 100 wt% H_2O[138,163,206]

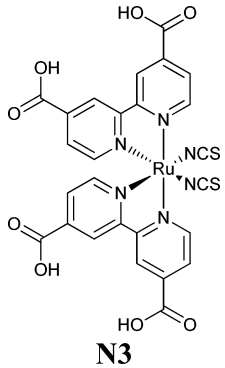

N3

Always with I^-/I_3^- with increasing H_2O content: 3 wt%,[124] 4 wt%,[43] 5 wt%,[303] 10 wt%,[294] 65 wt%,[138,203] and in 100 wt% H_2O[138,328]

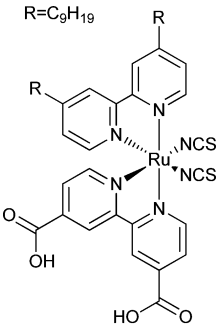

Z907

Always with I^-/I_3^- with increasing H_2O content: 10 wt%,[128] 50 wt%,[310] and in 100 wt% H_2O[206]

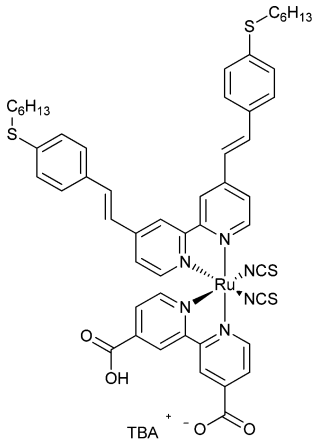

TG6

Always with I^-/I_3^- with increasing H_2O content: 20 wt%,[120] 50 wt%,[318] and in 100 wt% H_2O[120,206]

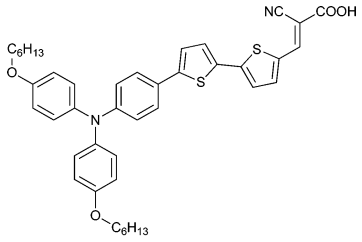

D21L6

I^-/I_3^- + 50 wt% H_2O[241]

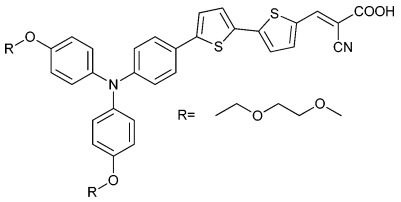

JK-310

I^-/I_3^- + 50 wt% H_2O[241]

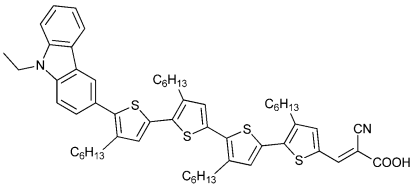

MK-2

$Fe(CN)_6^{4-}/Fe(CN)_6^{3-}$ in 100 wt% H_2O[182]
$[Co(bpy)_3]^{2+}/[Co(bpy)_3]^{3+}$ in 100 wt% H_2O[194,210]

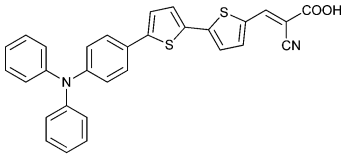

D5L6

I^-/I_3^- + 50 wt% H_2O[241]

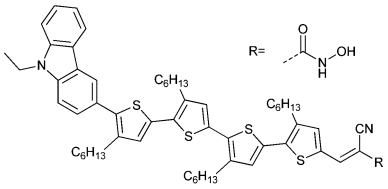

MK-2HA

I^-/I_3^- + 10 wt% H_2O[243]

Table 14 (*continued*)

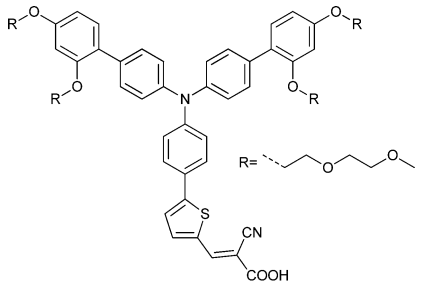

V35

I^-/I_3^- in 100 wt% H_2O[249]

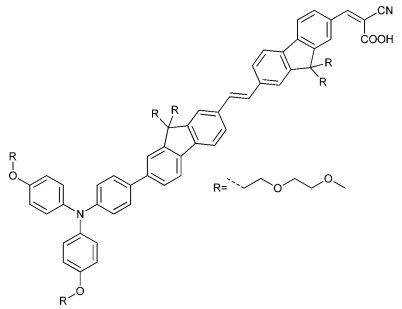

JK-259

I^-/I_3^- in 100 wt% H_2O[238]

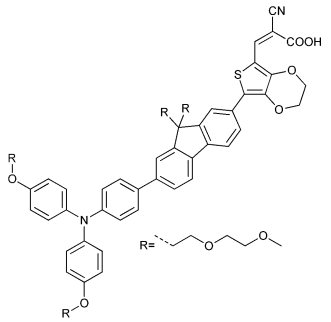

JK-262

I^-/I_3^- in 100 wt% H_2O[238]

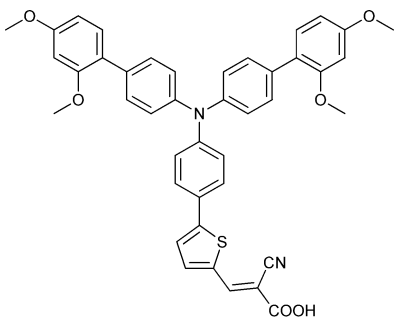

D45

TT^-EMI^+/DTT in 100 wt% H_2O[193]

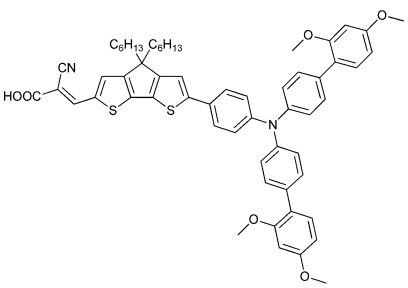

D51

TT^-EMI^+/DTT in 100 wt% H_2O[193]

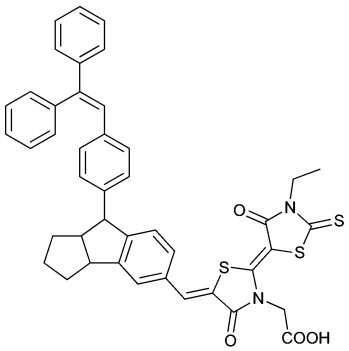

D149

I^-/I_3^- in 100 wt% H_2O[206]

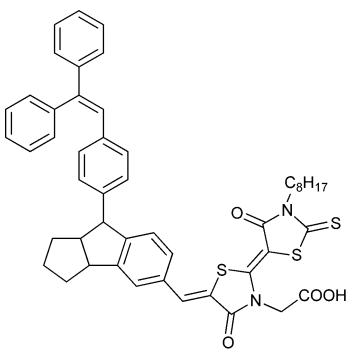

D205

$TEMPOL/TEMPOL^+$ in 100 wt% H_2O[274]

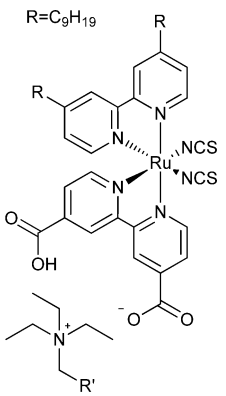

D907

I^-/I_3^- + 65 wt% H_2O[314]

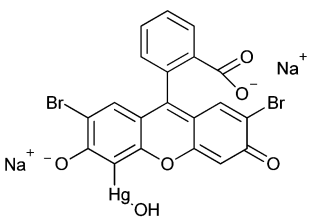

Merbromin

Fe^{2+}/Fe^{3+} + 65 wt% H_2O[204]

Natural dyes/pigments
CV-G with Ce^{3+}/Ce^{4+} + 30 wt% H_2O[178]
RhS with Ce^{3+}/Ce^{4+} + 65 wt% H_2O[174]
PG with I^-/I_3^- in 100 wt% H_2O[256]

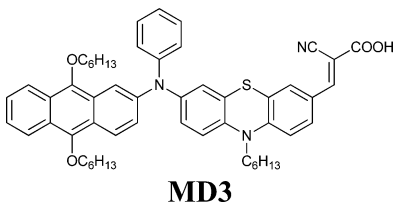

MD3

$TEMPO/I^-/I_3^-$ in 100 wt% H_2O[258]

research interest, very few literature reports useful to identify an optimum cathodic material have been available so far. Notwithstanding, some interesting studies have been already proposed, which will be hereby briefly summarised.

When using Co complexes as aqueous redox shuttles, Spiccia and coworkers observed a high charge transport resistance between the water-based electrolyte and the Pt counter electrode.[194] Thus, they screen-printed a mesoporous ITO film onto the FTO substrate, and then added a thermally-deposited Pt layer. The resulting cathode (13.5 μm-thick) led to an efficiency of 5.0% (4.2% with Pt only), which increased by another 0.1% after 48 h. The ITO/Pt cathode showed a R_{CE} equal to 1.6 Ω, around five times lower than that of pure Pt, along with an almost doubled exchange current (investigated by means of cyclic voltammetry), thus indicating improved electron transfer to the oxidized redox couple. The reason for this behaviour lied in the high surface area of the ITO mesoporous film, which enabled a higher Pt loading and facilitated the reduction of the oxidized species of the aqueous electrolyte at the counter electrode surface.

Poly(3,4-ethylenedioxythiophene) (PEDOT) is currently one of the most considered materials for the preparation of both rigid and flexible cathodes to be used in DSSCs based on alternative redox couples. Sun and coworkers tried to improve the FF of DSSCs assembled with a thiolate/disulphide redox couple by using PEDOT as a counter electrode.[193] However, they failed because of the poor stability of PEDOT in the aqueous electrolyte, which also resulted in its easy detachment from the FTO glass. Quite surprisingly, the opposite behavior was reported by Boschloo and coworkers with fully aqueous cells containing V35 dye and an iodide/triiodide redox couple.[249] Indeed, Table 15 shows that PEDOT counter electrodes outperformed Pt ones due to increased J_{sc} and V_{oc} values. Such a positive effect was attributed to the leaf-like PEDOT structure, which conferred a high-surface area to the cathode, thus increasing its catalytic activity. Moreover, a reduced tendency of the dye to desorb in the presence of PEDOT was observed: authors speculated that PEDOT partially trapped in its matrix the ions capable of being absorbed onto the surface of TiO_2,[270] preventing in this way the desorption of the dye. V35 was also tested with the best electrolyte reported by O'Regan and coworkers (see Section 9,[206]); however, the elevated concentration of GuI decreased significantly V_{oc} values (Table 15) due to the absorption of guanidinium cations on the TiO_2 surface.[271] Further optimization

Table 15 PV parameters (P_{in} = 1 sun) of V35-sensitized DSSCs assembled with different electrodes and electrolytes. Adapted and reprinted from ref. 249

Electrolyte	Cathode	J_{sc} (mA cm^{-2})	V_{oc} (V)	FF	η (%)
KI 4.0 M, I_2 20 mM and CDCA sat.	Pt	4.86	0.600	0.76	2.20
KI 4.0 M, I_2 20 mM and CDCA sat.	PEDOT	5.26	0.625	0.74	2.45
KI 2.0 M, I_2 10 mM and CDCA sat.	PEDOT	6.85	0.650	0.67	3.01
GuI 8.0 M, I_2 20 mM and CDCA sat.	PEDOT	5.76	0.550	0.62	1.97

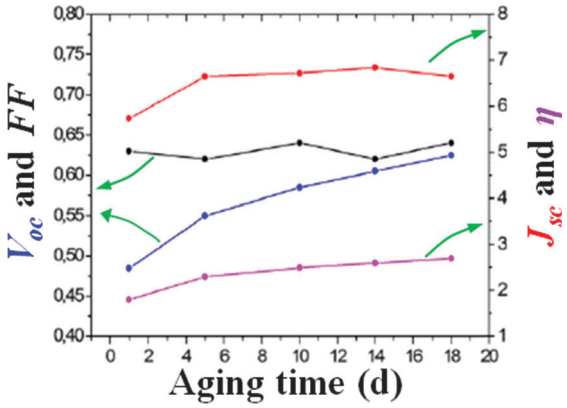

Fig. 20 Long-term stability under dark of DSSCs assembled with a fully aqueous electrolyte (KI 4.0 M and I_2 20 mM at pH 8.0) and a PEDOT counter electrolyte. Dye: V35. PV parameters were measured under P_{in} = 1 sun. Adapted and reprinted from ref. 249.

of iodine and CDCA concentrations yielded the highest efficiency recorded with V35 dye, namely 3.01% (4% under 0.5 sun). Noteworthy, all the electrolytes proposed by Boschloo and coworkers contained CDCA as a V_{oc}-improver agent: it did not shift significantly the TiO_2 CB,[272] but reduced the recombination processes.

To further demonstrate the long-term stability of the PEDOT-based aqueous cells, Boschloo and coworkers set up several aging tests, also studying the effect of the pH of the electrolyte on the PV parameters.[249] As shown in Fig. 20, both V_{oc} and FF were higher in the case of electrolytes (KI 4.0 M and I_2 20 mM) at pH 9.0; however, a lower photocurrent and an overall efficiency were obtained with respect to cells at pH 8.0. One very important aspect was given by fluctuations over time of the PV parameters (Fig. 20), and the better efficiencies were collected several days later device assembly. This is a typical characteristic of aqueous cells, thus scientific groups are suggested to monitor their devices over time rather than immediately abandoning their new materials due to low performance measured immediately after DSSC assembly.

Also materials other than PEDOT have surprisingly demonstrated increased performance and stability as cathodes in aqueous electrolyte-based DSSCs. In their pioneering work, Kim and coworkers revealed for the first time that the corrosion potential of silver metal increased in aqueous electrolytes containing Triton X-100.[156] The surfactant may in fact create a sort of protective layer on the Ag film surface which reduced the direct interaction with I_3^- ions, which in turn greatly diminished the dissolution of the metal. In the presence of the surfactant, an increased overpotential for the electron transfer from the Ag layer to I_3^- was additionally recorded. Such encouraging results unveiled the possibility of using Ag instead of the more expensive Pt in futuristic commercial DSSCs.

Very recently, the coating of the cathode surface with a polymeric film has been proposed to improve the electrode/electrolyte interfacial properties.[273] In this respect, Nishide and coworkers used 4-hydroxy-2,2,6,6-tetramethylpiperidinoxyl (TEMPOL, Fig. 21) as a redox mediator in an aqueous DSSC.[274]

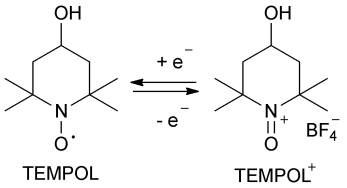

Fig. 21 Redox reaction of the TEMPOL mediator. Adapted from ref. 274.

TEMPOL is a hydrophilic TEMPO derivative, belonging to the class of nitroxide radical molecules, which have attracted remarkable attention as organic-based redox-active materials due to their rapid and reversible one-electron-transfer capability to form the corresponding oxoammonium cations.[275–277] This alternative redox mediator (to be added to the list shown in Section 8) was immobilized in a Nafion®:Pt two-layers cathode. Nafion® is typically used to prepare polymer electrolyte membranes,[278] but also as a trapping agent for electroactive cations in sensing and photoelectrochemical devices.[279,280] Exploiting its properties, a significant increase of both J_{sc} and FF values was evidenced with respect to the Pt-based cell, which was ascribed to the lower cell resistance due to the high efficiency in the regeneration reaction of the redox mediator as well as to the steep concentration gradient of the TEMPOL cation promoted by the Nafion® layer. In the presence of the Nafion®:Pt two-layers counter electrode and using the D205 dye, the overall cell efficiency increased from 0.11% (J_{sc} = 1.1 mA cm^{-2}, V_{oc} = 0.76 V, FF = 0.14) to 2.1% (J_{sc} = 4.5 mA cm^{-2}, V_{oc} = 0.69 V, FF = 0.64).

12. Cell sealing in the presence of water: a new intriguing challenge

Being the long-term stability a key objective of the present scientific research activity in the DSSC community, amounts of materials have been explored as sealants, such as thermoplastic hot-melt foils (*i.e.*, Surlyn®,[281] Bynel®,[282] *etc.*), UV curable glues[37] and glass frit (GF).[283,284] GF is believed to be one of the strongest candidate as a sealant material in DSSC glass modules, as it possesses the same characteristics of the substrate, thus optimum compatibility; moreover, it is non-permeable, stable under UV light and at elevated temperatures.[285–287] On the other hand, it has been quite difficult to find lead-free GF,[288] demonstrating at the same time low melting temperature and high chemical stability towards the redox mediator. Moreover, GF must not leach elements into the electrolyte, which could cause the depletion of the I_3^- ions.[115,289]

The use of an aqueous electrolyte opens up an amount of novel opportunities in the development of specific sealants for water-based DSSCs. A seminal work was proposed by Hinsch and coworkers, who fabricated Bi_2O_3–SiO_2–B_2O_3 and ZnO–SiO_2–Al_2O_3 GFs, with characteristic melting temperatures in the range of 400–520 °C.[290] When Bi_2O_3–SiO_2–B_2O_3 was coupled with an aqueous electrolyte (I_2 0.10 M, GuSCN 0.10 M and NBBI 0.50 M in MPII/ACN/H_2O), UV-Vis measurements revealed a significant decrease in the I_3^- absorbance with time (Fig. 22A),

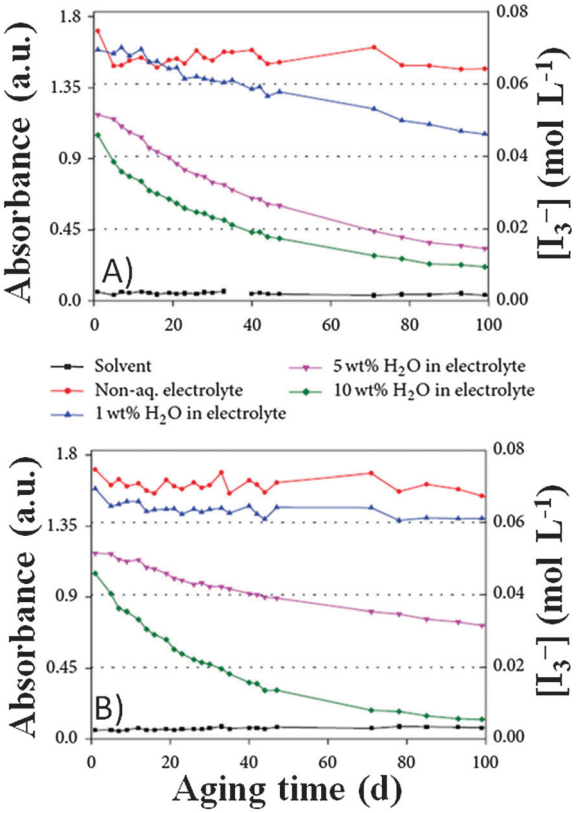

Fig. 22 Absorbance at 430 nm as a function of the aging time for DSSCs filled with solvent, non-aqueous electrolyte and redox electrolyte encompassing 1, 5 and 10 wt% H_2O, in the presence of different GFs as sealants: (A) Bi_2O_3–SiO_2–B_2O_3; (B) ZnO–SiO_2–Al_2O_3. Adapted and reprinted from ref. 290.

while energy dispersive X-ray (EDX) analysis revealed a precipitate of bismuth and iodine. Indeed, BiI_4^- formation was observed, and its absorption band at 460 nm competed with the one characteristic for the sensitizer.[291] As regards the ZnO–SiO_2–Al_2O_3 GF, the electrolyte bleached because of I_3^- depletion (Fig. 22B); EDX revealed the leakage of zinc from the GF. In turn, the metal formed a thermally stable compound with iodine,[292] being detrimental on the DSSC performance. Moreover, for both the GFs, the I_3^- depletion was enhanced while increasing the content of water in the electrolyte.

The GFs proposed by Hinsch and coworkers represent only the first example of the sealing material for aqueous DSSCs, thus other metal oxide formulations must be elaborated to assure the development of truly stable cells. However, in the case of aqueous DSSCs, also the polymeric sealants would return in vogue, since the water permeability would no longer be a problem for cell stability.

13. Quasi-solid electrolytes: the step forward

In Section 2, the main drawbacks of liquid electrolytes have been thoroughly discussed, volatility and difficulty of hermetic sealing being the most significant. We have already shown that

volatility may be remarkably reduced by introducing water as solvent of the redox mediator in place of ACN; nevertheless, the use of specifically developed quasi-solid electrolytes would clearly facilitate the operations of cell assembly and sealing, also guaranteeing a prolonged stability to the device. As a result, many research groups working on aqueous electrolytes have directed their efforts towards the realisation of water-based DSSCs in the quasi-solid state.

13.1 RTIL–water mixtures

The quasi-solidification of a liquid electrolyte is usually carried out through the introduction of RTILs or polymeric materials.[18,48,68] The pioneering work on the development of RTIL-laden polymer electrolytes was published by Mikoshiba and coworkers, who used water to face the slow I_3^- diffusion in the highly viscous RTILs.[293] By coupling MPII with different components (*e.g.*, LiI/TBP/I_2, TBP/I_2, LiI/I_2, I_2), it was observed that the addition of water improved the efficiency of N3-based cells, the best results being obtained using 5 wt% H_2O in the presence of LiI/I_2, while 10 wt% in the case of the LiI/TBP/I_2 system. The improvement was attributed to the reduced electrolyte viscosity and to the increased V_{oc}: a remarkable efficiency of 4.2% was obtained.

A more detailed analysis regarding the effects of water on the RTIL-based electrolytes was conducted by Hayase and coworkers.[294] As shown in Table 16, several additives were introduced to increase the conductivity of MPII: among all, water was demonstrated to be the best one, besides being the one having the lowest environmental impact. Table 17 shows that increasing the water content led to reduced viscosity (μ) and increased ionic conductivity (σ, also reflected in the improved diffusion coefficient for I_3^-). Other positive aspects were the R_{CE} decrease and E increase while increasing the amount of water. As regards the TiO_2 surface, when 8% of water was added in the electrolyte, it was observed that the flat band potential shifted positively from −1.11 to −1.01 eV, due to the adsorption of H_2O molecules onto the semiconductor.[82,83] This modified the characteristics of the electron diffusion in the nanostructured photoanode: electron lifetime (τ), electron diffusion constant (D) and electron diffusion length (L) decreased upon the introduction of water. This was due to the replacement of the Li^+ ions adsorbed onto the TiO_2 surface by water molecules, resulting in a less effective ambipolar diffusion of the electrons which, in turn, led to an increased electron recombination probability.

Imidazolium-based RTILs are very popular due to their peculiar characteristics of being solvents and salts at the same time. However, the synergistic effect of using mixtures of different ionic liquids has been also proposed to possibly improve the PV performance. Among all, bistriflimide ($TFSI^-$) gave excellent performance when combined with imidazolium-based RTILs.[295] Even if $TFSI^-$-based RTILs are generally considered as hydrophobic,[296,297] coulometric Karl Fischer titration enlighten the presence of significant amounts of water (*i.e.*, around 7 mol%) most likely absorbed from the ambient air.[298] To better unravel this phenomenon, Kim and coworkers theoretically investigated the effects of water on the microstructure as well as the transport properties of a mixture of 1-ethyl-3-methylimidazolium ($EMIm^+$), $TFSI^-$, I^- and I_3^-.[299] By considering a 0–25% mole fraction (χ_w) of water, three regimes were obtained (Fig. 23A):

– ice-like regime ($\chi_w < 7.69\%$, Fig. 23B), with water molecules mostly isolated and intercalated between two $EMIm^+$ and two $TFSI^-$ units, resulting in an ice-like entropy.

– Nano-cluster regime (χ_w = 7.69–14.29%, Fig. 23C), with nanosized water clusters bridged between two $EMIm^+$ and two $TFSI^-$ units.

– Liquid-like regime (χ_w = 14.29–25.00%, Fig. 23D), that is clusters composed of several water molecules located between $EMIm^+$ and $TFSI^-$ ions.

In order to examine the effect of water absorption on the transport properties of the electrolyte, the self-diffusion coefficients were measured based on the Green–Kubo relationship,[300] and it was found that the addition of water up to 10 mol% enhanced the diffusivity of both $EMIm^+$ and $TFSI^-$, with marginal variations in the diffusivity of I^- and I_3^-. More in detail, the increase of entropy and mobility of $EMIm^+$ caused local fluctuations in I^- and I_3^-, thus enhancing the rate of Grotthuss-like electron transfer[301] as well as the rate of oxidized

Table 16 μ and σ values of MPII-based electrolytes added with different additives in the 10 wt% ratio. Adapted and reprinted from ref. 294

Additive	μ (mPa s)	σ (mS cm^{-1})
Formamide	108	1.8
NMP	238	1.2
GBL	153	1.9
EC	104	1.5
PC	220	1.1
Diethoxyethane	139	2.1
EtOH	57	3.6
H_2O	18	15
Ethylene glycol	104	2.6

Table 17 μ, σ, apparent diffusion constant for I_3^- [$D(I_3^-)$], R_{CE}, E, τ, D and L values for MPII-based electrolytes with different water contents. Electrolytes tested were I_2 0.50 M in MPII:H_2O for μ, σ and $D(I_3^-)$; I_2 0.30 M in MPII:H_2O for R_{CE}; MPII 60 mM and I_2 10 mM in ACN/H_2O for E; LiI 0.50 M, I_2 0.30 M, TBP 0.58 M in MPII/H_2O for τ, D and L. P_{in} = 1 sun. Dye: N719. Note: we think that a factor of $10^{-5/-7}$ is missing in the reported $D(I_3^-)$ values. Adapted and reprinted from ref. 294

H_2O (wt%)	μ (mPa s)	σ (mS cm^{-1})	D (I_3^-) (cm^2 s^{-1})	R_{CE} (Ω cm^{-2})	E (mV)	τ (s)	D (cm^2 s^{-1})	L (cm)
0	564	0.7	6.5	3.04	—	0.32	1.36	0.66
1	285	1.35	9.5	1.99	0.09	—	—	—
5	52.8	5.81	23	0.24	0.17	0.12	1.23	0.38
10	19.2	14.12	34	0	0.24	0.12	1.23	0.38

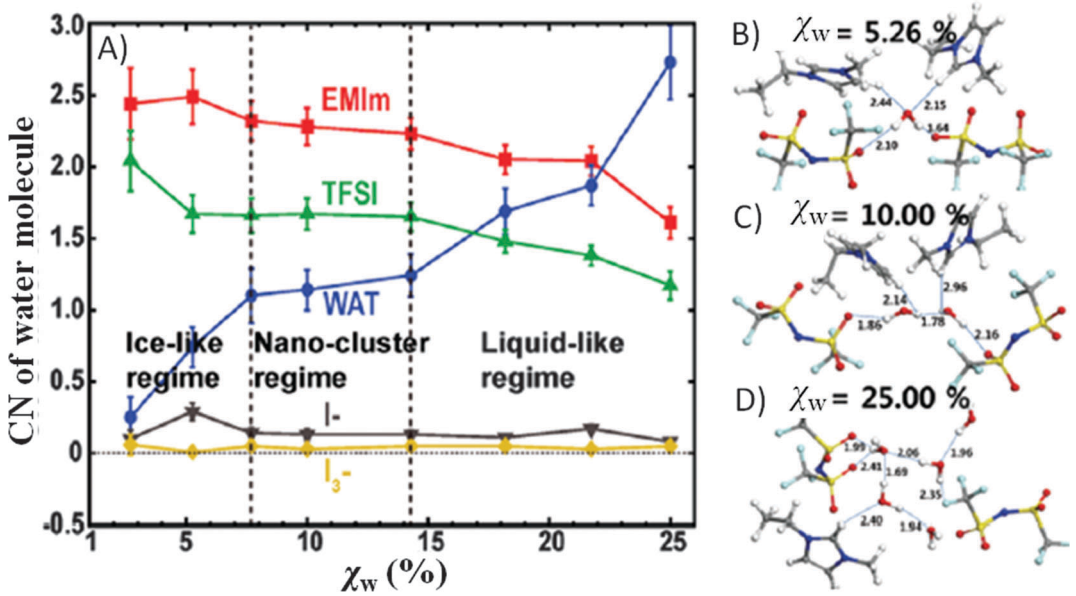

Fig. 23 (A) Dependence of water coordination (CN) on χ_w in the presence of the following mole fractions: $EMIm^+$ 0.50, $TFSI^-$ 0.36, I^- 0.13 and I_3^- 0.01. Representative water structure mediating $EMIm^+$–$TFSI^-$ interactions after 30 ns molecular dynamics for: (B) ice regime, (C) nanocluster regime, and (D) liquid-like regime. Adapted and reprinted from ref. 299.

dye reduction. On the other hand, when using high amounts of water, the large water clusters allowed water molecules to access the TiO_2 nanostructure, thus weakening the Lewis acid–base interaction of the carboxylic group of dye molecules with the anode particles. Based on all of these simulations, it was clear that the H_2O–RTIL system provided the best performance in the nanocluster regime, because of allowing spontaneous water absorption into the RTIL, retention in the RTIL phase by binding as nanoclusters to $EMIm^+$ or $TFSI^-$ ions and lubricating fluctuations in the RTIL to enhance Grotthuss electron transport.

13.2 Gel-polymer aqueous electrolytes

The second category of quasi-solid electrolytes is based on a polymeric matrix, capable of gelifying the redox mediator solution and trapping it within the macromolecular network.[302] In 2004, Hayase and coworkers firstly proposed an aqueous gel-polymer electrolyte obtained by reacting poly(vinylpyridine) (PVP, M_n = 80 000) with 1,2,4,5-tetra(bromomethyl)benzene to make chemically crosslinked ionomer structures.[303] The resulting polymer[304] trapped 0.30 M I_2 in MPII–H_2O mixtures, where water was useful to decrease the gel viscosity, thus guaranteeing a good physical contact between the gel and the mesopores of the photoanode. Moreover, $D(I_3^-)$ was improved upon water addition, because of the phase separation between PVP and MPII, which in turn retarded the interaction between the cations fixed on the polymer matrix and I_3^- ions.[305] Another advantage of water addition was the decrease in R_{CE}. As a further interesting aspect of their work, Hayase and coworkers carried out the treatment of the N719-sensitized photoanode with acetic acid, which bonded on the free TiO_2 sites. As a consequence, the electron recombination with I_3^-, which is the most relevant drawback of RTIL-based electrolytes, where high I_2 amounts are added to increase the limiting currents, was inhibited. An efficiency value of 2.4% (J_{sc} = 10.9 mA cm^{-2}, V_{oc} = 0.52 V, FF = 0.42) was obtained in the presence of 5 wt% H_2O.

In the field of gel-polymer electrolytes, PEG is one of the most successful material due to its ability to play the role as a host for several metal-salt systems, being at the same time a good binder for other phases.[306–308] Moreover, to achieve high ionic conductivity values, polymer blending with PEG is a valuable strategy.[309] With the aim of confirming the practical application of such an approach in an aqueous environment, Nateghi and coworkers prepared a gel-polymer electrolyte consisting of poly(vinylpyrrolidone) (PVPi, M_n = 40 000, 2 wt%), PEG 400 4 wt%, KI 0.20 M and I_2 40 mM in ACN/H_2O.[310] The effect of water concentration on the polyiodide formation was investigated by analyzing the intensity ratio between the polyiodide (I_n^-) and the I_3^- species: a decrease of the I_n^-/I_3^- ratio occurred upon water addition. Theoretical calculations indicated that I_n^- species were more effective electron acceptors than I_3^- due to more delocalized charges. This facilitated the reaction with electrons due to reduced repulsion;[311] moreover, the decrease of the I_n^-/I_3^- ratio contributed to reduce the charge recombination losses. As a consequence, V_{oc} values of the aqueous quasi-solid DSSCs increased because of water addition; this effect was also due to water adsorption onto the TiO_2 surface. On the other hand, the presence of water negatively affected the J_{sc} values, due to the lower concentration of I_3^- in the aqueous electrolyte and the detachment of the adsorbed Z907 dye molecules. Overall, cells with 50 wt% H_2O showed an efficiency equal to 2.31% (J_{sc} = 7.37 mA cm^{-2}, V_{oc} = 0.63 V, FF = 0.50), while in the absence of water the average value was 2.88% (J_{sc} = 13.7 mA cm^{-2}, V_{oc} = 0.58 V, FF = 0.35). When tested for their stability (under dark, 65 °C, 85% RH),

aqueous cells were able to retain the 63% of their initial efficiency after 168 h of operation, remarkably better than the 12% retention for the ACN-based quasi-solid DSSCs, thus further confirming the positive aspects of the lower volatility of aqueous electrolytes.

Amphiphilic block copolymers (ABCs) represent an emerging class of macromolecular matrices, because of their ability to self-assemble into liquid crystalline phases such as cubic, hexagonal and/or lamellar; in these configurations, polymer gels exhibit enhanced σ values with respect to other crystalline phases.[312,313] Being the behaviour of ABCs more relevant in water-based solvents, Soni and coworkers prepared gel-polymer electrolytes with Pluronic F77 $[HO(CH_2CH_2O)_{52}(CH_2CH(CH_3)O)_{35}(CH_2CH_2O)_{52}H]$ and Pluronic P-123 $[HO(CH_2CH_2O)_{20}(CH_2CH(CH_3)O)_{70}(CH_2CH_2O)_{20}H]$.[314] These are triblock copolymers (widely known as poloxamers) composed of a central hydrophobic chain of poly(propylene oxide) (PPO) flanked by two hydrophilic chains of poly(ethylene oxide) (PEO). F77 (M_n = 6600), P-123 (M_n = 5750) or pure PEG (M_n = 6000) were introduced in the 35 wt% ratio in aqueous electrolytes containing BMII 2.0 M, I_2 50 mM and TBP 0.50 M: under these conditions, the cubic phase was obtained, which is the crystalline phase of ABCs having the highest σ, due to the presence of interconnected bi-continuous channels. The conductivity trend showed in Table 18 followed the sequence P-123 > F77 > PEG: in fact, due to the lower amount of PEO units in the P-123 gel-polymer electrolyte, the degree of hydration per PEO chain was found to be higher when compared to that of F77, which promoted ion mobility. Moreover, the size of the F77 micellar core (Fig. 24A) was smaller than that of P-123. As regards PEG, it did not form a microcrystalline ordered gel, thus I_3^- ions could not diffuse so faster as in P-123- and F77-based electrolytes. However, as shown in Table 18, despite the lower σ, when introduced in quasi-solid DSSCs F77-based systems demonstrated higher J_{sc} and V_{oc} values than P-123-based ones. Indeed, while P-123 formed a gel with very high viscosity, F77 showed remarkable structural polymorphism (Fig. 24B): by lowering its temperature, a conversion into the simple micellar solution having reduced μ occurred. Thus, F77 gels could diffuse into the photoanode nanopores at low temperature (ensuring the efficient regeneration of the oxidized dye in the whole electrode), while maintaining a gel-like consistence above 37 °C. Moreover, the higher PPO content in the P-123 gel hindered the accessibility of TBP, thus lowering the cell photovoltage with respect to that of the F77-based cell. Stability tests were carried out over 500 h and only around 3% reduction in the overall performance of DSSCs based on ABCs occurred; in contrast, dye desorption was observed in the case of PEG-based gels, due to the highly hydrated polymer chains.

Another elegant strategy to prepare electrolytes being effectively water as well as solvent leakage resistant is the use of thixotropic three-dimensional (3D) networks,[315] the latter obtained by a chemical, photochemical or thermal route.[316,317] To this purpose, Ko and coworkers used xanthan gum ($M_n = 2 \times 10^6$), a water soluble and environmentally friendly polysaccharide rich in hydroxyl groups ready to form a 3D network, the viscosity of which reversibly decreases upon application of an external stress.[318] After a thorough optimization of the stability of all the ingredients in the reactive formulation – a key aspect in this field, where apolar, polar and ionic substances are concurrently used – a 1 : 1 mixture of xanthan gum (3 wt% in H_2O) and liquid electrolyte (PMII 4.0 M, I_2 0.30 M, TBP 1.5 M

Table 18 Effect of the ABCs : H_2O 35 : 65 matrices on both electrolyte (BMII 2.0 M, I_2 50 mM and TBP 0.50 M) and DSSC PV parameters (P_{in} = 1 sun). An ACN-based cell is also reported for comparison purposes. Dye: D907. Adapted and reprinted from ref. 314

Matrix	σ (mS cm^{-1})	D (I_3^-) (cm^2 s^{-1})	J_{sc} (mA cm^{-2})	V_{oc} (V)	FF	η (%)
ACN	—	—	16.8	0.676	0.54	6.5
P-123	14.8	4.3×10^{-7}	4.6	0.491	0.57	1.3
F77	11.1	3.4×10^{-7}	6.2	0.595	0.53	2.1
PEG	8.8	2.6×10^{-7}	2.1	0.600	0.44	0.6

Table 19 Effect of liquid (PMII 4.0 M, I_2 0.30 M, TBP 1.5 M and GuSCN 0.20 M in MPN or MPN : H_2O 1 : 1) and quasi-solid (1 : 1 in xanthan gum 3 wt% in H_2O and PMII 4.0 M, I_2 0.30 M, TBP 1.5 M and GuSCN 0.20 M in MPN) electrolytes on different electrochemical and PV parameters (P_{in} = 1 sun). Dye: TG6. Adapted and reprinted from ref. 318

Electrolyte	D (I_3^-) (cm^2 s^{-1})	J_{sc} (mA cm^{-2})	V_{oc} (V)	FF	η (%)
MPN	1.15×10^{-5}	12.86	0.59	0.61	5.23
MPN:H_2O	5.60×10^{-6}	9.69	0.68	0.76	4.99
MPN:H_2O:xantan gum	3.78×10^{-6}	9.49	0.65	0.77	4.78

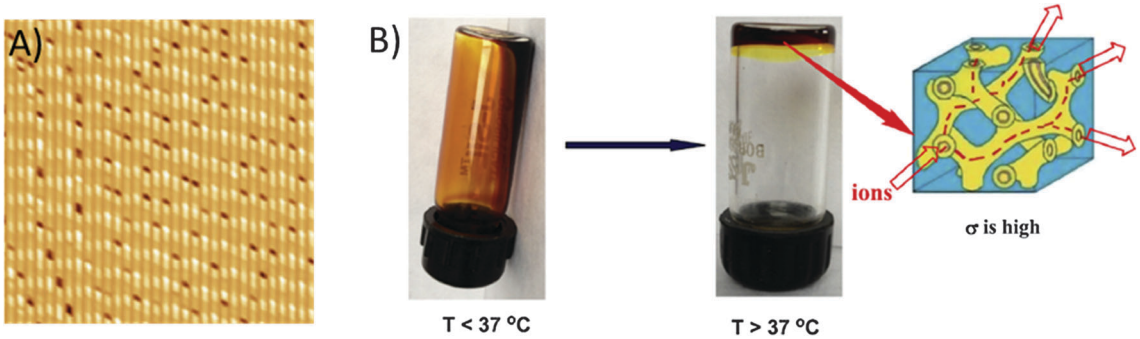

Fig. 24 (A) AFM image of a F77-based gel-polymer electrolyte coated onto a glass substrate. Black dark spots prove the existence of a circular area ranging from 3 to 5 nm, which might be the core of F77 micelles consisting of hydrophobic PPO moieties. The contrast of this area to the rest of the film could be due to the penetration of relatively hydrophobic I_3^- into the PPO core. (B) Photos and schematic illustration of the structural polymorphism of a F77-based gel-polymer electrolyte. Adapted and reprinted from ref. 314.

Table 20 PV performance (P_{in} = 1 sun) of DSSCs assembled with aqueous electrolytes. Data are presented in order of increasing amounts of water in the electrolytes; in the case of equal water amount, data are presented in order of increasing efficiency. Efficiency loss with respect to the initial value (η_{loss}) is also reported when aging tests were performed

Anode[a]	Dye[b]	Electrolyte	H_2O (%)	Cathode[c]	J_{sc} (mA cm^{-2})	V_{oc} (V)	FF	η (%)	η_{loss}[d]	Ref.
TiO_2 (11.5 μm T + 14.5 μm SL) + $TiCl_4$	N719	BMII 0.70 M, I_2 30 mM, GuSCN 0.10 M, TBP 0.50 M and AOT 2.0 mM in ACN:VAN	0.018	Pt	17.5	0.85	0.73	10.8	2% (1000 h, 1 sun)	172
TiO_2	N3	LiI 0.50 M and 50 mM I_2 in MPN	3	—	14.1	0.54	0.59	4.5	—	124
TiO_2 (4.5 μm)	N3	LiI 0.10 M and I_2 10 mM in MPN	4	Pt foil	1.96	0.541	0.67	4.8	—	43
BL + TiO_2 (10 μm)	N719	LiI 0.10 M, HDMII 0.60 M, I_2 50 mM, TBP 0.50 M and Triton X-100 20 mM in MPN	4	Pt	11.77	0.81	0.62	5.9	29% (7 d, dark)	156
TiO_2 (9 μm) + CH_3COOH[e]	N3	I_2 0.30 M, PVP 2% and TBMB 2% in MPII	5	Pt	10.9	0.52	0.42	2.4	—	303
TiO_2 (12 μm)	N719	DMPII 0.50 M, LiI 0.10 M, I_2 50 mM and $BBEG_n$ (n = 1) 0.50 M in ACN	10	Pt	4.19	0.8	0.69	2.31	7% (135 h)	145
TiO_2 (12 μm)	N719	DMPII 0.50 M, LiI 0.10 M, I_2 50 mM and $BBEG_n$ (n = 3) 0.50 M in ACN	10	Pt	5.75	0.8	0.64	2.96	40% (135 h)	145
$TiCl_4$ + TiO_2 (25 μm) + $TiCl_4$	MK-2HA	MPII 2.0 M, LiI 0.10 M, I_2 0.20 M, TBP 0.50 M in ACN	10	Pt	8.1	0.69	0.72	4.02	2.5% (200 h, dark)	243
TiO_2	N3	LiI 0.50 M, TBP 0.58 M and I_2 0.30 M in MPII	10	Pt	8.8	0.67	0.72	4.2[f]	—	293
TiO_2	N3	LiI 0.50 M, I_2 0.30 M and TBP 0.58 M in MPII	10	Pt	8.8	0.67	0.72	4.2[f]	—	294
BL + TiO_2 (10 μm) + $TiCl_4$	Z907 + CDCA	PMII 1.0 M, I_2 0.15 M, GuSCN 0.10 M and NBBI 0.50 M in MPN or ACN/VAN	10	Pt	15.67	0.68	0.71	7.52	7% (1000 h, 1 sun)	128
TiO_2 (7 μm) + $TiCl_4$	TG6	PMII 2.0 M, I_2 50 mM, GuSCN 0.10 M and TBP 0.50 M in MPN	20	Pt	8.5	0.84	0.73	5.2	Gain 2% (750 h, 1 sun, 35 °C)[g]	120
ZrO_2 (17.3 μm)	CV-G	$Ce(NO_3)_3$ 0.10 M and $Ce(NO_3)_4$ 50 mM in EtOH	30	Pt	0.52	0.624	0.53	0.688	—	178
$TiCl_4$ + TiO_2 (9 μm T + 5 μm SL)	Z907	KI 0.20 M, I_2 40 mM, PEG 4 wt% and PVP 2 wt% in ACN/VAN	50	Pt	7.368	0.625	0.5	2.306	37% (168 h, 1 sun)	310
TiO_2 (T + SL)	D5L6	PMII 2.0 M, I_2 50 mM, GuSCN 0.10 M, TBP 0.50 M and Triton X-100 1% in MPN	50	Pt	6.22	0.75	0.73	3.4	—	241
TiO_2 (T + SL)	JK-310	PMII 2.0 M, I_2 50 mM, GuSCN 0.10 M, TBP 0.50 M and Triton X-100 1% in MPN	50	Pt	6.62	0.75	0.76	3.77	—	241
TiO_2 (T + SL)	D21L6	PMII 2.0 M, I_2 50 mM, GuSCN 0.10 M, TBP 0.50 M and Triton X-100 1% in MPN	50	Pt	7.46	0.77	0.77	4.41	—	241
TiO_2 (12 μm T + 7 μm SL) + $TiCl_4$	TG6	PMII 4.0 M, I_2 0.30 M, TBP 1.5 M, GuSCN 0.20 M and xanthan gum 3 wt% in MPN	50	Pt	9.5	0.65	0.77	4.78	7% (288 h, dark, 65 °C, 85% RH)	318
TiO_2 (12 μm T + 7 μm SL) + $TiCl_4$	TG6	PMII 1.96 M, I_2 0.15 M, TBP 0.75 M and GuSCN 0.10 M in MPN	50	Pt	9.7	0.68	0.76	4.99	48% (288 h, dark, 65 °C, 85% RH)	318
BL + TiO_2 (12 μm) + $TiCl_4$	D907	BMII 2.0 M, I_2 50 mM and TBP 0.50 M in PEG	65	Pt	2.1	0.6	0.44	0.6	—	314
TiO_2 + Au NPs	MB	$FeCl_2$ 0.10 M, $FeCl_3$ 50 mM and $LiNO_3$ 0.10 M in EtOH	65	Ag	5.96	0.46	0.65	0.95	—	204
BL + TiO_2 (12 μm) + $TiCl_4$	D907	BMII 2.0 M, I_2 50 mM and TBP 0.50 M in P123	65	Pt	4.6	0.491	0.57	1.3	—	314
TiO_2 (15 μm)	N719	KI 0.50 M and I_2 25 mM in EtOH	65	Pt	4.24	0.51	0.60	1.3	—	138
TiO_2 (1.8 μm)	RhS	$Ce(NO_3)_3$ 0.10 M and 50 mM $Ce(NO_3)_4$ in EtOH	65	Ag	10.9	0.496	0.27	1.49	—	174
TiO_2 (15 μm)	N3	KI 0.50 M and I_2 25 mM in EtOH	65	Pt	4.94	0.55	0.63	1.7	—	138
BL + TiO_2 (12 μm) + $TiCl_4$	D907	BMII 2.0 M, I_2 50 mM and TBP 0.50 M in F77	65	Pt	6.2	0.595	0.53	2.1	3% (500 h)	314
TiO_2 (20 μm) + UV/O_3	N3 + TBP	KI 0.50 M and I_2 25 mM in EtOH	65	Pt	5.8	0.6	0.63	2.2	—	203
TiO_2 (3.3 μm)	PG	NaI 1.0 M and I_2 0.10 M	100	Pt	2.2[h]	0.44[h]	—	—	0% (24 h, under light[h])	256
TiO_2 (10 μm)	N3	LiI 0.10 M, I_2 10 mM, 0.5 wt% κ-carrageenan and HNO_3 (pH 2)	100	Pt plate	2.69	0.442	0.48	0.586	—	328
TiO_2 (15 μm)	N719	KI 0.50 M and I_2 25 mM	100	Pt	2.14	0.44	0.64	0.6	—	138
TiO_2 (15 μm)	N3	KI 0.50 M and I_2 25 mM	100	Pt	3.61	0.47	0.65	1.1	50% (75 d, dark, RT)	138

Table 20 (*continued*)

Anode[a]	Dye[b]	Electrolyte	H_2O (%)	Cathode[c]	J_{sc} (mA cm^{-2})	V_{oc} (V)	FF	η (%)	η_{loss}[d]	Ref.
$TiCl_4$ + TiO_2 (20 μm T + 4 μm SL) + $TiCl_4$	JK-259	PMII 2.0 M, I_2 50 mM, GuSCN 0.10 M, TBP 0.50 M and Triton X-100 1%	100	Pt	2.28	0.66	0.79	1.16	—	238
$TiCl_4$ + TiO_2 (3 μm T + 5 μm SL) + $TiCl_4$	V35	KI 4.0 M and I_2 20 mM, pH 8	100	PEDOT	5.60	0.485	0.63	1.71	Gain 58% (18 d, dark)	249
TiO_2 (8.9 μm) + $TiCl_4$	Z907 + CDCA	NaI 2.0 M, I_2 20 mM, GuSCN 0.50 M and CDCA until saturation	100	Pt	4.91	0.62	0.64	1.88	—	206
TiO_2	*cis*-$Ru(II)L_2(H_2O)_2^{2-i}$	KI 0.10 M and I_3^- 1.0 mM	100	Pt flag	0.38	0.52	0.7	2.0[j]	0% (4 d, 0.07 sun)	118
TiO_2 (2.8 μm T + 3.1 μm SL)	D205	TEMPOL 1.0 M and $NaBF_4$ 1.0 M	100	Pt:Teflon	4.5	0.69	0.64	2.1	—	274
$TiCl_4$ + TiO_2 (20 μm T + 4 μm SL) + $TiCl_4$	JK-262	PMII 2.0 M, I_2 50 mM, GuSCN 0.10 M, TBP 0.50 M and Triton X-100 1%	100	Pt	3.78	0.68	0.82	2.1	—	238
$TiCl_4$ + TiO_2 (3 μm T + 5 μm SL) + $TiCl_4$	V35	KI 4.0 M, I_2 20 mM and CDCA until saturation	100	Pt	4.86	0.600	0.76	2.20	—	249
TiO_2 (7 μm) + $TiCl_4$	TG6	PMII 2.0 M, I_2 50 mM, GuSCN 0.10 M, TBP 0.50 M and Triton X-100 1%	100	Pt	4.7	0.74	0.69	2.4	—	120
$TiCl_4$ + TiO_2 (3 μm T + 2 μm SL) + $TiCl_4$	D45	TT^-EMI^+ 0.20 M, DTT 0.20 M, TBP 0.50 M and 1% Triton X-100	100	Pt	7.2	0.65	0.55	2.6	37% (4 h, 1 sun, RT)	193
TiO_2 (8.9 μm) + $TiCl_4$	TG6	NaI 2.0 M, I_2 20 mM, GuSCN 0.50 M and CDCA until saturation	100	Pt	7.34	0.59	0.63	2.64	—	206
$TiCl_4$ + TiO_2 (3 μm T + 5 μm SL) + $TiCl_4$	V35	KI 2.0 M, I_2 10 mM and CDCA until saturation	100	PEDOT	6.85	0.650	0.67	3.01	—	249
TiO_2 (4.4 μm) + $TiCl_4$	N719	NaI 2.0 M, I_2 20 mM, GuSCN 1.0 M, HNO_3 (pH 3) and CDCA until saturation	100	Pt	8.5	0.59	0.63	3.08	—	206
$TiCl_4$ + TiO_2 (3 μm T + 2 μm SL) + $TiCl_4$	D51	TT^-EMI^+ 0.20 M, DTT 0.60 M, TBP 0.50 M and 1% Triton X-100	100	Pt	9.5	0.61	0.59	3.5	—	193
TiO_2 (13.3 μm)	N719 + CDCA	NaI 2.0 M, I_2 0.20 M, GuSCN 0.10 M and FC-134 0.2 wt%	100	Pt	10.97	0.53	0.68	3.96	63% (50 d, 1 sun, RT, UV filter)	163
TiO_2 (4.5 μm) + $TiCl_4$	D149	GuI 8.0 M, I_2 20 mM and CDCA until saturation	100	Pt	10.02	0.61	0.67	4.06	—	206
BL + TiO_2 (1.3 μm *T* + 5 μm SL) + $TiCl_4$	MK-2	$K_4Fe(CN)_6$ 0.40 M, $K_3Fe(CN)_6$ 40 mM, KCl 0.10 M, Trizma-HCl buffer 50 mM (pH 8) and Tween 20 0.1%	100	Pt mirror	7.2	0.76	0.75	4.1	50% (2 h)	182
TiO_2 (1 μm T + 3 μm SL)	MK-2	$[Co(bpy)_3]^{2+}$ 0.20 M, $[Co(bpy)_3]^{3+}$ 40 mM, NMBI 0.70 M NMBI and PEG 300 1%	100	Pt	8.3	0.68	0.72	4.2	10% (90 d, dark)	194
TiO_2 (9 μm T + 3 μm SL)	MD3	TEMPO 0.40 M, $NOBF_4$ 0.40 M, LiI 0.10 M, I_2 50 mM, DMPII 0.60 M, GuSCN 0.10 M and Tween 20 0.1%	100	Pt	9.56	0.77	0.67	4.96	—	258
TiO_2 (1 μm T + 3 μm SL)	MK-2	$[Co(bpy)_3]^{2+}$ 0.20 M, $[Co(bpy)_3]^{3+}$ 40 mM, NMBI 0.70 M NMBI and PEG 300 1%	100	Pt:ITO	9.8	0.69	0.74	5	Gain 2% (2 d, dark)	194
TiO_2 (1 μm T + 3 μm SL) + $TiCl_4$	MK-2	$[Co(bpy)_3](NO_3)_2$ 0.20 M, $[Co(bpy)_3](NO_3)_3$ 40 mM, NMBI 0.70 M and PEG 300 1 wt%	100	Pt	10.17	0.821	0.68	5.64	0% (500 h, dark)	210

[a] T means transparent layer, SL scattering layer, BL blocking layer. When "$TiCl_4$" is written before "TiO_2", it means that the treatment has been carried out to fabricate a BL. When "$TiCl_4$" is reported after "TiO_2", it means that the treatment has been performed after mesoporous TiO_2 deposition. "TiO_2" alone means that further data were not reported. [b] If a coadsorbent was employed, it has been reported in the table. [c] When "Pt" alone is reported, it means that Pt has been sputtered or thermally deposited following the traditional procedures. [d] If available, aging test conditions have been reported in the table. [e] Photoanodes were dipped in 1% acetic acid solution in toluene for 5 min, followed by rinsing with toluene. [f] Same PV data were reported by the same group in two different papers. [g] The cell was stored for 7 months in the dark before starting the aging test. [h] P_{in} not reported. [i] L is the 2,2′-bipyridyl-4,4′-dicarboxylate ligand. [j] P_{in} = 0.07 sun.

and GuSCN 0.20 M in MPN) was selected. As reported in Table 19, resulting aqueous DSSCs, both liquid and quasi-solid, showed higher V_{oc} and FF, but lower J_{sc} values with respect to the MPN-based liquid counterpart. The decrease in J_{sc} was related to the desorption of the dye from the TiO_2 electrode surface. Actually, even if the hydrophobic TG6 dye was used, it was not possible to fully prevent the dye molecules from being desorbed; moreover, the I_3^- diffusion coefficient was decreased when water was introduced. As regards V_{oc}, both E of the electrolyte and the CB of the TiO_2 positively shifted in the presence of aqueous electrolytes; however, the shift was found to be more significant for E, thus resulting in enhanced photovoltage values. Noteworthy, the quasi-solid aqueous cell exhibited a performance in terms of overall efficiency comparable with that of the liquid one (*i.e.*, 4.78% *vs.* 4.99%): this was ascribed to the thixotropic nature of the gel-polymer matrix, which could infiltrate as a liquid into the photoanode, in spite of the scarce wetting ability typically observed when solid polymer electrolytes are used,[319,320] being their macromolecular chain radius of gyration larger than the pore size of TiO_2.[69,321,322] During extreme 288 h aging tests (65 °C and 85% RH), the water-based liquid DSSC retained around 50% of its initial efficiency, while the quasi-solid one remarkably provided the 93% of its initial value. Such results demonstrated that the xanthan gum was able not only to prevent the leakage of the solvent from the DSSC, but also to reduce the number of dye molecules desorbed from the photoanode at high temperature.

As evidenced in the present section, the overall performances of quasi-solid water-based DSSCs are definitely interesting, particularly because of the excellent long-term stability demonstrated by these devices. Nevertheless, there is still room for further improvements. As an example, in terms of materials selection, a highly ambitious challenge would be the replacement of the oil-derived polymer matrixes by means of biosourced ones.[57,323–326] In the field of water-based DSSCs, a first attempt has been proposed by Kaneko and coworkers, who reported that polysaccharides such as agarose and κ-carrageenan[327] can form a tight and elastic solid able to retain the aqueous electrolyte (LiI 0.10 M and I_2 10 mM in H_2O, pH 2).[328] Detachment of the N3 dye from the TiO_2 electrode was not observed even after prolonged irradiation times; moreover EIS analysis showed that the electron donation from the I^- to the oxidized sensitizer took place in a similar way both in the quasi-solid and in the liquid state. Unfortunately, the authors published only a preliminary efficiency value of 0.586% (J_{sc} = 2.69 mA cm^{-2}, V_{oc} = 0.442 V, FF = 0.48) in the presence of 0.5 wt% κ-carrageenan, without any optimization of the electrolyte composition which, in our opinion, could have led to definitely higher performance.

14. Conclusions

DSSC represents the most widely studied device for the conversion of solar energy into electricity, particularly when low costs and good performance are envisaged. In this review article, the key role of water, being one of the most promising research strategy in the field of DSSCs, has been elucidated and thoroughly discussed by analysing the most significant literature reports, with particular attention to the impressive results achieved during the last three years.

After an exhaustive analysis of the interactions between water and the other cell components – previously considered exclusively harmful – we have shown how the solvent-of-life may adequately replace the traditionally used organic solvents. This would make DSSCs cheaper as well as less dangerous in terms of flammability and toxicity, thus even more environmentally friendly. In order to fabricate efficient aqueous DSSCs, several research groups worldwide are involved in an impressive scientific work, proposing new dyes, photoelectrodes, counter electrodes, redox couples, additives and sealants. As summarized in Table 20, the results obtained so far in terms of efficiency and durability are promising, sometimes outstanding, and fully justify the recent boom in the research and development of aqueous DSSCs.

Summarising, it seems that the main factor that negatively affects the efficiency of aqueous DSSC if compared to those based on organic solvents is the quality of the photoanode/electrolyte interface. Indeed, excessive hydrophilicity of the dye-sensitized surface favours sensitizer molecule desorption, thus decreasing the photocurrent and the stability over time; on the other hand, highly hydrophobic dyes do not allow the complete wettability of the electrode which, in turn, results in a less effective regeneration process for aqueous electrolytes. An optimum between these two extremes has not been achieved so far, and the creation of an intimate photoanode/electrolyte interface will be one of the main research goals in the coming years. At present, the most effective strategies towards realistic aqueous DSSCs include the use of cobalt complexes (preferably in the gel form) as redox mediators, hydrophobic dyes combined/functionalized with surfactants or weakly hydrophilic dyes obtained by the modification of already available sensitizers, and water-tolerant counter electrodes with a wide surface area. However, the study of aqueous DSSCs is at an early stage and comparative studies that could greatly improve the knowledge of these systems are still lacking.

The sum of the above reported intriguing features accounts for the promising prospects of the novel materials described here to be effectively implemented in the emerging business of aqueous DSSC manufacturing. The use of water in solar energy conversion devices was intended to be a big bet by a great part of the scientific community but, based on the results discussed in this review article, it may very soon become the key for success of this green technology to finally enter into the mass production stage.

Abbreviations

ABC	Amphiphilic block copolymer
ACN	Acetonitrile
AOT	Bis(2-ethylhexyl) sulfosuccinate sodium salt
$BBEG_n$	Bis-benzimidazole derivatives containing an ethylene glycol repeating unit

BMII	1-Butyl-3-methylimidazolium iodide
CA	Contact angle
CB	Conduction band
CDCA	Chenodeoxycholic acid
CPMD	Car–Parrinello molecular dynamics
CTAB	Hexadecyltrimethylammonium bromide
CV-G	Green part of *Codiaeum varie*
D	Electron diffusion constant
D(ion)	Apparent diffusion constant for the given ion
DMHII	3-Hexyl-1,2-dimethylimidazolium iodide
DMPII	1,2-Dimethyl-3-propylimidazolium iodide
DRIFT	Diffuse-reflectance infrared Fourier transform
DSSC	Dye-sensitized solar cell
DTT	3,3′-Dithiobis[4-methyl-(1,2,4)-triazole]
E	Redox mediator potential
E_c	CB energy
E_f	Fermi level electrochemical potential
EC	Ethylene carbonate
EDX	Energy dispersive X-ray analysis
EIS	Electrochemical impedance spectroscopy
$EMIm^+$	1-Ethyl-3-methylimidazolium
FC-134	*N*,*N*,*N*-Trimethyl-3-(perfluorooctyl sulfonamido)-propan-1-aminium iodide
FF	Fill factor
FK-1	Triethylammonium perfluorooctane sulphonate
FTIR	Fourier transform infrared
GBL	γ-Butyrolactone
GF	Glass frit
GuI	Guanidinium iodide
GuSCN	Guanidinium thiocyanate
HDMII	1-Hexyl-2,3-dimethylimidazolium iodide
HMII	1-Hexyl-3-methylimidazolium iodide
IPCE	Incident photon to current efficiency
I_{sc}	Short-circuit current
J_{dl}	Diffusion limited current
J_{sc}	Short-circuit current density
L	Electron diffusion length
MAN	Methoxyacetonitrile
MPII	1-Methyl-3-propylimidazolium iodide
MPN	3-Methoxypropionitrile
NBBI	*N*-Butylbenzimidazole
NMBI	*N*-Methylbenzimidazole
NMP	*N*-Methylpyrrolidone
NPs	Nanoparticles
ODTS	Octadecyltrichlorosilane
PC	Propylene carbonate
PEDOT	Poly(3,4-ethylenedioxythiophene)
PEG	Poly(ethylene glycol)
PEO	Poly(ethylene oxide)
PES	Photoelectron spectroscopy
PG	Pomegranate
P_{in}	Irradiation intensity
PMII	1-Propyl-3-methylimidazolium iodide
PPO	Poly(propylene oxide)
PSC	Perovskite solar cell
PV	Photovoltaic
PVP	Poly(vinylpyridine)
PVPi	Poly(vinylpyrrolidone)
R_{CE}	Charge transfer resistance at the counter electrode
RH	Relative humidity
RhS	Rhoeo spathacea
R_s	Series resistance
RT	Room temperature
RTIL	Room temperature ionic liquid
TAS	Transient adsorption spectroscopy
TBA	Tetrabutylammonium
TBAI	Tetrabutylammonium iodide
TBP	4-*tert*-Butylpyridine
TCO	Transparent conductive oxide
TDDFT	Time-dependent density functional theory
TEMPOL	4-Hydroxy-2,2,6,6-tetramethylpiperidinoxyl
$TFSI^-$	Bistriflimide
TT^-EMI^+	1-Ethyl-3-methylimidazolium 4-methyl-1,2,4-triazole-3-thiolate
UV-Vis	Ultraviolet-visible
VAN	Valeronitrile
V_{oc}	Open-circuit voltage
3D	Three-dimensional
η	Cell efficiency
λ_{max}	Absorption maximum
μ	Viscosity
σ	Ionic conductivity
τ	Electron lifetime
χ_w	Mole fraction of water

Acknowledgements

C.B. gratefully acknowledges financial support by DSSCX project (PRIN 2010-2011, 20104XET32) from Ministero dell'Istruzione, dell'Università e della Ricerca.

References

1 R. A. Mulhall and J. R. Bryson, Energy price risk and the sustainability of demand side supply chains, *Appl. Energy*, 2014, **123**, 327–334.
2 P. Faria, T. Soares, Z. Vale and H. Morais, Distributed generation and demand response dispatch for a virtual power player energy and reserve provision, *Renewable Energy*, 2014, **66**, 686–695.
3 T. C. Kandpal and L. Broman, Renewable energy education: a global status review, *Renewable Sustainable Energy Rev.*, 2014, **34**, 300–324.
4 D. Neves, C. A. Silva and S. Connors, Design and implementation of hybrid renewable energy systems on micro-communities: a review on case studies, *Renewable Sustainable Energy Rev.*, 2014, **31**, 935–946.
5 G. D. A. Jebaselvi and S. Paramasivam, Analysis on renewable energy systems, *Renewable Sustainable Energy Rev.*, 2013, **28**, 625–634.

6 M. Grätzel, Photoelectrochemical cells, *Nature*, 2001, **414**, 338–344.
7 C. J. Brabec, M. Heeney, I. McCulloch and J. Nelson, Influence of blend microstructure on bulk heterojunction organic photovoltaic performance, *Chem. Soc. Rev.*, 2011, **40**, 1185–1199.
8 J. Li and A. C. Grimsdale, Carbazole-based polymers for organic photovoltaic devices, *Chem. Soc. Rev.*, 2010, **39**, 2399–2410.
9 A. Bessette and G. S. Hanan, Design, synthesis and photophysical studies of dipyrromethene-based materials: Insights into their applications in organic photovoltaic devices, *Chem. Soc. Rev.*, 2014, **43**, 3342–3405.
10 M. T. Dang and J. D. Wuest, Using volatile additives to alter the morphology and performance of active layers in thin-film molecular photovoltaic devices incorporating bulk heterojunctions, *Chem. Soc. Rev.*, 2013, **42**, 9105–9126.
11 E. D. Dunlop and D. Halton, The performance of crystalline silicon photovoltaic solar modules after 22 years of continuous outdoor exposure, *Prog. Photovoltaics*, 2006, **14**, 53–64.
12 A. Shah, P. Torres, R. Tscharner, N. Wyrsch and H. Keppner, Photovoltaic technology: the case for thin-film solar cells, *Science*, 1999, **285**, 692–698.
13 L. Dou, J. You, Z. Hong, Z. Xu, G. Li, R. A. Street and Y. Yang, 25th anniversary article: a decade of organic/polymeric photovoltaic research, *Adv. Mater.*, 2013, **25**, 6642–6671.
14 B. C. O'Regan and M. Grätzel, A low-cost, high-efficiency solar cell based on dye-sensitized colloidal TiO_2 films, *Nature*, 1991, **353**, 737–740.
15 T. Kawashima, T. Ezure, K. Okada, H. Matsui, K. Goto and N. Tanabe, FTO/ITO double-layered transparent conductive oxide for dye-sensitized solar cells, *J. Photochem. Photobiol., A*, 2004, **164**, 199–202.
16 P. Roy, D. Kim, K. Lee, E. Spiecker and P. Schmuki, TiO_2 nanotubes and their application in dye-sensitized solar cells, *Nanoscale*, 2010, **2**, 45–59.
17 Y. Qina and Q. Peng, Ruthenium sensitizers and their applications in dye-sensitized solar cells, *Int. J. Photoenergy*, 2012, **2012**, 291579.
18 F. Bella and R. Bongiovanni, Photoinduced polymerization: an innovative, powerful and environmentally friendly technique for the preparation of polymer electrolytes for dye-sensitized solar cells, *J. Photochem. Photobiol., C*, 2013, **16**, 1–21.
19 S. Thomas, T. G. Deepak, G. S. Anjusree, T. A. Arun, S. V. Nair and A. S. Nair, A review on counter electrode materials in dye-sensitized solar cells, *J. Mater. Chem. A*, 2014, **2**, 4474–4490.
20 M. Grätzel, Dye-sensitized solar cells, *J. Photochem. Photobiol., C*, 2003, **4**, 145–153.
21 A. Hagfeldt, G. Boschloo, L. Sun, L. Kloo and H. Pettersson, Dye-Sensitized Solar Cells, *Chem. Rev.*, 2010, **110**, 6595–6663.
22 B. E. Hardin, H. J. Snaith and M. D. McGehee, The renaissance of dye-sensitized solar cells, *Nat. Photonics*, 2012, **6**, 162–169.
23 G. Griffini, F. Bella, F. Nisic, C. Dragonetti, D. Roberto, M. Levi, R. Bongiovanni and S. Turri, Multifunctional luminescent down-shifting fluoropolymer coatings: a straightforward strategy to improve the UV-light harvesting ability and long-term outdoor stability of organic dye-sensitized solar cells, *Adv. Energy Mater.*, 2015, **5**, 1401312.
24 D. Rosestolato, J. Fregoni, S. Ferro and A. De Battisti, Influence of the nature of the electrode material and process variables on the kinetics of the chlorine evolution reaction. the case of IrO_2-based electrocatalysts, *Electrochim. Acta*, 2014, **139**, 180–189.
25 M. Law, L. E. Greene, J. C. Johnson, R. Saykally and P. Yang, Nanowire dye-sensitized solar cells, *Nat. Mater.*, 2005, **4**, 455–459.
26 U. Bach, D. Lupo, P. Comte, J. E. Moser, F. Weissörtel, J. Salbeck, H. Spreitzer and M. Grätzel, Solid-state dye-sensitized mesoporous TiO_2 solar cells with high photon-to-electron conversion efficiencies, *Nature*, 1998, **395**, 583–585.
27 X. Wang, L. Zhi and K. Müllen, Transparent, conductive graphene electrodes for dye-sensitized solar cells, *Nano Lett.*, 2008, **8**, 323–327.
28 G. K. Mor, K. Shankar, M. Paulose, O. K. Varghese and C. A. Grimes, Use of highly-ordered TiO_2 nanotube arrays in dye-sensitized solar cells, *Nano Lett.*, 2006, **6**, 215–218.
29 S. Mathew, A. Yella, P. Gao, R. Humphry-Baker, B. F. E. Curchod, N. Ashari-Astani, I. Tavernelli, U. Rothlisberger, M. K. Nazeeruddin and M. Grätzel, Dye-sensitized solar cells with 13% efficiency achieved through the molecular engineering of porphyrin sensitizers, *Nat. Chem.*, 2014, **6**, 242–247.
30 H. Li, Z. Yang, L. Qiu, X. Fang, H. Sun, P. Chen, S. Pan and H. Peng, Stable wire-shaped dye-sensitized solar cells based on eutectic melts, *J. Mater. Chem. A*, 2014, **2**, 3841–3846.
31 J. M. Pringle, Recent progress in the development and use of organic ionic plastic crystal electrolytes, *Phys. Chem. Chem. Phys.*, 2013, **15**, 1339–1351.
32 T. M. Brown, F. De Rossi, F. Di Giacomo, G. Mincuzzi, V. Zardetto, A. Realea and A. Di Carlo, Progress in flexible dye solar cell materials, processes and devices, *J. Mater. Chem. A*, 2014, **2**, 10788–10817.
33 F. Bella, A. Lamberti, A. Sacco, S. Bianco, A. Chiodoni and R. Bongiovanni, Novel electrode and electrolyte membranes: towards flexible dye-sensitized solar cell combining vertically aligned TiO_2 nanotube array and light-cured polymer network, *J. Membr. Sci.*, 2014, **470**, 125–131.
34 Y. G. Tropsha and N. G. Harvey, Activated rate theory treatment of oxygen and water transport through silicon oxide/poly(ethylene terephthalate) composite barrier structures, *J. Phys. Chem. B*, 1997, **101**, 2259–2266.
35 A. Yella, H. W. Lee, H. N. Tsao, C. Yi, A. K. Chandiran, M. K. Nazeeruddin, E. W. G. Diau, C. Y. Yeh, S. M. Zakeeruddin and M. Grätzel, Porphyrin-sensitized solar cells with cobalt(II/III)-based redox electrolyte exceed 12 percent efficiency, *Science*, 2011, **334**, 629–634.

36 G. Oskam, B. V. Bergeron, G. J. Meyer and P. C. Searson, Pseudohalogens for dye-sensitized TiO_2 photoelectrochemical cells, *J. Phys. Chem. B*, 2001, **105**, 6867–6873.
37 F. Bella, A. Sacco, G. P. Salvador, S. Bianco, E. Tresso, C. F. Pirri and R. Bongiovanni, First pseudohalogen polymer electrolyte for dye-sensitized solar cells promising for *in situ* photopolymerization, *J. Phys. Chem. C*, 2013, **117**, 20421–20430.
38 S. Ferrere, A. Zaban and B. A. Gregg, Dye sensitization of nanocrystalline tin oxide by perylene derivatives, *J. Phys. Chem. B*, 1997, **101**, 4490–4493.
39 Y. Liu, J. R. Jennings and Q. Wang, Efficient dye-sensitized solar cells using a tetramethylthiourea redox mediator, *ChemSusChem*, 2013, **6**, 2124–2131.
40 Y. Bai, Q. Yu, N. Cai, Y. Wang, M. Zhang and P. Wang, High-efficiency organic dye-sensitized mesoscopic solar cells with a copper redox shuttle, *Chem. Commun.*, 2011, **47**, 4376–4378.
41 T. Daeneke, T. H. Kwon, A. B. Holmes, N. W. Duffy, U. Bach and L. Spiccia, High-efficiency dye-sensitized solar cells with ferrocene-based electrolytes, *Nat. Chem.*, 2011, **3**, 211–215.
42 F. Kato, A. Kikuchi, T. Okuyama, K. Oyaizu and H. Nishide, Nitroxide radicals as highly reactive redox mediators in dye-sensitized solar cells, *Angew. Chem., Int. Ed.*, 2012, **51**, 10177–10180.
43 Y. Liu, A. Hagfeldt, X. R. Xiao and S. E. Lindquist, Investigation of influence of redox species on the interfacial energetics of a dye-sensitized nanoporous TiO_2 solar cell, *Sol. Energy Mater. Sol. Cells*, 1998, **55**, 267–281.
44 G. Boschloo, L. Häggman and A. Hagfeldt, Quantification of the effect of 4-*tert*-butylpyridine addition to I^-/I_3^- redox electrolytes in dye-sensitized nanostructured TiO_2 solar cells, *J. Phys. Chem. B*, 2006, **110**, 13144–13150.
45 C. N. Zhang, Y. Huang, Z. P. Huo, S. H. Chen and S. Y. Dai, Photoelectrochemical effects of guanidinium thiocyanate on dye-sensitized solar cell performance and stability, *J. Phys. Chem. C*, 2009, **113**, 21779–21783.
46 V. Gutmann, Empirical parameters for donor and acceptor properties of solvents, *Electrochim. Acta*, 1976, **21**, 661–670.
47 J. Wu, Z. Lan, S. Hao, P. Li, J. Lin, M. Huang, L. Fang and Y. Huang, Progress on the electrolytes for dye-sensitized solar cells, *Pure Appl. Chem.*, 2008, **80**, 2241–2258.
48 D. R. Macfarlane, N. Tachikawa, M. Forsyth, J. M. Pringle, P. C. Howlett, G. D. Elliott, J. H. Davis, M. Watanabe, P. Simon and C. A. Angell, Energy applications of ionic liquids, *Energy Environ. Sci.*, 2014, **7**, 232–250.
49 M. Wang, C. Grätzel, S. M. Zakeeruddin and M. Grätzel, Recent developments in redox electrolytes for dye-sensitized solar cells, *Energy Environ. Sci.*, 2012, **5**, 9394–9405.
50 J. Cong, X. Yang, L. Kloo and L. Sun, Iodine/iodide-free redox shuttles for liquid electrolyte-based dye-sensitized solar cells, *Energy Environ. Sci.*, 2012, **5**, 9180–9194.
51 G. Boschloo and A. Hagfeldt, Characteristics of the iodide/triiodide redox mediator in dye-sensitized solar cells, *Acc. Chem. Res.*, 2009, **42**, 1819–1826.
52 S. Yanagida, Y. Yu and K. Manseki, Iodine/iodide-free dye-sensitized solar cells, *Acc. Chem. Res.*, 2009, **42**, 1827–1838.
53 Z. Yu, N. Vlachopoulos, M. Gorlov and L. Kloo, Liquid electrolytes for dye-sensitized solar cells, *Dalton Trans.*, 2011, **40**, 10289–10303.
54 N. Jiang, T. Sumitomo, T. Lee, A. Pellaroque, O. Bellon, D. Milliken and H. Desilvestro, High temperature stability of dye solar cells, *Sol. Energy Mater. Sol. Cells*, 2013, **119**, 36–50.
55 M. F. Aziz, I. M. Noor, B. Sahraoui and A. K. Arof, Dye-sensitized solar cells with PVA-KI-EC-PC gel electrolytes, *Opt. Quantum Electron.*, 2014, **46**, 133–141.
56 N. T. Dintcheva, M. Furlani, W. J. M. J. S. R. Jayasundara, T. M. W. J. Bandara, B. E. Mellander and F. P. La Mantia, Rheological behavior of PAN-based electrolytic gel containing tetrahexylammonium and magnesium iodide for photoelectrochemical applications, *Rheol. Acta*, 2013, **52**, 881–889.
57 F. Bella, J. R. Nair and C. Gerbaldi, Towards green, efficient and durable quasi-solid dye-sensitized solar cells integrated with a cellulose-based gel-polymer electrolyte optimized by a chemometric DoE approach, *RSC Adv.*, 2013, **3**, 15993–16001.
58 F. Bella, D. Pugliese, J. R. Nair, A. Sacco, S. Bianco, C. Gerbaldi, C. Barolo and R. Bongiovanni, A UV-crosslinked polymer electrolyte membrane for quasi-solid dye-sensitized solar cells with excellent efficiency and durability, *Phys. Chem. Chem. Phys.*, 2013, **15**, 3706–3711.
59 F. Bella, E. D. Ozzello, A. Sacco, S. Bianco and R. Bongiovanni, Polymer electrolytes for dye-sensitized solar cells prepared by photopolymerization of PEG-based oligomers, *Int. J. Hydrogen Energy*, 2014, **39**, 3036–3045.
60 B. Wang, S. Chang, L. T. L. Lee, S. Zheng, K. Y. Wong, Q. Li, X. Xiao and T. Chen, Improving pore filling of gel electrolyte and charge transport in photoanode for high-efficiency quasi-solid-state dye-sensitized solar cells, *ACS Appl. Mater. Interfaces*, 2013, **5**, 8289–8293.
61 S. Yuan, Q. Tang, B. He and P. Yang, Efficient quasi-solid-state dye-sensitized solar cells employing polyaniline and polypyrrole incorporated microporous conducting gel electrolytes, *J. Power Sources*, 2014, **254**, 98–105.
62 S. Yuan, Q. Tang, B. Hu, C. Ma, J. Duan and B. He, Efficient quasi-solid-state dye-sensitized solar cells from graphene incorporated conducting gel electrolytes, *J. Mater. Chem. A*, 2014, **2**, 2814–2821.
63 K. C. Huang, R. Vittal and K. C. Ho, Effects of crown ethers in nanocomposite silica-gel electrolytes on the performance of quasi-solid-state dye-sensitized solar cells, *Sol. Energy Mater. Sol. Cells*, 2010, **94**, 675–679.
64 W. S. Chi, D. K. Roh, S. J. Kim, S. Y. Heo and J. H. Kim, Hybrid electrolytes prepared from ionic liquid-grafted alumina for high-efficiency quasi-solid-state dye-sensitized solar cells, *Nanoscale*, 2013, **5**, 5341–5348.
65 Z. Lan, J. Wu, D. Wang, S. Hao, J. Lin and Y. Huang, Quasi-solid-state dye-sensitized solar cells based on a sol–gel organic–inorganic composite electrolyte containing an organic iodide salt, *Sol. Energy*, 2007, **81**, 117–122.

66 F. Bella, E. D. Ozzello, S. Bianco and R. Bongiovanni, Photo-polymerization of acrylic/methacrylic gel-polymer electrolyte membranes for dye-sensitized solar cells, *Chem. Eng. J.*, 2013, **225**, 873–879.

67 D. Song, W. Cho, J. H. Lee and Y. S. Kang, Toward higher energy conversion efficiency for solid polymer electrolyte dye-sensitized solar cells: ionic conductivity and TiO_2 pore-filling, *J. Phys. Chem. Lett.*, 2014, **5**, 1249–1258.

68 J. N. de Freitas, A. F. Nogueira and M. A. De Paoli, New insights into dye-sensitized solar cells with polymer electrolytes, *J. Mater. Chem.*, 2009, **19**, 5279–5294.

69 Y. Wang, Recent research progress on polymer electrolytes for dye-sensitized solar cells, *Sol. Energy Mater. Sol. Cells*, 2009, **93**, 1167–1175.

70 G. R. A. Kumara, J. K. Tiskumara, C. S. K. Ranasinghe, I. S. Rathnayake, W. M. N. M. B. Wanninayake, E. N. Jayaweera, L. R. A. K. Bandara and R. M. G. Rajapakse, Efficient solid-state dye-sensitized n-ZnO/D-358 dye/p-CuI solar cell, *Electrochim. Acta*, 2013, **94**, 34–37.

71 C. D. Bailie, E. L. Unger, S. M. Zakeeruddin, M. Grätzel and M. D. McGehee, Melt-infiltration of spiro-OMeTAD and thermal instability of solid-state dye-sensitized solar cells, *Phys. Chem. Chem. Phys.*, 2014, **16**, 4864–4870.

72 B. W. Park, L. Yang, E. M. J. Johansson, N. Vlachopoulos, A. Chams, C. Perruchot, M. Jouini, G. Boschloo and A. Hagfeldt, Neutral, polaron, and bipolaron states in PEDOT prepared by photoelectrochemical polymerization and the effect on charge generation mechanism in the solid-state dye-sensitized solar cell, *J. Phys. Chem. C*, 2013, **117**, 22484–22491.

73 C. Y. Hsu, Y. C. Chen, R. Y. Y. Lin, K. C. Ho and J. T. Lin, Solid-state dye-sensitized solar cells based on spirofluorene (spiro-OMeTAD) and arylamines as hole transporting materials, *Phys. Chem. Chem. Phys.*, 2012, **14**, 14099–14109.

74 B. Li, L. Wang, B. Kang, P. Wang and Y. Qiu, Review of recent progress in solid-state dye-sensitized solar cells, *Sol. Energy Mater. Sol. Cells*, 2006, **90**, 549–573.

75 J. Bouclé and J. Ackermann, Solid-state dye-sensitized and bulk heterojunction solar cells using TiO_2 and ZnO nanostructures: recent progress and new concepts at the borderline, *Polym. Int.*, 2012, **61**, 355–373.

76 M. Liu, M. B. Johnston and H. J. Snaith, Efficient planar heterojunction perovskite solar cells by vapour deposition, *Nature*, 2013, **501**, 395–398.

77 A. Marchioro, J. Teuscher, D. Friedrich, M. Kunst, R. Van De Krol, T. Moehl, M. Grätzel and J. E. Moser, Unravelling the mechanism of photoinduced charge transfer processes in lead iodide perovskite solar cells, *Nat. Photonics*, 2014, **8**, 250–255.

78 C. Roldán-Carmona, O. Malinkiewicz, A. Soriano, G. Mínguez Espallargas, A. Garcia, P. Reinecke, T. Kroyer, M. I. Dar, M. K. Nazeeruddin and H. J. Bolink, Flexible high efficiency perovskite solar cells, *Energy Environ. Sci.*, 2014, **7**, 994–997.

79 H. Zhou, Q. Chen, G. Li, S. Luo, T. B. Song, H. S. Duan, Z. Hong, J. You, Y. Liu and Y. Yang, Interface engineering of highly efficient perovskite solar cells, *Science*, 2014, **345**, 542–546.

80 National Center for Photovoltaics (NCPV) at NREL, http://www.nrel.gov/ncpv.

81 M. K. Nazeeruddin, A. Kay, I. Rodicio, R. Humphry-Baker, E. Mueller, P. Liska, N. Vlachopoulos and M. Grätzel, Conversion of light to electricity by *cis*-X_2bis(2,2′-bipyridyl-4,4′-dicarboxylate)ruthenium(II) charge-transfer sensitizers (X = Cl^-, Br^-, I^-, CN^-, and SCN^-) on nanocrystalline TiO_2 electrodes, *J. Am. Chem. Soc.*, 1993, **115**, 6382–6390.

82 H. Lindström, S. Södergren, A. Solbrand, H. Rensmo, J. Hjelm, A. Hagfeldt and S. E. Lindquist, Li^+ ion insertion in TiO_2 (anatase). 2. Voltammetry on nanoporous films, *J. Phys. Chem. B*, 1997, **101**, 7717–7722.

83 B. Enright, G. Redmond and D. Fitzmaurice, Spectroscopic determination of flatband potentials for polycrystalline TiO_2 electrodes in mixed solvent systems, *J. Phys. Chem.*, 1994, **98**, 6195–6200.

84 S. Y. Huang, G. Schlichthörl, A. J. Nozik, M. Grätzel and A. J. Frank, Charge recombination in dye-sensitized nanocrystalline TiO_2 solar cells, *J. Phys. Chem. B*, 1997, **101**, 2576–2582.

85 H. G. Agrell, J. Lindgren and A. Hagfeldt, Degradation mechanisms in a dye-sensitized solar cell studied by UV-Vis and IR spectroscopy, *Sol. Energy*, 2003, **75**, 169–180.

86 H. L. Lu, T. F. R. Shen, S. T. Huang, Y. L. Tung and T. C. K. Yang, The degradation of dye sensitized solar cell in the presence of water isotopes, *Sol. Energy Mater. Sol. Cells*, 2011, **95**, 1624–1629.

87 Y. Cho, L. B. Sagle, S. Iimura, Y. Zhang, J. Kherb, A. Chilkoti, J. M. Scholtz and P. S. Cremer, Hydrogen bonding of β-turn structure is stabilized in D_2O, *J. Am. Chem. Soc.*, 2009, **131**, 15188–15193.

88 D. Lacelle, M. Fontaine, A. P. Forest and S. Kokelj, High-resolution stable water isotopes as tracers of thaw unconformities in permafrost: a case study from western Arctic Canada, *Chem. Geol.*, 2014, **368**, 85–96.

89 M. K. Nazeeruddin, E. Muller, R. Humphry-Baker, N. Vlachopoulos and M. Grätzel, Redox regulation in ruthenium(II) polypyridyl complexes and their application in solar energy conversion, *J. Chem. Soc., Dalton Trans.*, 1997, 4571–4578.

90 H. Lindstrom, S. Sodergren, A. Solbrand, H. Rensmo, J. Hjelm, A. Hagfeldt and S. E. Lindquist, Li^+ ion insertion in TiO_2 (anatase). 1. Chronoamperometry on CVD films and nanoporous films, *J. Phys. Chem. B*, 1997, **101**, 7710–7716.

91 M. Chabanel and Z. Wang, Vibrational study of ionic association in aprotic solvents. 6. Dimerization of lithium, sodium, and potassium isothiocyanate ion pairs in tetrahydrofuran and in 1,3-dioxolane, *J. Phys. Chem.*, 1984, **88**, 1441–1445.

92 E. H. Hardy, A. Zygar, M. D. Zeidler, M. Holz and F. D. Sacher, Isotope effect on the translational and rotational motion in liquid water and ammonia, *J. Chem. Phys.*, 2001, **114**, 3174–3181.

93 M. Turrion, B. Macht, P. Salvador and H. Tributsch, Imaging techniques for the study of photodegradation of dye sensitization cells, *Z. Phys. Chem.*, 1999, **212**, 51–57.
94 H. Tributsch, A. Barkschat, T. Moehl and B. Macht, The function of TiO_2 with respect to sensitizer stability in nanocrystalline dye solar cells, *Int. J. Photoenergy*, 2008, **2008**, 814951.
95 B. Macht, M. Turrion, A. Barkschat, P. Salvador, K. Ellmer and H. Tributsch, Patterns of efficiency and degradation in dye sensitization solar cells measured with imaging techniques, *Sol. Energy Mater. Sol. Cells*, 2002, **73**, 163–173.
96 A. J. Bard, *Encyclopedia of the Electrochemistry of the Elements*, Marcel Dekker, New York, 1973, vol. 1, p. 93.
97 K. Nakamoto, *Infrared and Raman Spectra of Inorganic and Coordination Compounds*, Wiley, New York, 1978.
98 M. J. Scott, M. Woodhouse, B. A. Parkinson and C. M. Elliott, Spatially resolved current-voltage measurements – Evidence for nonuniform photocurrents in dye-sensitized solar cells, *J. Electrochem. Soc.*, 2008, **155**, B290–B293.
99 T. A. G. Risbridger, F. A. Castro and P. J. Cameron, Two-dimensional photocurrent and transmission mapping of aqueous dye-sensitized solar cells, *J. Phys. Chem. C*, 2012, **116**, 22253–22260.
100 J. H. Yum, P. Walter, S. Huber, D. Rentsch, T. Geiger, F. Nüesch, F. De Angelis, M. Grätzel and M. K. Nazeeruddin, Efficient far red sensitization of nanocrystalline TiO_2 films by an unsymmetrical squaraine dye, *J. Am. Chem. Soc.*, 2007, **129**, 10320–10321.
101 D. Pugliese, A. Lamberti, F. Bella, A. Sacco, S. Bianco and E. Tresso, TiO_2 nanotubes as flexible photoanode for back-illuminated dye-sensitized solar cells with hemi-squaraine organic dye and iodine-free transparent electrolyte, *Org. Electron.*, 2014, **15**, 3715–3722.
102 A. Vittadini, A. Selloni, F. P. Rotzinger and M. Gräztel, Structure and energetics of water adsorbed at TiO_2 anatase (101) and (001) surfaces, *Phys. Rev. Lett.*, 1998, **81**, 2954–2957.
103 F. De Angelis, S. Fantacci and R. Gebauer, Simulating dye-sensitized TiO_2 heterointerfaces in explicit solvent: absorption spectra, energy levels, and dye desorption, *J. Phys. Chem. Lett.*, 2011, **2**, 813–817.
104 A. Tilocca and A. Selloni, Vertical and lateral order in adsorbed water layers on anatase TiO_2(101), *Langmuir*, 2004, **20**, 8379–8384.
105 R. Katoh, A. Furube, M. Kasuya, N. Fuke, N. Koide and L. Han, Photoinduced electron injection in black dye sensitized nanocrystalline TiO_2 films, *J. Mater. Chem.*, 2007, **17**, 3190–3196.
106 T. Takamuku, M. Tabata, A. Yamaguchi, J. Nishimoto, M. Kumamoto, H. Wakita and T. Yamaguchi, Liquid structure of acetonitrile-water mixtures by X-ray diffraction and infrared spectroscopy, *J. Phys. Chem. B*, 1998, **102**, 8880–8888.
107 X. Grabuleda, C. Jaime and P. A. Kollman, Molecular dynamics simulation studies of liquid acetonitrile: new six-site model, *J. Comput. Chem.*, 2000, **21**, 901–908.
108 M. Sumita, K. Sodeyama, L. Han and Y. Tateyama, Water contamination effect on liquid acetonitrile/TiO_2 anatase (101) interface for durable dye-sensitized solar cell, *J. Phys. Chem. C*, 2011, **115**, 19849–19855.
109 M. Iannuzzi, A. Laio and M. Parrinello, Efficient exploration of reactive potential energy surfaces using Car-Parrinello molecular dynamics, *Phys. Rev. Lett.*, 2003, **90**, 238302.
110 C. Anselmi, E. Mosconi, M. Pastore, E. Ronca and F. De Angelis, Adsorption of organic dyes on TiO_2 surfaces in dye-sensitized solar cells: interplay of theory and experiment, *Phys. Chem. Chem. Phys.*, 2012, **14**, 15963–15974.
111 J. Weidmann, Th. Dittrich, E. Konstantinova, I. Lauermann, I. Uhlendorf and F. Koch, Influence of oxygen and water related surface defects on the dye sensitized TiO_2 solar cell, *Sol. Energy Mater. Sol. Cells*, 1999, **56**, 153–165.
112 G. Smestad, Testing of dye sensitized TiO_2 solar cells II: theoretical voltage output and photoluminescence efficiencies, *Sol. Energy Mater. Sol. Cells*, 1994, **32**, 273–278.
113 P. E. de Jongh and D. Vanmaekelbergh, Investigation of the electronic transport properties of nanocrystalline particulate TiO_2 electrodes by intensity-modulated photocurrent spectroscopy, *J. Phys. Chem. B*, 1997, **101**, 2716–2722.
114 V. E. Henrich, G. Dresselhaus and H. J. Zeiger, Chemisorbed phases of H_2O on TiO_2 and $SrTiO_3$, *Solid State Commun.*, 1977, **24**, 623–626.
115 T. Kitamura, K. Okada, H. Matsui and N. Tanabe, Durability of dye-sensitized solar cells and modules, *J. Sol. Energy Eng.*, 2010, **132**, 021105.
116 J. Desilvestro, M. Grätzel, L. Kavan, J. Moser and J. Augustynski, Highly efficient sensitization of titanium dioxide, *J. Am. Chem. Soc.*, 1985, **107**, 2988–2990.
117 M. Matsumura, S. Matsudaira, H. Tsubomura, M. Takata and H. Yanagida, Dye Sensitization and Surface Structures of Semiconductor Electrodes, *Ind. Eng. Chem. Prod. Res. Dev.*, 1980, **19**, 415–421.
118 P. Liska, N. Vlachopoulos, M. K. Nazeeruddin, P. Comte and M. Grätzel, *cis*-diaquabis(2,2′-bipyridyl-4,4′-dicarboxylate)-ruthenium(II) sensitizes wide band gap oxide semiconductors very efficiently over a broad spectral range in the visible, *J. Am. Chem. Soc.*, 1988, **110**, 3686–3687.
119 N. Vlachopoulos, P. Liska, J. Augustynski and M. Grätzel, Very efficient visible light energy harvesting and conversion by spectral sensitization of high surface area polycrystalline titanium dioxide films, *J. Am. Chem. Soc.*, 1988, **110**, 1216–1220.
120 C. H. Law, S. C. Pathirana, X. Li, A. Y. Anderson, P. R. F. Barnes, A. Listorti, T. H. Ghaddar and B. O'Regan, Water-based electrolytes for dye-sensitized solar cells, *Adv. Mater.*, 2010, **22**, 4505–4509.
121 B. C. O'Regan, K. Walley, M. Juozapavicius, A. Anderson, F. Matar, T. Ghaddar, S. M. Zakeeruddin, C. Klein and J. R. Durrant, Structure/function relationships in dyes for solar energy conversion: a two-atom change in dye structure and the mechanism for its effect on cell voltage, *J. Am. Chem. Soc.*, 2009, **131**, 3541–3548.
122 F. Matar, T. H. Ghaddar, K. Walley, T. DosSantos, J. R. Durrant and B. C. O'Regan, A new ruthenium

polypyridyl dye, TG6, whose performance in dye-sensitized solar cells is surprisingly close to that of N719, the 'dye to beat' for 17 years, *J. Mater. Chem.*, 2008, **18**, 4246–4253.

123 A. Juris, V. Balzani, F. Barigelletti, S. Campagna, P. Belser and A. von Zelewsky, Ru(II) polypyridine complexes: photophysics, photochemistry, eletrochemistry, and chemiluminescence, *Coord. Chem. Rev.*, 1988, **84**, 85–277.

124 H. Zhao, X. Yin, H. Li, Y. Lin and Y. X. Weng, Explanation of effect of added water on dye-sensitized nanocrystalline TiO_2 solar cell: correlation between performance and carrier relaxation kinetics, *Chin. Phys. Lett.*, 2007, **24**, 3272–3275.

125 H. N. Ghosh, J. B. Asbury, Y. Weng and T. Lian, Interfacial electron transfer between $Fe(II)(CN)_6^{4-}$ and TiO_2 nanoparticles: direct electron injection and nonexponential recombination, *J. Phys. Chem. B*, 1998, **102**, 10208–10215.

126 Y. X. Weng, Y. Q. Wang, J. B. Asbury, H. N. Ghosh and T. Lian, Back electron transfer from TiO_2 nanoparticles to $Fe^{III}(CN)_6^{3-}$: origin of non-single-exponential and particle size independent dynamics, *J. Phys. Chem. B*, 2000, **104**, 93–104.

127 H. Zhao, Q. Zhang and Y. X. Weng, Deep surface trap filling by photoinduced carriers and interparticle electron transport observed in TiO_2 nanocrystalline film with time-resolved visible and mid-IR transient spectroscopies, *J. Phys. Chem. C*, 2007, **111**, 3762–3769.

128 K. Zhu, S. R. Jang and A. J. Frank, Effects of water intrusion on the charge-carrier dynamics, performance, and stability of dye-sensitized solar cells, *Energy Environ. Sci.*, 2012, **5**, 9492–9495.

129 A. B. Heinzel, D. M. Teschner and R. Schumacher, Influence of water on the capacitance/potential distribution at the TiO_2/CH_3CN junction, *Ber. Bunsen Ges. Phys. Chem.*, 1981, **85**, 1117–1119.

130 M. A. Henderson, Structural sensitivity in the dissociation of water on TiO_2 single-crystal surfaces, *Langmuir*, 1996, **12**, 5093–5098.

131 G. Schlichthorl, N. G. Park and A. J. Frank, Evaluation of the charge-collection efficiency of dye-sensitized nanocrystalline TiO_2 solar cells, *J. Phys. Chem. B*, 1999, **103**, 782–791.

132 Q. Wang, Z. Zhang, S. M. Zakeeruddin and M. Grätzel, Enhancement of the performance of dye-sensitized solar cell by formation of shallow transport levels under visible light illumination, *J. Phys. Chem. C*, 2008, **112**, 7084–7092.

133 J. R. Jennings and Q. Wang, Influence of lithium ion concentration on electron injection, transport, and recombination in dye-sensitized solar cells, *J. Phys. Chem. C*, 2010, **114**, 1715–1724.

134 S. Sodergren, H. Siegbahn, H. Rensmo, H. Lindstrom, A. Hagfeldt and S. E. Lindquist, Lithium intercalation in nanoporous anatase TiO_2 studied with XPS, *J. Phys. Chem. B*, 1997, **101**, 3087–3090.

135 L. Tan, Z. Sun, W. Zhang, Y. Tang, S. Morimura and K. Kida, Production of bio-fuel ethanol from distilled grain waste eluted from Chinese spirit making process, *Bioprocess Biosyst. Eng.*, 2014, **37**, 2031–2038, DOI: 10.1007/s00449-014-1178-5.

136 G. J. Liu, H. Z. Ma, Y. Q. Ma, W. Y. Zhang, Q. H. Wang and J. Xiao, Research on immobilization carrier on ethanol fermentation from food waste, *Adv. Mater. Res.*, 2014, **878**, 466–472.

137 P. Avetta, F. Bella, A. Bianco Prevot, E. Laurenti, E. Montoneri, A. Arques and L. Carlos, Waste cleaning waste: photodegradation of monochlorophenols in the presence of waste-derived photosensitizer, *ACS Sustainable Chem. Eng.*, 2013, **1**, 1545–1550.

138 H. Saito, S. Uegusa, T. N. Murakami, N. Kawashima and T. Miyasaka, Fabrication and efficiency enhancement of water-based dye-sensitized solar cells by interfacial activation of TiO_2 mesopores, *Electrochemistry*, 2004, **72**, 310–316.

139 F. Bella, A. Sacco, D. Pugliese, M. Laurenti and S. Bianco, Additives and salts for dye-sensitized solar cells electrolytes: what is the best choice?, *J. Power Sources*, 2014, **264**, 333–343.

140 K. Hara, Y. Dan-Oh, C. Kasada, Y. Ohga, A. Shinpo, S. Suga, K. Sayama and H. Arakawa, Effect of additives on the photovoltaic performance of coumarin-dye-sensitized nanocrystalline TiO_2 solar cells, *Langmuir*, 2004, **20**, 4205–4210.

141 T. Le Bahers, F. Labat, T. Pauporté and I. Ciofini, Effect of solvent and additives on the open-circuit voltage of ZnO-based dye-sensitized solar cells: a combined theoretical and experimental study, *Phys. Chem. Chem. Phys.*, 2010, **12**, 14710–14719.

142 Z. Yu, M. Gorlov, G. Boschloo and L. Kloo, Synergistic effect of *N*-methylbenzimidazole and guanidinium thiocyanate on the performance of dye-sensitized solar cells based on ionic liquid electrolytes, *J. Phys. Chem. B*, 2010, **114**, 22330–22337.

143 D. Pugliese, F. Bella, V. Cauda, A. Lamberti, A. Sacco, E. Tresso and S. Bianco, A chemometric approach for the sensitization procedure of ZnO flowerlike microstructures for dye-sensitized solar cells, *ACS Appl. Mater. Interfaces*, 2013, **5**, 11288–11295.

144 V. Cauda, D. Pugliese, N. Garino, A. Sacco, S. Bianco, F. Bella, A. Lamberti and C. Gerbaldi, Multi-functional energy conversion and storage electrodes using flower-like zinc oxide nanostructures, *Energy*, 2014, **65**, 639–646.

145 H. L. Lu, Y. H. Lee, S. T. Huang, C. Su and T. C. K. Yang, Influences of water in bis-benzimidazole-derivative electrolyte additives to the degradation of the dye-sensitized solar cells, *Sol. Energy Mater. Sol. Cells*, 2011, **95**, 158–162.

146 D. Tikariha, K. K. Ghosh, P. Quagliotto and S. Ghosh, Mixed micellization properties of cationic monomeric and gemini surfactants, *J. Chem. Eng. Data*, 2010, **55**, 4162–4167.

147 P. Quagliotto, C. Barolo, N. Barbero, E. Barni, C. Compari, E. Fisicaro and G. Viscardi, Synthesis and characterization of highly fluorinated gemini pyridinium surfactants, *Eur. J. Org. Chem.*, 2009, 3167–3177.

148 D. Tikariha, B. Kumar, N. Singh, K. K. Ghosh and P. Quagliotto, Micellization behavior of cationic gemini surfactants in aqueous-ethylene glycol solution, *J. Surfactants Deterg.*, 2011, **14**, 555–562.

149 V. P. Torchilin, Structure and design of polymeric surfactant-based drug delivery systems, *J. Controlled Release*, 2001, **73**, 137–172.

150 D. A. Edwards, R. G. Luthy and Z. Liu, Solubilization of polycyclic aromatic hydrocarbons in micellar nonionic surfactant solutions, *Environ. Sci. Technol.*, 1991, **25**, 127–133.

151 D. Hidalgo, R. Messina, A. Sacco, D. Manfredi, S. Vankova, E. Garrone, G. Saracco and S. Hernández, Thick mesoporous TiO_2 films through a sol-gel method involving a non-ionic surfactant: characterization and enhanced performance for water photo-electrolysis, *Int. J. Hydrogen Energy*, 2014, **39**, 21512–21522, DOI: 10.1016/j.ijhydene.2014.02.163.

152 W. Chen, Y. Qiu, K. Yan and S. Yang, Surfactant directed self-assembly of size-tunable mesoporous titanium dioxide microspheres and their application in quasi-solid state dye-sensitized solar cells, *J. Power Sources*, 2011, **196**, 10806–10816.

153 S. Casino, F. Di Lupo, C. Francia, A. Tuel, S. Bodoardo and C. Gerbaldi, Surfactant-assisted sol gel preparation of high-surface area mesoporous TiO_2 nanocrystalline Li-ion battery anodes, *J. Alloys Compd.*, 2014, **594**, 114–121.

154 G. Meligrana, F. Di Lupo, S. Ferrari, M. Destro, S. Bodoardo, N. Garino and C. Gerbaldi, Surfactant-assisted mild hydrothermal synthesis to nanostructured mixed orthophosphates $LiMn_yFe_{1-y}PO_4$/C lithium insertion cathode materials, *Electrochim. Acta*, 2013, **105**, 99–109.

155 K. M. O'Malley, C. Z. Li, H. L. Yip and A. K. Y. Jen, Enhanced open-circuit voltage in high performance polymer/fullerene bulk-heterojunction solar cells by cathode modification with a C_{60} surfactant, *Adv. Energy Mater.*, 2012, **2**, 82–86.

156 Y. S. Jung, B. Yoo, M. K. Lim, S. Y. Lee and K. J. Kim, Effect of Triton X-100 in water-added electrolytes on the performance of dye-sensitized solar cells, *Electrochim. Acta*, 2009, **54**, 6286–6291.

157 S. G. Yan and J. T. Hupp, Semiconductor-based interfacial electron-transfer reactivity: decoupling kinetics from pH-dependent band energetics in a dye-sensitized titanium dioxide/aqueous solution system, *J. Phys. Chem.*, 1996, **100**, 6867–6870.

158 T. S. Kang, K. H. Chun, J. S. Hong, S. H. Moon and K. J. Kim, Enhanced stability of photocurrent-voltage curves in Ru(II)-dye-sensitized nanocrystalline TiO_2 electrodes with carboxylic acids, *J. Electrochem. Soc.*, 2000, **147**, 3049–3053.

159 N. G. Park, S. H. Chang, J. van der Lagemaat, K. J. Kim and A. J. Frank, Effect of cations on the open-circuit photovoltage and the charge-injection efficiency of dye-sensitized nanocrystalline rutile TiO_2 films, *Bull. Korean Chem. Soc.*, 2000, **21**, 985–988.

160 J. L. Anthony, E. J. Maginn and J. F. Brenneeke, Solution thermodynamics of imidazolium-based ionic liquids and water, *J. Phys. Chem. B*, 2001, **105**, 10942–10949.

161 A. Latini, F. K. Aldibaja, C. Cavallo and D. Gozzi, Benzonitrile based electrolytes for best operation of dye sensitized solar cells, *J. Power Sources*, 2014, **269**, 308–316.

162 A. Asghar, M. Emziane, H. K. Pak and S. Y. Oh, Outdoor testing and degradation of dye-sensitized solar cells in Abu Dhabi, *Sol. Energy Mater. Sol. Cells*, 2014, **128**, 335–342.

163 H. Zhang, L. Qiu, D. Xu, W. Zhang and F. Yan, Performance enhancement for water based dye-sensitized solar cells *via* addition of ionic surfactants, *J. Mater. Chem. A*, 2014, **2**, 2221–2226.

164 X. Chen, J. Zhao, J. Zhang, L. Qiu, D. Xu, H. Zhang, X. Han, B. Sun, G. Fu, Y. Zhang and F. Yan, Bis-imidazolium based poly(ionic liquid) electrolytes for quasi-solid-state dye-sensitized solar cells, *J. Mater. Chem.*, 2012, **22**, 18018–18024.

165 J. Xia, N. Masaki, M. Lira-Cantu, Y. Kim, K. Jiang and S. Yanagida, Influence of doped anions on poly(3,4-ethylenedioxythiophene) as hole conductors for iodine-free solid-state dye-sensitized solar cells, *J. Am. Chem. Soc.*, 2008, **130**, 1258–1263.

166 G. Kume, M. Gallotti and G. Nunes, Review on anionic/cationic surfactant mixtures, *J. Surfactants Deterg.*, 2008, **11**, 1–11.

167 A. K. Vikingstad, M. G. Aarra and A. Skauge, Effect of surfactant structure on foam–oil interactions: comparing fluorinated surfactant and alpha olefin sulfonate in static foam tests, *Colloids Surf., A*, 2006, **279**, 105–112.

168 Y. Tachibana, K. Hara, K. Sayama and H. Arakawa, Quantitative analysis of light-harvesting efficiency and electron-transfer yield in ruthenium-dye-sensitized nanocrystalline TiO_2 solar cells, *Chem. Mater.*, 2002, **14**, 2527–2535.

169 M. Zeman, R. A. C. M. M. van Swaaij, J. W. Metselaar and R. E. I. Schropp, Optical modeling of a-Si:H solar cells with rough interfaces: Effect of back contact and interface roughness, *J. Appl. Phys.*, 2000, **88**, 6436–6443.

170 S. Mastroianni, A. Lanuti, S. Penna, A. Reale, T. M. Brown, A. Di Carlo and F. Decker, Physical and electrochemical analysis of an indoor-outdoor ageing test of large-area dye solar cell devices, *ChemPhysChem*, 2012, **13**, 2925–2936.

171 B. C. O'Regan, L. Xiaoe and T. Ghaddar, Dye adsorption, desorption, and distribution in mesoporous TiO_2 films, and its effects on recombination losses in dye sensitized solar cells, *Energy Environ. Sci.*, 2012, **5**, 7203–7215.

172 E. H. Kong, J. Lim, Y. J. Chang, Y. H. Yoon, T. Park and H. M. Jang, Aerosol OT-water system coupled with triiodide/iodide (I_3^-/I^-) redox electrolytes for highly efficient dye-sensitized solar cells, *Adv. Energy Mater.*, 2013, **3**, 1344–1350.

173 E. Y. Sheu, S. H. Chen and J. S. Huang, Structure and growth of bis(2-ethylhexyl) sulfosuccinate micelles in aqueous solutions, *J. Phys. Chem.*, 1987, **91**, 3306–3310.

174 W. H. Lai, L. H. Su, L. G. Teoh and M. H. Hon, Commercial and natural dyes as photosensitizers for a water-based dye-

sensitized solar cell loaded with gold nanoparticles, *J. Photochem. Photobiol., A*, 2008, **195**, 307–313.

175 E. W. McFarland and J. Tang, A photovoltaic device structure based on internal electron emission, *Nature*, 2003, **421**, 616–618.

176 N. Chandrasekharan and P. V. Kamat, Improving the photoelectrochemical performance of nanostructured TiO_2 films by adsorption of gold nanoparticles, *J. Phys. Chem. B*, 2000, **104**, 10851–10857.

177 Y. Tian and T. Tatsuma, Mechanisms and applications of plasmon-induced charge Separation at TiO_2 films loaded with gold nanoparticles, *J. Am. Chem. Soc.*, 2005, **127**, 7632–7637.

178 Y. H. Su and Y. S. Lai, Performance enhancement of natural pigments on a high light transmission ZrO_2 nanoparticle layer in a water-based dye-sensitized solar cell, *Int. J. Energy Res.*, 2014, **38**, 436–443.

179 M. A. Taylor, R. E. Alonso, L. A. Errico, A. Lopez-Garcia, P. de la Presa, A. Svane and N. E. Christensen, Structural, electronic and hyperfine properties of pure and Ta-doped ZrO_2, *Phys. Rev. B: Condens. Matter Mater. Phys.*, 2012, **85**, 155202.

180 J. S. Lissau, J. M. Gardner and A. Morandeira, Photon upconversion on dye-sensitized nanostructured ZrO_2 films, *J. Phys. Chem. C*, 2011, **115**, 23226–23232.

181 H. Hug, M. Bader, P. Mair and T. Glatzel, Biophotovoltaics: natural pigments in dye-sensitized solar cells, *Appl. Energy*, 2014, **115**, 216–225.

182 T. Daeneke, Y. Uemura, N. W. Duffy, A. J. Mozer, N. Koumura, U. Bach and L. Spiccia, Aqueous dye-sensitized solar cell electrolytes based on the ferricyanide-ferrocyanide redox couple, *Adv. Mater.*, 2012, **24**, 1222–1225.

183 G. Gritzner, K. Danksagmüller and V. Gutmann, Outer-sphere coordination effects on the redox behaviour of the $Fe(CN)_6^{3-}/Fe(CN)_6^{4-}$ couple in non-aqueous solvents, *J. Electroanal. Chem.*, 1976, **72**, 177–185.

184 N. Koumura, Z. S. Wang, S. Mori, M. Miyashita, E. Suzuki and K. Hara, Alkyl-functionalized organic dyes for efficient molecular photovoltaics, *J. Am. Chem. Soc.*, 2006, **128**, 14256–14257.

185 M. Yang, D. W. Thompson and G. J. Meyer, Dual pathways for TiO_2 sensitization by $Na_2[Fe(bpy)(CN)_4]$, *Inorg. Chem.*, 2000, **39**, 3738–3739.

186 N. W. Duffy, L. M. Peter, R. M. G. Rajapakse and K. G. U. Wijayantha, A novel charge extraction method for the study of electron transport and interfacial transfer in dye sensitised nanocrystalline solar cells, *Electrochem. Commun.*, 2000, **2**, 658–662.

187 M. Guček, R. Susič and B. Pihlar, Investigation of UV-induced decomposition of hexacyanoferrate(II) and -(III) by capillary electrophoresis, *Chemosphere*, 1999, **39**, 2467–2478.

188 C. A. P. Arellano and S. S. Martinez, Effects of pH on the degradation of aqueous ferricyanide by photolysis and photocatalysis under solar radiation, *Sol. Energy Mater. Sol. Cells*, 2010, **94**, 327–332.

189 M. Wang, N. Chamberland, L. Breau, J. E. Moser, R. Humphry-Baker, B. Marsan, S. M. Zakeeruddin and M. Grätzel, An organic redox electrolyte to rival triiodide/iodide in dye-sensitized solar cells, *Nat. Chem.*, 2010, **2**, 385–389.

190 H. Tian, E. Gabrielsson, Z. Yu, A. Hagfeldt, L. Kloo and L. Sun, A thiolate/disulfide ionic liquid electrolyte for organic dye-sensitized solar cells based on Pt-free counter electrodes, *Chem. Commun.*, 2011, **47**, 10124–10126.

191 D. Li, H. Li, Y. Luo, K. Li, Q. Meng, M. Armand and L. Chen, Non-corrosive, non-absorbing organic redox couple for dye-sensitized solar cells, *Adv. Funct. Mater.*, 2010, **20**, 3358–3365.

192 H. Tian, X. Jiang, Z. Yu, L. Kloo, A. Hagfeldt and L. Sun, Efficient organic-dye-sensitized solar cells based on an iodine-free electrolyte, *Angew. Chem., Int. Ed.*, 2010, **49**, 7328–7331.

193 H. Tian, E. Gabrielsson, P. W. Lohse, N. Vlachopoulos, L. Kloo, A. Hagfeldt and L. Sun, Development of an organic redox couple and organic dyes for aqueous dye-sensitized solar cells, *Energy Environ. Sci.*, 2012, **5**, 9752–9755.

194 W. Xiang, F. Huang, Y. B. Cheng, U. Bach and L. Spiccia, Aqueous dye-sensitized solar cell electrolytes based on the cobalt(II)/(III) tris(bipyridine) redox couple, *Energy Environ. Sci.*, 2013, **6**, 121–127.

195 R. Jiang, A. Anderson, P. R. F. Barnes, L. Xiaoe, C. Law and B. C. O'Regan, 2000 hours photostability testing of dye sensitised solar cells using a cobalt bipyridine electrolyte, *J. Mater. Chem. A*, 2014, **2**, 4751–4757.

196 L. Y. Lin, M. H. Yeh, C. Y. Chen, R. Vittal, C. G. Wu and K. C. Ho, Surface modification of TiO_2 nanotube arrays with Y_2O_3 barrier layer: controlling charge recombination dynamics in dye-sensitized solar cells, *J. Mater. Chem. A*, 2014, **2**, 8281–8287.

197 W. Mekprasart, S. Suphankij, T. Tangcharoen, A. Simpraditpan and W. Pecharapa, Modification of dye-sensitized solar cell working electrode using TiO_2 nanoparticle/N-doped TiO_2 nanofiber composites, *Phys. Status Solidi A*, 2014, **211**, 1745–1751, DOI: 10.1002/pssa.201330566.

198 G. A. Sewvandi, X. Tao, T. Kusunose, Y. Tanaka, S. Nakanishi and Q. Feng, Modification of TiO_2 electrode with organic silane interposed layer for high-performance of dye-sensitized solar cells, *ACS Appl. Mater. Interfaces*, 2014, **6**, 5818–5826.

199 D. H. Kim, W. M. Seong, I. J. Park, E. S. Yoo, S. S. Shin, J. S. Kim, H. S. Jung, S. Lee and K. S. Hong, Anatase TiO_2 nanorod-decoration for highly efficient photoenergy conversion, *Nanoscale*, 2013, **5**, 11725–11732.

200 S. Lim, N. M. Huang, H. N. Lim and M. Mazhar, Surface modification of aerosol-assisted CVD produced TiO_2 thin film for dye sensitised solar cell, *Int. J. Photoenergy*, 2014, 586707.

201 J. R. Nair, M. Destro, C. Gerbaldi, R. Bongiovanni and N. Penazzi, Novel multiphase electrode/electrolyte composites for next generation of flexible polymeric Li-ion cells, *J. Appl. Electrochem.*, 2013, **43**, 137–145.

202 M. Flasque, A. N. Van Nhien, J. Swiatowska, A. Seyeux, C. Davoisne and F. Sauvage, Interface stability of a TiO_2/3-methoxypropionitrile-based electrolyte: first evidence for solid electrolyte interphase formation and implications, *ChemPhysChem*, 2014, **15**, 1126–1137.

203 T. N. Murakami, H. Saito, S. Uegusa, N. Kawashima and T. Miyasaka, Water-based dye-sensitized solar cells: interfacial activation of TiO_2 mesopores in contact with aqueous electrolyte for efficiency development, *Chem. Lett.*, 2003, 1154–1155.

204 Y. H. Su, W. H. Lai, L. G. Teoh, M. H. Hon and J. L. Huang, Layer-by-layer Au nanoparticles as a Schottky barrier in a water-based dye-sensitized solar cell, *Appl. Phys. A: Mater. Sci. Process.*, 2007, **88**, 173–178.

205 S. S. Zumdahl, *Chemical Principles*, Houghton Mifflin, New York, 2005.

206 C. Law, O. Moudam, S. Villarroya-Lidon and B. C. O'Regan, Managing wetting behavior and collection efficiency in photoelectrochemical devices based on water electrolytes; improvement in efficiency of water/iodide dye sensitised cells to 4%, *J. Mater. Chem.*, 2012, **22**, 23387–23394.

207 M. Wang, S. J. Moon, D. Zhou, F. Le Formal, N. L. Cevey-Ha, R. Humphry-Baker, C. Grätzel, P. Wang, S. M. Zakeeruddin and M. Grätzel, Enhanced-light-harvesting amphiphilic ruthenium dye for efficient solid-state dye-sensitized solar cells, *Adv. Funct. Mater.*, 2010, **20**, 1821–1826.

208 C. E. Richards, A. Y. Anderson, S. Martiniani, C. Law and B. C. O'Regan, The mechanism of iodine reduction by TiO_2 electrons and the kinetics of recombination in dye-sensitized solar cells, *J. Phys. Chem. Lett.*, 2012, **3**, 1980–1984.

209 L. I. Katzin and E. Gebert, The iodide-iodine-triiodide equilibrium and ion activity coefficient ratios, *J. Am. Chem. Soc.*, 1955, **77**, 5814–5819.

210 C. Dong, W. Xiang, F. Huang, D. Fu, W. Huang, U. Bach, Y. B. Cheng, X. Li and L. Spiccia, Controlling interfacial recombination in aqueous dye-sensitized solar cells by octadecyltrichlorosilane surface treatment, *Angew. Chem., Int. Ed.*, 2014, **53**, 6933–6937.

211 J. J. Nelson, T. J. Amick and C. M. Elliott, Mass transport of polypyridyl cobalt complexes in dye-sensitized solar cells with mesoporous TiO_2 photoanodes, *J. Phys. Chem. C*, 2008, **112**, 18255–18263.

212 S. Li, Y. Xiao, X. Wang and M. Cao, A ZnO-graphene hybrid with remarkably enhanced lithium storage capability, *Phys. Chem. Chem. Phys.*, 2014, **16**, 25846–25853.

213 X. Liang, D. Mei, M. Cao, D. Qu and B. Deng, Effects of structural patterns and degree of crystallinity on the performance of nanostructured ZnO as anode material for lithium-ion batteries, *J. Alloys Compd.*, 2015, **627**, 455–462.

214 J. Kim, S. A. Hong and J. Yoo, Continuous synthesis of hierarchical porous ZnO microspheres in supercritical methanol and their enhanced electrochemical performance in lithium ion batteries, *Chem. Eng. J.*, 2015, **266**, 179–188.

215 G. Yuan, G. Wang, H. Wang and J. Bai, Synthesis and electrochemical investigation of radial ZnO microparticles as anode materials for lithium-ion batteries, *Ionics*, 2014, **21**, 365–371.

216 M. Liang and J. Chen, Arylamine organic dyes for dye-sensitized solar cells, *Chem. Soc. Rev.*, 2013, **42**, 3453–3488.

217 J. N. Clifford, E. Martínez-Ferrero, A. Viterisi and E. Palomares, Sensitizer molecular structure-device efficiency relationship in dye sensitized solar cells, *Chem. Soc. Rev.*, 2011, **40**, 1635–1646.

218 Y. Wu and W. Zhu, Organic sensitizers from D-π-A to D-A-π-A: Effect of the internal electron-withdrawing units on molecular absorption, energy levels and photovoltaic performances, *Chem. Soc. Rev.*, 2013, **42**, 2039–2058.

219 A. S. Polo, M. K. Itokazu and N. Y. Murakami Iha, Metal complex sensitizers in dye-sensitized solar cells, *Coord. Chem. Rev.*, 2004, **248**, 1343–1361.

220 M. K. Nazeeruddin, S. M. Zakeeruddin, J. J. Lagref, P. Liska, P. Comte, C. Barolo, G. Viscardi, K. Schenk and M. Grätzel, Stepwise assembly of amphiphilic ruthenium sensitizers and their applications in dye-sensitized solar cell, *Coord. Chem. Rev.*, 2004, **248**, 1317–1328.

221 R. Argazzi, N. Y. Murakami Iha, H. Zabri, F. Odobel and C. A. Bignozzi, Design of molecular dyes for application in photoelectrochemical and electrochromic devices based on nanocrystalline metal oxide semiconductors, *Coord. Chem. Rev.*, 2004, **248**, 1299–1316.

222 Z. Chen, F. Li and C. Huang, Organic D-π-A dyes for dye-sensitized solar cell, *Curr. Org. Chem.*, 2007, **11**, 1241–1258.

223 G. Cicero, G. Musso, A. Lamberti, B. Camino, S. Bianco, D. Pugliese, F. Risplendi, A. Sacco, N. Shahzad, A. M. Ferrari, B. Ballarin, C. Barolo, E. Tresso and G. Caputo, Combined experimental and theoretical investigation of the hemi-squaraine/TiO_2 interface for dye sensitized solar cells, *Phys. Chem. Chem. Phys.*, 2013, **15**, 7198–7203.

224 J. Park, C. Barolo, F. Sauvage, N. Barbero, C. Benzi, P. Quagliotto, S. Coluccia, D. Di Censo, M. Grätzel, M. K. Nazeeruddin and G. Viscardi, Symmetric *vs.* asymmetric squaraines as photosensitisers in mesoscopic injection solar cells: a structure-property relationship study, *Chem. Commun.*, 2012, **48**, 2782–2784.

225 J. Park, G. Viscardi, C. Barolo and N. Barbero, Near-infrared sensitization in dye-sensitized solar cells, *Chimia*, 2013, **67**, 129–135.

226 A. Abbotto, F. Sauvage, C. Barolo, F. De Angelis, S. Fantacci, M. Grätzel, N. Manfredi, C. Marinzi and M. K. Nazeeruddin, Panchromatic ruthenium sensitizer based on electron-rich heteroarylvinylene π-conjugated quaterpyridine for dye-sensitized solar cells, *Dalton Trans.*, 2011, **40**, 234–242.

227 K. Hara, T. Sato, R. Katoh, A. Furube, T. Yoshihara, M. Murai, M. Kurashige, S. Ito, A. Shinpo, S. Suga and H. Arakawa, Novel conjugated organic dyes for efficient dye-sensitized solar cells, *Adv. Funct. Mater.*, 2005, **15**, 246–252.

228 C. Barolo, J. H. Yum, E. Artuso, N. Barbero, D. Di Censo, M. G. Lobello, S. Fantacci, F. De Angelis, M. Grätzel,

M. K. Nazeeruddin and G. Viscardi, A simple synthetic route to obtain pure trans-ruthenium(II) complexes for dye-sensitized solar cell applications, *ChemSusChem*, 2013, **6**, 2170–2180.

229 B. Bozic-Weber, E. C. Constable and C. E. Housecroft, Light harvesting with Earth abundant d-block metals: development of sensitizers in dye-sensitized solar cells (DSCs), *Coord. Chem. Rev.*, 2013, **257**, 3089–3106.

230 W. M. Campbell, K. W. Jolley, P. Wagner, K. Wagner, P. J. Walsh, K. C. Gordon, L. Schmidt-Mende, M. K. Nazeeruddin, Q. Wang, M. Grätzel and D. L. Officer, Highly efficient porphyrin sensitizers for dye-sensitized solar cells, *J. Phys. Chem. C*, 2007, **111**, 11760–11762.

231 S. M. Zakeeruddin, M. K. Nazeeruddin, R. Humphry-Baker, P. Pechy, P. Quagliotto, C. Barolo, G. Viscardi and M. Grätzel, Design, synthesis, and application of amphiphilic ruthenium polypyridyl photosensitizers in solar cells based on nanocrystalline TiO_2 films, *Langmuir*, 2002, **18**, 952–954.

232 N. Vlachopoulos, P. Liska, A. J. McEvoy and M. Grätzel, Efficient spectral sensitisation of polycrystalline titanium dioxide photoelectrodes, *Surf. Sci.*, 1987, **189–190**, 823–831.

233 M. K. Nazeeruddin, R. Humphry-Baker, P. Liska and M. Grätzel, Investigation of sensitizer adsorption and the influence of protons on current and voltage of a dye-sensitized nanocrystalline TiO_2 solar cell, *J. Phys. Chem. B*, 2003, **107**, 8981–8987.

234 M. Hahlin, E. M. J. Johansson, R. Schölin, H. Siegbahn and H. Rensmo, Influence of water on the electronic and molecular surface structures of Ru-dyes at nanostructured TiO_2, *J. Phys. Chem. C*, 2011, **115**, 11996–12004.

235 E. M. J. Johansson, T. Edvinsson, M. Odelius, D. P. Hagberg, L. Sun, A. Hagfeldt, H. Siegbahn and H. Rensmo, Electronic and molecular surface structure of a polyene-diphenylaniline dye adsorbed from solution onto nanoporous TiO_2, *J. Phys. Chem. C*, 2007, **111**, 8580–8586.

236 T. Marinado, D. P. Hagberg, M. Hedlund, T. Edvinsson, E. M. J. Johansson, G. Boschloo, H. Rensmo, T. Brinck, L. Sun and A. Hagfeldt, Rhodanine dyes for dye-sensitized solar cells: spectroscopy, energy levels and photovoltaic performance, *Phys. Chem. Chem. Phys.*, 2009, **11**, 133–141.

237 E. M. J. Johansson, P. G. Karlsson, M. Hedlund, D. Ryan, H. Siegbahn and H. Rensmo, Photovoltaic and interfacial properties of heterojunctions containing dye-sensitized dense TiO_2 and tri-arylamine derivatives, *Chem. Mater.*, 2007, **19**, 2071–2078.

238 H. Choi, B. S. Jeong, K. Do, M. J. Ju, K. Song and J. Ko, Aqueous electrolyte based dye-sensitized solar cells using organic sensitizers, *New J. Chem.*, 2013, **37**, 329–336.

239 S. J. Moon, J. H. Yum, R. Humphry-Baker, K. M. Karlsson, D. P. Hagberg, T. Marinado, A. Hagfeldt, L. Sun, M. Grätzel and M. K. Nazeeruddin, Highly efficient organic sensitizers for solid-state dye-sensitized solar cells, *J. Phys. Chem. C*, 2009, **113**, 16816–16820.

240 J. H. Yum, D. P. Hagberg, S. J. Moon, K. M. Karlsson, T. Marinado, L. Sun, A. Hagfeldt, M. K. Nazeeruddin and M. Grätzel, A light-resistant organic sensitizer for solar-cell applications, *Angew. Chem., Int. Ed.*, 2009, **48**, 1576–1580.

241 H. Choi, J. Han, M. S. Kang, K. Song and J. Ko, Aqueous electrolytes based dye-sensitized solar cells using I^-/I_3^- redox couple to achieve $\geq$ 4% power conversion efficiency, *Bull. Korean Chem. Soc.*, 2014, **35**, 1433–1439.

242 C. Chen, X. Yang, M. Cheng, F. Zhang and L. Sun, Degradation of cyanoacrylic acid-based organic sensitizers in dye-sensitized solar cells, *ChemSusChem*, 2013, **6**, 1270–1275.

243 C. Koenigsmann, T. S. Ripolles, B. J. Brennan, C. F. A. Negre, M. Koepf, A. C. Durrell, R. L. Milot, J. A. Torre, R. H. Crabtree, V. S. Batista, G. W. Brudvig, J. Bisquert and C. A. Schmuttenmaer, Substitution of a hydroxamic acid anchor into the MK-2 dye for enhanced photovoltaic performance and water stability in a DSSC, *Phys. Chem. Chem. Phys.*, 2014, **16**, 16629–16641.

244 Z. S. Wang, N. Koumura, Y. Cui, M. Takahashi, H. Sekiguchi, A. Mori, T. Kubo, A. Furube and K. Hara, Hexylthiophene-functionalized carbazole dyes for efficient molecular photovoltaics: tuning of solar-cell performance by structural modification, *Chem. Mater.*, 2008, **20**, 3993–4003.

245 T. N. Murakami, E. Yoshida and N. Koumura, Carbazole dye with phosphonic acid anchoring groups for long-term heat stability of dye-sensitized solar cells, *Electrochim. Acta*, 2014, **131**, 174–183.

246 W. R. McNamara, R. C. Snoeberger III, G. Li, C. Richter, L. J. Allen, R. L. Milot, C. A. Schmuttenmaer, R. H. Crabtree, G. W. Brudvig and V. S. Batista, Hydroxamate anchors for water-stable attachment to TiO_2 nanoparticles, *Energy Environ. Sci.*, 2009, **2**, 1173–1175.

247 W. R. McNamara, R. L. Milot, H. E. Song, R. C. Snoeberger III, V. S. Batista, C. A. Schmuttenmaer, G. W. Brudvig and R. H. Crabtree, Water-stable, hydroxamate anchors for functionalization of TiO_2 surfaces with ultrafast interfacial electron transfer, *Energy Environ. Sci.*, 2010, **3**, 917–923.

248 D. P. Hagberg, X. Jiang, E. Gabrielsson, M. Linder, T. Marinado, T. Brinck, A. Hagfeldt and L. Sun, *J. Mater. Chem.*, 2009, **19**, 7232–7238.

249 V. Leandri, H. Ellis, E. Gabrielsson, L. Sun, G. Boschloo and A. Hagfeldt, Organic hydrophilic dye for water-based dye-sensitized solar cells, *Phys. Chem. Chem. Phys.*, 2014, **16**, 19964–19971, DOI: 10.1039/C4CP02774D.

250 R. C. White, J. E. Benedetti, A. D. Gonalves, W. Romão, B. G. Vaz, M. N. Eberlin, C. R. D. Correia, M. A. De Paoli and A. F. Nogueira, Synthesis, characterization and introduction of a new ion-coordinating ruthenium sensitizer dye in quasi-solid state TiO2 solar cells, *J. Photochem. Photobiol., A*, 2011, **222**, 185–191.

251 C. Shi, S. Dai, K. Wang, X. Pan, L. Zeng, L. Hu, F. Kong and L. Guo, Influence of various cations on redox behavior of I^- and I_3^- and comparison between KI complex with 18-crown-6 and 1,2-dimethyl-3-propylimidazolium iodide in dye-sensitized solar cells, *Electrochim. Acta*, 2005, **50**, 2597–2602.

252 S. Ito, T. Saitou, H. Imahori, H. Uehara and N. Hasegawa, Fabrication of dye-sensitized solar cells using natural dye for food pigment: monascus yellow, *Energy Environ. Sci.*, 2010, **3**, 905–909.

253 D. Zhang, S. M. Lanier, J. A. Downing, J. L. Avent, J. Lum and J. L. McHale, Betalain pigments for dye-sensitized solar cells, *J. Photochem. Photobiol., A*, 2008, **195**, 72–80.

254 D. Yu, G. Zhu, S. Liu, B. Ge and F. Huang, Photocurrent activity of light-harvesting complex II isolated from spinach and its pigments in dye-sensitized TiO_2 solar cell, *Int. J. Hydrogen Energy*, 2013, **38**, 16740–16748.

255 C. I. Oprea, A. Dumbrava, I. Enache, A. Georgescu and M. A. Gîrţu, A combined experimental and theoretical study of natural betalain pigments used in dye-sensitized solar cells, *J. Photochem. Photobiol., A*, 2012, **240**, 5–13.

256 Q. Dai and J. Rabani, Photosensitization of nanocrystalline TiO_2 films by pomegranate pigments with unusually high efficiency in aqueous medium, *Chem. Commun.*, 2001, 2142–2143.

257 M. Gil, I. C. Garcia-Viguera, F. Artés and F. A. Tomás-Barberán, Changes in pomegranate juice pigmentation during ripening, *J. Sci. Food Agric.*, 1995, **68**, 77–81.

258 R. Y. Y. Lin, T. M. Chuang, F. L. Wu, P. Y. Chen, T. C. Chu, J. S. Ni, M. S. Fan, Y. H. Lo, K. C. Ho and J. T. Lin, Anthracene/phenothiazine π-conjugated sensitizers for dye-sensitized solar cells using redox mediator in organic and water-based solvents, *ChemSusChem*, 2015, **8**, 105–113.

259 H. Bonnemann, G. Khelashvili, S. Behrens, A. Hinsch, K. Skupien and E. Dinjus, Role of the platinum nanoclusters in the iodide/triiodide redox system of dye solar cells, *J. Cluster Sci.*, 2007, **18**, 141–155.

260 S. Ahmad, J. H. Yum, H. J. Butt, M. K. Nazeeruddin and M. Grätzel, Efficient platinum-free counter electrodes for dye-sensitized solar cell applications, *ChemPhysChem*, 2010, **11**, 2814–2819.

261 A. M. Ritzmann, M. Pavone, A. B. Muñoz-García, J. A. Keith and E. A. Carter, *Ab initio* DFT + *U* analysis of oxygen transport in $LaCoO_3$: The effect of Co^{3+} magnetic states, *J. Mater. Chem. A*, 2014, **2**, 8060–8074.

262 G. Syrrokostas, A. Siokou, G. Leftheriotis and P. Yianoulis, Degradation mechanisms of Pt counter electrodes for dye sensitized solar cells, *Sol. Energy Mater. Sol. Cells*, 2012, **103**, 119–127.

263 F. Hao, P. Dong, Q. Luo, J. Li, J. Lou and H. Lin, Recent advances in alternative cathode materials for iodine-free dye-sensitized solar cells, *Energy Environ. Sci.*, 2013, **6**, 2003–2019.

264 H. Xu, C. Zhang, Z. Wang, S. Pang, X. Zhou, Z. Zhang and G. Cui, Nitrogen-doped carbon and iron carbide nanocomposites as cost-effective counter electrodes of dye-sensitized solar cells, *J. Mater. Chem. A*, 2014, **2**, 4676–4681.

265 E. Ramasamy, C. Jo, A. Anthonysamy, I. Jeong, J. K. Kim and J. Lee, Soft-template simple synthesis of ordered mesoporous titanium nitride-carbon nanocomposite for high performance dye-sensitized solar cell counter electrodes, *Chem. Mater.*, 2012, **24**, 1575–1582.

266 J. M. Pringle, V. Armel and D. R. MacFarlane, Electrodeposited PEDOT-on-plastic cathodes for dye-sensitized solar cells, *Chem. Commun.*, 2010, **46**, 5367–5369.

267 Z. Tang, J. Wu, M. Zheng, Q. Tang, Q. Liu, J. Lin and J. Wang, High efficient PANI/Pt nanofiber counter electrode used in dye-sensitized solar cell, *RSC Adv.*, 2012, **2**, 4062–4064.

268 J. Chen, F. Meng, X. Gui, H. Sun, Z. Zeng, Z. Li, Y. Zhou and Z. Tang, The application of a three dimensional CNT-sponge as the counter electrode for dye-sensitized solar cells, *Carbon*, 2012, **50**, 5624–5627.

269 Z. Wang, P. Li, Y. Chen, J. He, J. Liu, W. Zhang and Y. Li, Phosphorus-doped reduced graphene oxide as an electrocatalyst counter electrode in dye-sensitized solar cells, *J. Power Sources*, 2014, **263**, 246–251.

270 H. S. Park, S. J. Ko, J. S. Park, J. Y. Kim and H.-K. Song, Redox-active charge carriers of conducting polymers as a tuner of conductivity and its potential window, *Sci. Rep.*, 2013, **3**, 2454.

271 N. Kopidakis, N. R. Neale and A. J. Frank, Effect of an adsorbent on recombination and band-edge movement in dye-sensitized TiO_2 solar cells: evidence for surface passivation, *J. Phys. Chem. B*, 2006, **110**, 12485–12489.

272 T. Marinado, M. Hahlin, X. Jiang, M. Quintana, E. M. J. Johansson, E. Gabrielsson, S. Plogmaker, D. P. Hagberg, G. Boschloo, S. M. Zakeeruddin, M. Grätzel, H. Siegbahn, L. Sun, A. Hagfeldt and H. Rensmo, Surface molecular quantification and photoelectrochemical characterization of mixed organic dye and coadsorbent layers on TiO_2 for dye-sensitized solar cells, *J. Phys. Chem. C*, 2010, **114**, 11903–11910.

273 K. S. Lee, Y. Jun and J. H. Park, Controlled dissolution of polystyrene nanobeads: transition from liquid electrolyte to gel electrolyte, *Nano Lett.*, 2012, **12**, 2233–2237.

274 R. Kato, F. Kato, K. Oyaizu and H. Nishide, Redox-active hydroxy-TEMPO radical immobilized in Nafion layer for an aqueous electrolyte-based and dye-sensitized solar cell, *Chem. Lett.*, 2014, 480–482.

275 J. Min, J. Won, Y. S. Kang and S. Nagase, Benzimidazole derivatives in the electrolyte of new-generation organic dye-sensitized solar cells with an iodine-free redox mediator, *J. Photochem. Photobiol., A*, 2011, **219**, 148–153.

276 W. Zhang, L. Qiu, X. Chen and F. Yan, Imidazolium functionalized bis-2,2,6,6-tetramethyl-piperidine-1-oxyl (TEMPO) bi-redox couples for highly efficient dye-sensitized solar cells, *Electrochim. Acta*, 2014, **117**, 48–54.

277 Z. Zhang, P. Chen, T. N. Murakami, S. M. Zakeeruddin and M. Grätzel, The 2,2,6,6-tetramethyl-l-piperidinyloxy radical: an efficient, iodine-free redox mediator for dye-sensitized solar cells, *Adv. Funct. Mater.*, 2008, **18**, 341–346.

278 L. Napoli, J. Franco, H. Fasoli and A. Sanguinetti, Conductivity of Nafion® 117 membrane used in polymer electrolyte fuel cells, *Int. J. Hydrogen Energy*, 2014, **39**, 8656–8660.

279 M. Krishnan, X. Zhang and A. J. Bard, Polymer films on electrodes. 14. Spectral sensitization of n-type SnO_2 and

voltammetry at electrodes modified with Nafion films containing $Ru(bpy)_3^{2+}$, *J. Am. Chem. Soc.*, 1984, **106**, 7371–7380.

280 T. Tamura and H. Kawakami, Aligned electrospun nanofiber composite membranes for fuel cell electrolytes, *Nano Lett.*, 2010, **10**, 1324–1328.

281 Y. H. Lai, C. Y. Lin, J. G. Chen, C. C. Wang, K. C. Huang, K. Y. Liu, K. F. Lin, J. J. Lin and K. C. Ho, Enhancing the performance of dye-sensitized solar cells by incorporating nanomica in gel electrolytes, *Sol. Energy Mater. Sol. Cells*, 2010, **94**, 668–674.

282 S. Ito, K. Takahashi, S. I. Yusa, M. Saito and T. Shigetomi, Ultradurable dye-sensitized solar cells under 120 °C using cross-linkage dye and ionic-liquid electrolyte, *Int. J. Photoenergy*, 2013, **2013**, 501868.

283 J. Kim, D. Kim, S. Hwang and H. Kim, Highly efficient and stable dye-sensitized solar cells from adding low melting point glass frits, *Met. Mater. Int.*, 2012, **18**, 539–544.

284 F. Ribeiro, J. Maçaira, I. Mesquita, J. Gabriel, L. Andrade and A. Mendes, Laser assisted dye-sensitized solar cell sealing: from small to large cells areas, *J. Renewable Sustainable Energy*, 2014, **6**, 011208.

285 A. Hinsch, S. Behrens, M. Berginc, H. Bönnemann, H. Brandt, A. Drewitz, F. Einsele, D. Faßler, D. Gerhard, H. Gores, R. Haag, T. Herzig, S. Himmler, G. Khelashvili, D. Koch, G. Nazmutdinova, U. Opara-Krasovec, P. Putyra, U. Rau, R. Sastrawan, T. Schauer, C. Schreiner, S. Sensfuss, C. Siegers, K. Skupien, P. Wachter, J. Walter, P. Wasserscheid, U. Würfel and M. Zistler, Material development for dye solar modules: results from an integrated approach, *Prog. Photovoltaics*, 2008, **16**, 489–501.

286 H. Chen, S. Wang, H. Lin, G. Wang, S. Wang and G. Yang, Stability of dye sensitized solar cells with glass frit sealant, *Key Eng. Mater.*, 2012, **512–515**, 1619–1624.

287 R. Sastrawan, J. Beier, U. Belledin, S. Hemming, A. Hinsch, R. Kern, C. Vetter, F. M. Petrat, A. Prodi-Schwab, P. Lechner and W. Hoffmann, A glass frit-sealed dye solar cell module with integrated series connections, *Sol. Energy Mater. Sol. Cells*, 2006, **90**, 1680–1691.

288 W. J. Lee, E. Ramasamy, D. Y. Lee and J. S. Song, Glass frit overcoated silver grid lines for nano-crystalline dye sensitized solar cells, *J. Photochem. Photobiol., A*, 2006, **183**, 133–137.

289 A. Hauch and A. Georg, Diffusion in the electrolyte and charge-transfer reaction at the platinum electrode in dye-sensitized solar cells, *Electrochim. Acta*, 2001, **46**, 3457–3466.

290 K. F. Jensen, M. M. Rahman, W. Veurman, H. Brandt, C. Im, J. Wilde, A. Hinsch and J. J. Lee, Glass frit dissolution influenced by material composition and the water content in iodide/triiodide electrolyte of dye-sensitized solar cells, *Int. J. Photoenergy*, 2013, **2013**, 696052.

291 O. Horváth and I. Mikó, Spectra, equilibrium and photoredox chemistry of iodobismuthate(III) complexes in acetonitrile, *Inorg. Chim. Acta*, 2000, **304**, 210–218.

292 H. Wakita, G. Johansson, M. Sandström, P. L. Goggin and H. Ohtaki, Structure determination of zinc iodide complexes formed in aqueous solution, *J. Solution Chem.*, 1991, **20**, 643–668.

293 S. Mikoshiba, S. Murai, H. Sumino and S. Hayase, Another role of LiI/*tert*-butylpyridine in room-temperature molten salt electrolytes containing water for dye-sensitized solar cell, *Chem. Lett.*, 2002, 1156–1157.

294 S. Mikoshiba, S. Murai, H. Sumino, T. Kado, D. Kosugi and S. Hayase, Ionic liquid type dye-sensitized solar cells: increases in photovoltaic performances by adding a small amount of water, *Curr. Appl. Phys.*, 2005, **5**, 152–158.

295 J. Zhang, Y. Cui, X. Zhang, Q. Sun, J. Zheng, P. Wang, J. Feng and Y. Zhu, LiTFSI as a plastic salt in the quasi-solid state polymer electrolyte for dye-sensitized solar cells, *C. R. Chim.*, 2013, **16**, 195–200.

296 T. Welton, Room-temperature ionic liquids: solvents for synthesis and catalysis, *Chem. Rev.*, 1999, **99**, 2071–2084.

297 R. Kawano, H. Matsui, C. Matsuyama, A. Sato, M. Susan, N. Tanabe and M. Watanabe, High performance dye-sensitized solar cells using ionic liquids as their electrolytes, *J. Photochem. Photobiol., A*, 2004, **164**, 87–92.

298 L. Cammarata, S. G. Kazarian, P. A. Salter and T. Welton, Molecular states of water in room temperature ionic liquids, *Phys. Chem. Chem. Phys.*, 2001, **3**, 5192–5200.

299 J. Jeon, H. Kim, W. A. Goddard, T. A. Pascal, G. I. Lee and J. K. Kang, The role of confined water in ionic liquid electrolytes for dye-sensitized solar cells, *J. Phys. Chem. Lett.*, 2012, **3**, 556–559.

300 D. J. Searles and D. J. Evans, Fluctuation theorem and Green-Kubo relations, *J. Chem. Phys.*, 2000, **112**, 9727–9735.

301 V. K. Thorsmolle, G. Rothenberger, D. Topgaard, J. C. Brauer, D. B. Kuang, S. M. Zakeeruddin, B. Lindman, M. Grätzel and J. E. Moser, Extraordinarily efficient conduction in a redox-active ionic liquid, *ChemPhysChem*, 2011, **12**, 145–149.

302 F. Bella, R. Bongiovanni, R. S. Kumar, M. A. Kulandainathan and A. M. Stephan, Light cured networks containing metal organic frameworks as efficient and durable polymer electrolytes for dye-sensitized solar cells, *J. Mater. Chem. A*, 2013, **1**, 9033–9036.

303 S. Sakaguchi, H. Ueki, T. Kato, T. Kado, R. Shiratuchi, W. Takashima, K. Kaneto and S. Hayase, Quasi-solid dye sensitized solar cells solidified with chemically cross-linked gelators: control of TiO_2/gel electrolytes and counter Pt/gel electrolytes interfaces'', *J. Photochem. Photobiol., A*, 2004, **164**, 117–122.

304 S. Murai, S. Mikoshiba, H. Sumino and S. Hayase, Quasi-solid dye-sensitized solar cells containing chemically cross-linked gel: How to make gels with a small amount of gelator, *J. Photochem. Photobiol., A*, 2002, **148**, 33–39.

305 S. Murai, S. Mikoshiba, H. Sumino, T. Kato and S. Hayase, Quasi-solid dye sensitised solar cells filled with phase-separated chemically cross-linked ionic gels, *Chem. Commun.*, 2003, 1534–1535.

306 W. C. Lai and C. C. Chen, Novel poly(ethylene glycol) gel electrolytes prepared using self-assembled 1,3:2,4-dibenzylidene-d-sorbitol, *Soft Matter*, 2014, **10**, 312–319.

307 C. Song, L. Zhang, Y. Wang, X. Yan and D. Zhao, Synthesis and optimization of P(MMA-BA-MAA)/PEG-based polymer gel electrolytes, *J. Mater. Sci.*, 2013, **48**, 8153–8162.

308 S. Xu, H. Hu, B. Sebo, B. Chen, Q. Tai and X. Zhao, Modification of nanocrystalline porous films by poly(ethyleneglycol) for quasi-solid dye-sensitized solar cells, *J. Power Sources*, 2011, **196**, 10817–10821.

309 D. A. Rand, Battery system for electric vehicles: state of art review, *J. Power Sources*, 1979, **4**, 101–143.

310 S. Mozaffari, M. R. Nateghi and M. Borhanizarandi, Effects of water-based gel electrolyte on the charge recombination and performance of dye-sensitized solar cells, *J. Solid State Electrochem.*, 2014, **18**, 2589–2598, DOI: 10.1007/s10008-014-2508-x.

311 J. E. Benedetti, A. D. Goncalves, A. Formiga, M. A. De Paoli, X. Li, J. R. Durrant and A. F. Nogueira, A polymer gel electrolyte composed of a poly(ethylene oxide) copolymer and the influence of its composition on the dynamics and performance of dye-sensitized solar cells, *J. Power Sources*, 2010, **195**, 1246–1255.

312 S. S. Soni, K. B. Fadadu and A. Gibaud, Ionic conductivity through thermoresponsive polymer gel: ordering matters, *Langmuir*, 2012, **28**, 751–756.

313 V. K. Aswal and P. S. Goyal, Small-angle neutron scattering diffractometer at Dhruva reactor, *Curr. Sci.*, 2000, **79**, 947–953.

314 S. S. Soni, K. B. Fadadu, R. L. Vekariya, J. Debgupta, K. D. Patel, A. Gibaud and V. K. Aswal, Effect of self-assembly on triiodide diffusion in water based polymer gel electrolytes: an application in dye solar cell, *J. Colloid Interface Sci.*, 2014, **425**, 110–117.

315 J. Y. Kim, T. H. Kim, D. Y. Kim, N. G. Park and K. D. Ahn, Novel thixotropic gel electrolytes based on dicationic bis-imidazolium salts for quasi-solid-state dye-sensitized solar cells, *J. Power Sources*, 2008, **175**, 692–697.

316 S. Erdur, G. Yilmaz, D. Goen Colak, I. Cianga and Y. Yagci, Poly(phenylenevinylene)s as sensitizers for visible light induced cationic polymerization, *Macromolecules*, 2014, **47**, 7296–7302.

317 J. Xu and C. Boyer, Visible light photocatalytic thiol-ene reaction: an elegant approach for fast polymer postfunctionalization and step-growth polymerization, *Macromolecules*, 2015, **48**, 520–529.

318 S. J. Park, K. Yoo, J. Y. Kim, J. Y. Kim, D. W. Lee, B. Kim, H. Kim, J. H. Kim, J. Cho and M. J. Ko, Water-based thixotropic polymer gel electrolyte for dye-sensitized solar cells, *ACS Nano*, 2013, **7**, 4050–4056.

319 M. Imperiyka, A. Ahmad, S. A. Hanifah and F. Bella, A UV-prepared linear polymer electrolyte membrane for dye-sensitized solar cells, *Physica B*, 2014, **450**, 151–154.

320 F. Bella, M. Imperiyka and A. Ahmad, Photochemically produced quasi-linear copolymers for stable and efficient electrolytes in dye-sensitized solar cells, *J. Photochem. Photobiol., A*, 2014, **289**, 73–80.

321 C. L. Chen, H. Teng and Y. L. Lee, *In situ* gelation of electrolytes for highly efficient gel-state dye-sensitized solar cells, *Adv. Mater.*, 2011, **23**, 4199–4204.

322 L. Jin, Z. Wu, T. Wei, J. Zhai and X. Zhang, Dye-sensitized solar cell based on blood mimetic thixotropy sol-gel electrolyte, *Chem. Commun.*, 2011, **47**, 997–999.

323 A. Chiappone, F. Bella, J. R. Nair, G. Meligrana, R. Bongiovanni and C. Gerbaldi, Structure-performance correlation of nanocellulose-based polymer electrolytes for efficient quasi-solid DSSCs, *ChemElectroChem*, 2014, **1**, 1350–1358.

324 M. H. Khanmirzaei and S. Ramesh, Studies on biodegradable polymer electrolyte rice starch (RS) complexed with lithium iodide, *Ionics*, 2014, **20**, 691–695.

325 G. P. Salvador, D. Pugliese, F. Bella, A. Chiappone, A. Sacco, S. Bianco and M. Quaglio, New insights in long-term photovoltaic performance characterization of cellulose-based gel electrolytes for stable dye-sensitized solar cells, *Electrochim. Acta*, 2014, **146**, 44–51.

326 F. Bella, A. Chiappone, J. R. Nair, G. Meligrana and C. Gerbaldi, Effect of different green cellulosic matrices on the performance of polymeric dye-sensitized solar cells, *Chem. Eng. Trans.*, 2014, **41**, 211–216.

327 F. Bella, N. N. Mobarak, F. N. Jumaah and A. Ahmad, From seaweeds to biopolymeric electrolytes for third generation solar cells: An intriguing approach, *Electrochim. Acta*, 2014, **151**, 306–311.

328 M. Kaneko, T. Nomura and C. Sasaki, Photoinduced charge separation in an aqueous phase using nanoporous TiO_2 film and a quasi-solid made of natural products, *Macromol. Rapid Commun.*, 2003, **24**, 444–446.